

Université de Montréal

**Complexes pinceurs de type POCOP de Nickel (II):
Synthèse, caractérisation, réactivité et applications
catalytiques**

Par

Abderrahmen Salah

Département de Chimie

Faculté des Arts et des Sciences

Mémoire présenté à la Faculté des études supérieures

En vue de l'obtention du grade de M.Sc.

En chimie

Juin 2011

© Salah Abderrahmen, 2011

Université de Montréal
Faculté des études supérieures

Ce mémoire intitulé :

**Complexes pinceurs de type POCOP de Nickel (II):
Synthèse, caractérisation, réactivité et applications
catalytiques**

Présenté par :

Abderrahmen Salah

A été évalué par un jury composé des personnes suivantes :

Pr. Garry Hanan, président-rapporteur

Pr. Davit Zargarian, directeur de recherche

Pr. André Beauchamp, membre du jury

Résumé

Ce mémoire décrit la synthèse, la caractérisation spectroscopique et l'étude de la réactivité catalytique d'une nouvelle série de complexes pinceurs de Ni(II) formés à partir du ligand POCOP^{Ph} ($\kappa^P, \kappa^C, \kappa^P$ -2,6-{Ph₂PO}₂C₆H₄), très peu étudié dans le cas du nickel. Les études décrites dans ce mémoire examinent l'effet des substituants des phosphines sur les propriétés spectroscopiques et électrochimiques ainsi que les activités catalytiques.

La synthèse du ligand a été améliorée par rapport à la procédure connue dans la littérature en diminuant le temps de réaction à 30 min et la température jusqu'à température ambiante. Les composés pinceur ($\kappa^P, \kappa^C, \kappa^P$ -2,6-{Ph₂PO}₂C₆H₃)NiX ont été obtenus avec des rendements variant entre 60% et 88%. Le premier complexe a été synthétisé en faisant réagir le précurseur NiBr₂(NCCH₃)_x avec le ligand POCOP^{Ph} pour donner (POCOP^{Ph})NiBr. Ce dernier réagit par la suite avec les sels d'argent et de potassium pour donner 4 nouveaux complexes soient : (POCOP^{Ph})NiCN, (POCOP^{Ph})NiOTf, (POCOP^{Ph})NiOAc et (POCOP^{Ph})NiONO₂ (OTf = triflate et OAc = acetate). Vu la réactivité limitée du dérivé bromure, le dérivé (POCOP^{Ph})NiOTf a été utilisé pour la préparation du composé (POCOP^{Ph})NiCCPh. Le dérivé Ni-OTf a été utilisé également pour la synthèse des complexes (POCOP^{Ph})NiR qui ont été détectés par RMN. Ces complexes (POCOP^{Ph})NiR ont montré une stabilité trop faible et donnent des nouveaux complexes de type (POCOP^{Ph})NiX en échangeant l'halogène avec le Mg ou de type (POCOP^{Ph})NiOH en s'hydrolysant. Les espèces cationiques [(POCOP^{Ph})NiNCR][OTf] (R= Me, CHCH₂, CHCHMe, C(Me)CH₂, NCCH₂CH₂N(Ph)H) ont été obtenues facilement et avec des bon rendements à partir du (POCOP^{Ph})NiOTf.

Tous les composés obtenus ont été caractérisés par la spectroscopie RMN (^1H , $^{13}\text{C}\{^1\text{H}\}$, $^{31}\text{P}\{^1\text{H}\}$, $^{19}\text{F}\{^1\text{H}\}$), la spectroscopie IR et la spectroscopie UV-vis. L'analyse élémentaire et l'analyse par la diffraction des rayons X, dont le but est de résoudre la structure à l'état solide, ont été utilisées pour la plupart des complexes. Des études de voltampérométrie cyclique ont été menées pour déterminer la densité électronique des centres métalliques et l'effet des phosphines sur cette propriété électrochimique.

Dans le but de déterminer l'effet des substituants des phosphines sur l'activité catalytique des complexes, nous avons évalué les réactivités catalytiques des deux complexes $(\text{POCOP}^{\text{Ph}})\text{NiOTf}$ et $(\text{POCOP}^{i\text{-Pr}})\text{NiOTf}$ dans la réaction d'hydroamination des oléfines activés et plus spécifiquement l'acrylonitrile. Après optimisation des conditions expérimentales, on a constaté que la réactivité des deux composés sont similaires mais une grande différence apparaît après l'ajout des additifs. En effet, le complexe $(\text{POCOP}^{i\text{-Pr}})\text{NiOTf}$ donne une bonne activité catalytique en présence de la triéthylamine, tandis que cette activité diminue considérablement en présence d'eau, contrairement au complexe $(\text{POCOP}^{\text{Ph}})\text{NiOTf}$ qui est plus actif en présence d'eau. Dans le cas du complexe $(\text{POCOP}^{\text{Ph}})\text{NiOTf}$, on a pu montrer que la base se coordonne au nickel dans le produit formé après la réaction d'hydroamination, ce qui diminue l'activité de ce complexe dans certains cas. Également on a exploré la réaction de l'addition du lien O-H sur l'acrylonitrile, et étonnamment le complexe $(\text{POCOP}^{\text{Ph}})\text{NiOTf}$ est beaucoup plus actif que son homologue $(\text{POCOP}^{i\text{-Pr}})\text{NiOTf}$ dans le cas des alcools aromatiques. Par contre, les alcools aliphatiques restent un défi majeur pour ce genre de complexe. Le mécanisme de cette réaction qui a été proposé montre que l'alcoololyse passe par les deux

intermédiaires $(POCOP^{Ph})NiOAr$ et $[(POCOP^{Ph})NiOAr][HOAr]$ mais l'isolation de ces intermédiaires observés par RMN semble être difficile.

Mots clés : nickel, complexe pinceur, POCOP, catalyse, hydroamination, hydroalcoxylation, voltampérométrie cyclique, diffraction de rayons X, RMN, GC-MS.

Abstract

This thesis describes the synthesis, spectroscopic characterization and the catalytic activities of a new family of pincer complexes of Ni (II) starting from the ligand POCOP^{Ph} ($\kappa^P, \kappa^C, \kappa^P$ -2,6-{Ph₂PO}₂C₆H₄) for which very few nickel complexes have been reported previously. We discuss the influence of *P*-substituents on the spectroscopic, electrochemical and catalytic activities of these complexes.

The synthesis of POCOP^{Ph} has been improved comparatively to the procedure reported in the literature by reducing the reaction time to 30 minutes and the temperature to room temperature. The complex ($\kappa^P, \kappa^C, \kappa^P$ -2,6-{Ph₂PO}₂C₆H₃)NiBr was obtained with 88% yield by reacting the precursor NiBr₂(NCCH₃)_x with POCOP^{Ph}. This complex was then reacted with various silver and potassium salts to give the following complexes (POCOP^{Ph})NiCN, (POCOP^{Ph})NiOTf, (POCOP^{Ph})NiOAc and (POCOP^{Ph})NiONO₂ (OTf = triflate et OAc = acetate). The limited reactivity of the bromo derivative led us to use (POCOP^{Ph})NiOTf for the preparation of some of the desired derivatives, such as (POCOP^{Ph})NiCCPh. Attempts to prepare the desired alkyl derivatives (POCOP^{Ph})NiR were not successful, but we were able to detect these derivatives using NMR. The thermal instability of (POCOP^{Ph})NiR led to formation of new (POCOP^{Ph})NiX complexes by halogen exchange with MgX₂ or (POCOP^{Ph})NiOH by hydrolysis. The cationic species [(POCOP^{Ph})NiNCR][OTf] (R = Me, CHCH₂, CHCHMe, C(Me)CH₂, NCCH₂CH₂N(Ph)H) also were obtained easily from the (POCOP^{Ph})NiOTf with good yields.

All these complexes were characterized by elemental analysis, NMR spectroscopy (¹H, ¹³C{¹H}, ³¹P{¹H}, ¹⁹F{¹H}), IR spectroscopy and UV-vis spectroscopy. For most

complexes analysis by X-ray diffraction allowed us to establish their solid state structures. A few studies by cyclic voltammetry have been done to determine the electronic density of the metal center and the *P*-substituent influence on this characteristic.

In order to investigate the effect of phosphine substituents on the catalytic activities of this type of complexes, catalytic studies were undertaken with the following two complexes (POCOP^{Ph}) NiOTf and ($\text{POCOP}^{\text{i-Pr}}$) NiOTf in hydroamination of activated olefins specifically acrylonitrile. After optimization of experimental conditions, it was found that both complexes have similar activities but what makes a huge difference is the use of additives. Indeed, ($\text{POCOP}^{\text{i-Pr}}$) NiOTf showed good catalytic activity in the presence of triethylamine as base but this activity decreased significantly in the presence of water. The opposite was observed with (POCOP^{Ph}) NiOTf complex: it was shown that triethylamine coordinates to the nickel center in this complex and hence reduces its activity in some cases. We also explored other reactions such as the addition of the O-H bond in aromatic alcohols to acrylonitrile, and it was surprising that (POCOP^{Ph}) NiOTf is much more active than its homologous ($\text{POCOP}^{\text{i-Pr}}$)- NiOTf . However aliphatic alcohols remain a major challenge for this kind of complex. Mechanistic studies suggest that this reaction passes through the following intermediates (POCOP^{Ph}) NiOAr and $[(\text{POCOP}^{\text{Ph}})\text{NiOAr}][\text{HOAr}]$. These species were observed by NMR but not isolated.

Keywords: nickel, pincer complex, POCOP-type, catalysis, hydroamination, hydroalkoxylation, cyclic voltammetry, alcoholysis, X-ray diffraction, NMR, GC-MS

Table des matières

Résumé	iii
Abstract	vi
Table des matières	viii
Liste des tableaux	xii
Liste des figures	xiii
Liste des abréviations	xvi
Remerciements	xix
Chapitre 1 : Introduction	1
1.1 Généralité sur les complexes pinceurs	3
1.2 Ligands pinceur de type POCOP	5
1.3 Les complexes pinceurs de type POCOP	7
1.4 Activité catalytique des complexes pinceurs de type POCOP vs PCP.....	9
1.4.1 Reactions de couplage	10
1.4.2. Coordination et activation des petites molécules.....	14
1.4.3. Activation des lien C-C et C-H.....	16
1.4.4. Hydroamination des oléfines activés.....	19
1.5 Description des travaux	21
1.6 Références.....	22
Chapitre 2 : The Impact of <i>P</i> -Substituents on the Structures, Spectroscopic Properties, and Reactivities of POCOP-Type Pincer Complexes of Nickel(II).....	28
2.1. Abstract.....	29

2.2. Introduction.....	30
2.3. Results and Discussion.....	31
2.3.1 Synthesis	31
2.3.2 Spectroscopic characterization.....	34
2.3.3 Solid state characterization.....	39
2.3.4 Cyclic voltammetry measurements.....	44
2.3.5 Reactivity tests.....	45
2.4 Conclusion.....	47
2.5 Experimental Section.....	48
2.5.1 General.....	48
2.5.2 Synthesis of 1,3-(OPPh ₂) ₂ C ₆ H ₄ (ligand a).....	49
2.5.3. Synthesis of (POCOP ^{Ph})NiBr (1).....	49
2.5.4. Synthesis of (POCOP ^{Ph})NiCN (2).....	50
2.5.5. Synthesis of (POCOP ^{Ph})Ni(OSO ₂ CF ₃).....	51
2.5.6. Synthesis of (POCOP ^{Ph})Ni(OCOCH ₃).....	52
2.5.7. Synthesis of (POCOP ^{Ph})Ni(ONO ₂)(5).....	52
2.5.8 Synthesis of (POCOP ^{Ph})Ni(C≡CPh) (6).....	53
2.5.9. Crystal Structure Determinations.....	54
2.6 Acknowledgements.....	55
2.7 References.....	55
2.8 Supporting Informations.....	59

Chapitre 3 : Hydroamination and Alcoholytic Promoted by the Pincer	
Complex $\{\kappa^P, \kappa^C, \kappa^P\text{-}2,6\text{-}(\text{Ph}_2\text{PO})_2\text{C}_6\text{H}_3\}\text{Ni}(\text{OSO}_2\text{CF}_3)$	67
3.1. Abstract.....	68
3.2. Introduction.....	69
3.3. Results and Discussion.....	72
3.3.1. Synthesis and characterization of cationic precursors.....	73
3.3.2. Relative stabilities of complexes 1, 2a, and 3.....	78
3.3.3. Catalytic hydroamination of acrylonitrile catalyzed by the triflate derivatives 1 and 3.....	81
3.3.4. Hydroamination with crotonitrile and methacrylonitrile.....	85
3.3.5. Catalytic alcoholytic of acrylonitrile.....	86
3.3.6. Mechanistic insights.....	88
3.3.7. On the mechanism of alcoholytic reactions catalyzed by 1.....	95
3.4. Conclusion.....	97
3.5. Experimental Section.....	99
3.5.1. General.....	99
3.5.2. Synthesis of $[\{\kappa^P, \kappa^C, \kappa^P\text{-}2,6\text{-}(\text{Ph}_2\text{PO})_2\text{C}_6\text{H}_3\}\text{Ni}(\text{NCCH}_3)][\text{OSO}_2\text{CF}_3]$ (2a).....	100
3.5.3. General procedure for preparation of $[\{\kappa^P, \kappa^C, \kappa^P\text{-}2,6\text{-}(\text{Ph}_2\text{PO})_2\text{C}_6\text{H}_3\}\text{Ni}(\text{NCR})][\text{OSO}_2\text{CF}_3]$ (2).....	101
3.5.3.1. $[\{\kappa^P, \kappa^C, \kappa^P\text{-}2,6\text{-}(\text{Ph}_2\text{PO})_2\text{C}_6\text{H}_3\}\text{Ni}(\text{NCCH}=\text{CH}_2)][\text{OSO}_2\text{CF}_3]$ (2b).....	101
3.5.3.2. $[\{\kappa^P, \kappa^C, \kappa^P\text{-}2,6\text{-}(\text{Ph}_2\text{PO})_2\text{C}_6\text{H}_3\}\text{Ni}(\text{NCCH}=\text{CHMe})][\text{OSO}_2\text{CF}_3]$ (2c).....	102
3.5.3.3. $[\{\kappa^P, \kappa^C, \kappa^P\text{-}2,6\text{-}(\text{Ph}_2\text{PO})_2\text{C}_6\text{H}_3\}\text{Ni}(\text{NCC}(\text{Me})=\text{CH}_2)][\text{OSO}_2\text{CF}_3]$ (2d).....	102

3.5.3.4. [$\{\kappa^P, \kappa^C, \kappa^P$ -2,6-(Ph ₂ PO) ₂ C ₆ H ₃ }Ni(NCCH ₂ CH ₂ N(Ph)H)][OSO ₂ CF ₃] (2e).....	103
3.5.4 Synthesis of $\{\kappa^P, \kappa^C, \kappa^P$ -2,6-(Ph ₂ PO) ₂ C ₆ H ₃ }Ni{O(3-Me-C ₆ H ₄)} (5).....	104
3.5.5 Typical procedure used for catalytic hydroamination of cyano olefins.....	104
3.5.6 Typical procedure used for catalytic alcoholysis of acrylonitrile.....	105
3.5.7. Crystal Structure Determinations.....	105
3.6. Acknowledgements.....	106
3.8 References.....	107
3.7 Supporting Informations.....	114
Chapitre IV : Conclusion générale	120
4.1 Synthèse des ligands et des complexes.....	120
4.2 L'effet du changement des phosphines sur les propriétés catalytiques et spectroscopiques.....	122
4.3 Limitation et perspectives	124

Liste des tableaux

Table 2.1. IR data for complexes 2 and 6 and related compounds	37
Table 2.2. Lowest energy electronic transitions for the complexes (POCOP)NiX.....	39
Table 2.3. Crystal Data Collection and Refinement Parameters for Complexes 1-6.....	40
Table 2.4. Selected Bond Distances (Å) and Angles (deg) for Complexes 1-6.....	41
Table 2.5. Redox potentials.....	45
Table 2.6. ^1H NMR data for complexes 1-6.....	61
Table 2.7. $^{13}\text{C}\{^1\text{H}\}$ NMR data for complexes 1-6	62
Table 3.1. UV-visible data for the cationic adducts $[(\text{POCOP}^{\text{Ph}})\text{Ni}(\text{NCR})]^+$	73
Table 3.2. Crystal Data Collection and Refinement Parameters for Complexes 2a, 2e, 3 and 4.....	76
Table 3.3. Selected Bond Distances (Å) and Angles (deg) for 2a, 1, and their POCOP $^{i\text{-Pr}}$ analogues.....	77
Table 3.4. Catalytic activities for hydroamination of acrylonitrile.....	83
Table 3.5. Catalyzed alcoholysis of acrylonitrile.....	87
Table 3.6. Values of v (CN) for various RCN and their Ni adducts.....	95
Table 3.7. ^1H NMR data for complexes 2a-e and 5.....	116
Table 3.8. $^{13}\text{C}\{^1\text{H}\}$ NMR data for complexes 2a-e and 5.....	116

Liste des figures

Figure 1.1. Structure générale de complexes pinceurs.....	3
Figure 1.2. Exemples de complexes pinceurs.....	5
Figure 1.3. Schéma général de synthèses de ligand POCOP.....	6
Figure 1.4. les voies les plus citées dans la littérature de la synthèse de POCOP ligand..	6
Figure 1.5. Intermédiaires de réaction durant la formation de complexes pinceurs.....	7
Figure1.6. Exemples de réactions de formation des complexes pinceurs avec des précurseurs de faible D.O.....	8
Figure 1.7. Exemples de réactions de formation des complexes pinceurs avec des précurseurs métalliques à fort D.O	9
Figure 1.8. Schéma général du couplage du Heck.....	10
Figure 1.9. Premiers complexes pinceurs de Palladium utilisés dans le couplage de Heck.....	11
Figure 1.10. Schéma général de la réaction de couplage de Suzuki.....	12
Figure 1.11. Complexes Catalyseurs de Palladium utilisés en couplage de Suzuki.....	12
Figure 1.12. Complexe pinceur de Pd pour la réaction de couplage de Suzuki.....	13
Figure 1.13. Exemples De complexes PCP et POCOP coordonnant divers petites molécules.....	15
Figure 1.14. Travaux de Goldman.....	16
Figure 1.15. Trois mécanismes d'activation de lien C-H aromatique.....	17
Figure 1.16. Travaux de Milstein avec PCP de Rh et de Brookhart avec ses complexes PCP et POCOP d'Ir.....	18

Figure 1.17. Travaux de Szabo avec ces complexes POCOP de Pd.....	19
Figure 1.18. Schéma général de la réaction d'hydroamination.....	19
Figure 1.19. Exemples des complexes PCP et POCOP étudié en hydroamination.....	21
Figure 2.1. PCP, POCOP and POCN pincer type complexes of Nickel	31
Figure 2.2. Synthesis of ligand and complexes.....	32
Figure 2.3. Attempts of synthesis of alkyl derivetives.....	34
Figure 2.4. UV-Vis spectra for compelxes 1 and (POCOP ^{i-Pr})NiBr, recorded using CH ₂ Cl ₂ solutions (1.11×10^{-4} M).....	38
Figure2.5. ORTEP diagrams for complexes 1-6	42
Figure 2.6. Cyclic Valtammograms of complexes 3 and 4 (1 mM solutions in CH ₂ Cl ₂) containing 0.1 M [NBu ₄][PF ₆].....	45
Figure 2.7. UV-Vis of (POCOP ^{i-Pr})Ni-OCOCH ₃ in CH ₂ Cl ₂ Concentration = $1.054 \cdot 10^{-4}$ mol/L.....	63
Figure 2.8. UV-Vis of (POCOP ^{i-Pr})Ni-OSO ₂ CF ₃ in CH ₂ Cl ₂ Concentration = $1.054 \cdot 10^{-4}$ mol/L.....	63
Figure 2.9. UV-Vis of complex 2 in CH ₂ Cl ₂ Concentration = $1.11 \cdot 10^{-4}$ mol/L.....	64
Figure 2.10. UV-Vis of complex 3 in CH ₂ Cl ₂ Concentration = $1.27 \cdot 10^{-4}$ mol/L.....	64
Figure 2.11. UV-Vis of complex 4 in CH ₂ Cl ₂ Concentration = $5.60 \cdot 10^{-5}$ mol/L.....	65
Figure 2.12. UV-Vis of complex 5 in CH ₂ Cl ₂ Concentration = $5.80 \cdot 10^{-4}$ mol/L.....	65
Figure 2.13. UV-Vis of complex 6 in CH ₂ Cl ₂ Concentration = $7.85 \cdot 10^{-5}$ mol/L.....	66
Figure 3.1. PCP and POCOP type pincer complexes.....	70
Figure 3.2. Synthesis path of complex 2a	74
Figure 3.3. ORTEP diagram for complex 2a	78

Figure 3.4. Reaction of triflate derivatives under ambient air.....	79
Figure 3.5. ORTEP diagram for complex 3	80
Figure 3.6. ORTEP diagram for complex 4	80
Figure 3.7. Equation of hydroamination of acrylonitrile	83
Figure 3.8. Equation of alcoholysis of acrylonitrile	86
Figure 3.9. ORTEP diagram for complex 2e	91
Figure 3.10. Reactivity of complexes 1 and 2b	92
Figure 3.11. Proposed mechanism of Hydroamination of acrylonitrile.....	93
Figure 3.12. Mechanism of alcoholysis of acrylonitrile.....	97
Figure 3.13. UV-Vis of (POCOP^{i-Pr})NiNCMe in CH ₂ Cl ₂ Concentration = 1.25 10 ⁻⁴ mol/L.....	117
Figure 3.14. UV-Vis of complex 5 in CH ₂ Cl ₂ Concentration = 1.26 10 ⁻⁵ mol/L.....	117
Figure 3.15. UV-Vis of complex 2a in CH ₂ Cl ₂ Concentration = 1.25 10 ⁻⁴ mol/L.....	118
Figure 3.16. UV-Vis of complex 2b in CH ₂ Cl ₂ Concentration = 1.25 10 ⁻⁴ mol/L.....	118
Figure 3.17. UV-Vis of complex 2c in CH ₂ Cl ₂ Concentration = 1.25 10 ⁻⁴ mol/L.....	119
Figure 3.18. UV-Vis of complex 2d in CH ₂ Cl ₂ Concentration = 1.25 10 ⁻⁴ mol/L.....	119
Figure 4.1. Synthèse des ligands.....	120
Figure 4.2. Synthèse des complexes.....	121
Figure 4.3. Mécanisme de l'hydroamination.....	123
Figure 4.4. Mécanisme de l'hydroalkoxylation.....	124
Figure 4.5. Nouveau complexes et intermédiaire réactionnels de type POCOP	125

Liste des abréviations

★ Å :	Angstrom
★ Ac :	acyle
★ Ar :	aryle
★ δ :	déplacement chimique
★ cat. :	catalyseur
★ cod :	<i>1,5-cyclooctadiène</i>
★ Cp :	cyclopentadiènyle
★ d :	doublet
★ D :	deutérium
★ DMAP :	4-diméthylaminopyridine
★ D.O. :	degré d'oxydation
★ dppe :	1,2- bis(diphénylphosphino)éthane
★ dppp :	1,3-bis(diphénylphosphino)propane
★ equiv :	équivalents
★ Et :	éthyle
★ EWG :	<i>electronwithdrawing</i>
★ F :	facteur de structure
★ GC :	<i>gas chromatography</i>
★ h :	heure
★ i :	ipso
★ i-Pr :	isopropyle
★ IR :	infrarouge

★ J :	constante de couplage
★ L :	ligand neutre
★ m :	méta
★ m :	multiplet
★ m/z :	masse/charge
★ min :	minute
★ Me :	méthyl
★ MLCT :	<i>metal to ligand charge transfer</i>
★ NMR :	<i>nuclear magnetic resonance</i>
★ n-Bu :	<i>n</i> -butyle
★ NEt ₃ :	triéthylamine
★ o :	ortho
★ OAc :	acetate
★ OTf :	triflate
★ ORTEP :	<i>Oak ridge thermal ellipsoid program</i>
★ p :	para
★ Ph :	phényle
★ POCOP ^{i-Pr} :	1,3-(OP(i-Pr ₂)) ₂ C ₆ H ₄
★ POCOP ^{Ph} :	1,3-(OPPh ₂) ₂ C ₆ H ₄
★ ppm :	parties par million
★ qq :	quasiquadruplet
★ R :	groupe alkyle
★ RMN :	résonance magnétique nucléaire

- ★ s : singulet
 - ★ MS : *mass spectrometry*
 - ★ t : triplet
 - ★ r.t. : *room temperature*
 - ★ *t*-Bu : *tert*-butyle
 - ★ THF : tétrahydrofurane
 - ★ X : ligand anionique
-

Remerciements

Tout d'abord, je tiens à remercier mon directeur de recherche, le professeur Davit Zargarian, pour la confiance qu'il m'a accordée en m'accueillant dans son groupe. Je le remercie également pour son soutien et ses nombreux et précieux conseils, ainsi que pour toutes les discussions intéressantes que nous avons eues ensemble.

J'adresse mes sincères remerciements au professeur Garry Hanan et au professeur André L. Beauchamp pour avoir accepté de juger ce travail en tant que président rapporteur et membre du jury.

Ensuite, je tien également à remercier à Dr. Michel Simard et surtout Madame Francine Bélanger-Gariépy pour leur aide et patience lors des analyses de diffraction des rayons X. Grace à eux, j'ai pu apprendre cette technique fort précieuse pour moi. De plus, je remercie Elena Nadezhina pour sa patience avec mes analyses élémentaires.

Un grand merci à mon ancien collègue et mon cher ami Dr. Denis Spasyuk qui m'a initié aux manipulations sous atmosphère inerte et qui m'a appris la chimie des pinceurs.

Je ne serais oublier de remercier tout mes collègues Xavier, Dr. Laure ben hamou également ma stagiaire Xaroline et tout mes amis surtout Kévin Ruffray pour tout les PEPSI time qu'on a eu ensemble.

Je remercie particulièrement mes parents pour leur confiance soutien et patience ainsi que tout les membres de ma petite et grande famille.

Bonne lecture
Abderrahmen Salah

Chapitre 1: Introduction

La contribution à la résolution des problèmes environnementaux constitue un des grands défis actuels pour la chimie, celle-ci étant considérée comme la plus grande source de pollution.

En effet, les processus de synthèse de certains produits essentiels pour l'industrie et plus spécifiquement l'industrie pharmaceutique, nécessitent plusieurs étapes dont chacune exige de l'énergie, ce qui augmente les coûts et diminue le rendement en polluant l'atmosphère. Pour résoudre un tel type de problème, différentes solutions ont été mises en œuvre dans tous les domaines de la chimie, tels que la recherche de sources d'énergies renouvelables¹ comme l'énergie solaire, l'utilisation de l'hydrogène comme une source propre, la conversion de gaz inerte comme le méthane et l'azote qui est envisageable mais dans des conditions de température et de pression sévères. Pour cela d'autres domaines ont pris le défi d'augmenter l'efficacité des réactions en jouant sur plusieurs facteurs, en diminuant l'énergie ou le nombre d'étapes ou en réduisant la quantité de réactifs et en augmentant la vitesse des réactions².

Une des voies les plus efficaces pour atteindre ces objectifs est le développement des complexes organométalliques de métaux de transition, en tant que catalyseurs pour les réactions chimiques. Car ils ont montré des réactivités importantes tout en utilisant des conditions moins exigeantes et en diminuant le nombre d'étapes. Ainsi, il s'est avéré qu'au niveau structural la combinaison de ligands et d'un métal donne naissance dans certains cas à des composés thermiquement très stables et robustes, et présentant des réactivités intéressantes comme celle des composés de type pinceur³.

Ces derniers se présentent comme une combinaison d'un métal de transition et d'un ligand tridentate, ce qui donne une configuration ou géométrie rigide de type plan carré dans la plupart des complexes pinceurs.

Récemment, plusieurs groupes de recherche ont publié des travaux sur une classe spécifique des complexes pinceurs, symétriques, où le métal central se lie avec deux phosphores et un carbone : on les nomme les complexes pinceurs de type PCP ou PXCXP (X = C, O, N, S).

Le groupe du Pr Davit Zargarian⁴ étudie les complexes pinceurs de Nickel encore très peu étudiés en commençant par les diphosphinito-complexes (PCP et POCOP). D'anciens membres du groupe ont étudié les complexes pinceurs PCP et POCOP de Ni comme respectivement Annie Castonguay dans le cadre de son projet de doctorat et Valerica Pandarus dans le cadre de son projet de maîtrise. Maintenant l'intérêt est ciblé sur les groupements ``R`` portés par les phosphores. Grâce à leur réactivité catalytique et leur voie de synthèse les diphosphinito-complexes ont attiré notre attention. Par exemple, ce type de complexes est un très bon catalyseur pour l'addition de Kharasch⁵, le couplage de Heck⁶, et celui de Suzuki⁷, ou encore la déshydrogénération des alcanes⁸ et l'addition de Mickael⁹.

Les phosphores influencent la densité électronique sur le métal. La modification des groupements R permet de moduler les propriétés électroniques et stériques des phosphinites, et donc influence la réactivité du centre métallique : c'est dans ce cadre que s'inscrit mon projet de maîtrise.

Ainsi, ce projet a pour but dans un premier temps d'augmenter l'efficacité des réactions catalytiques en changeant les groupements qui se trouvent sur les phosphores, et

dans un second temps une étude structurale et électronique des complexes $\text{POC}_{\text{sp}^2}\text{OP}$ du Nickel synthétisés.

1.1 Généralité sur les complexes pinceurs

En 1976, les premiers complexes pinceurs ont été synthétisés par Shaw^{3b} : il a en effet rapporté des complexes pinceurs avec tous les métaux de transition d¹⁰ et d⁹. Ceci a été le premier modèle de coordination tridenté où une liaison σ métal-carbone est stabilisée par la formation de métallacycles. En général les complexes pinceurs sont formés d'un ligand tridentate et d'un métal de transition où le ligand est connecté au métal par au moins une liaison σ métal-carbone.

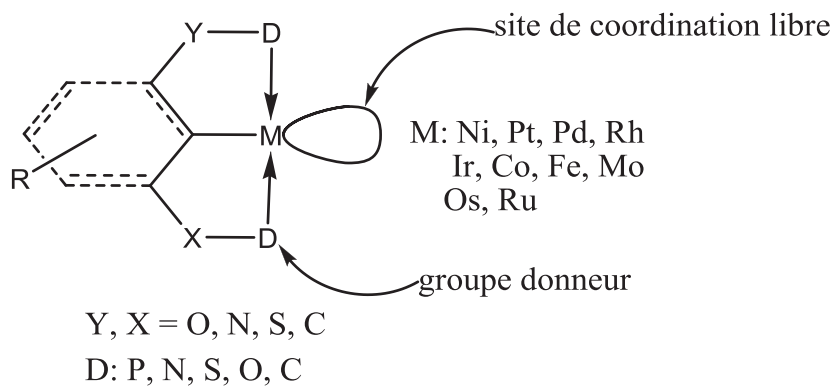


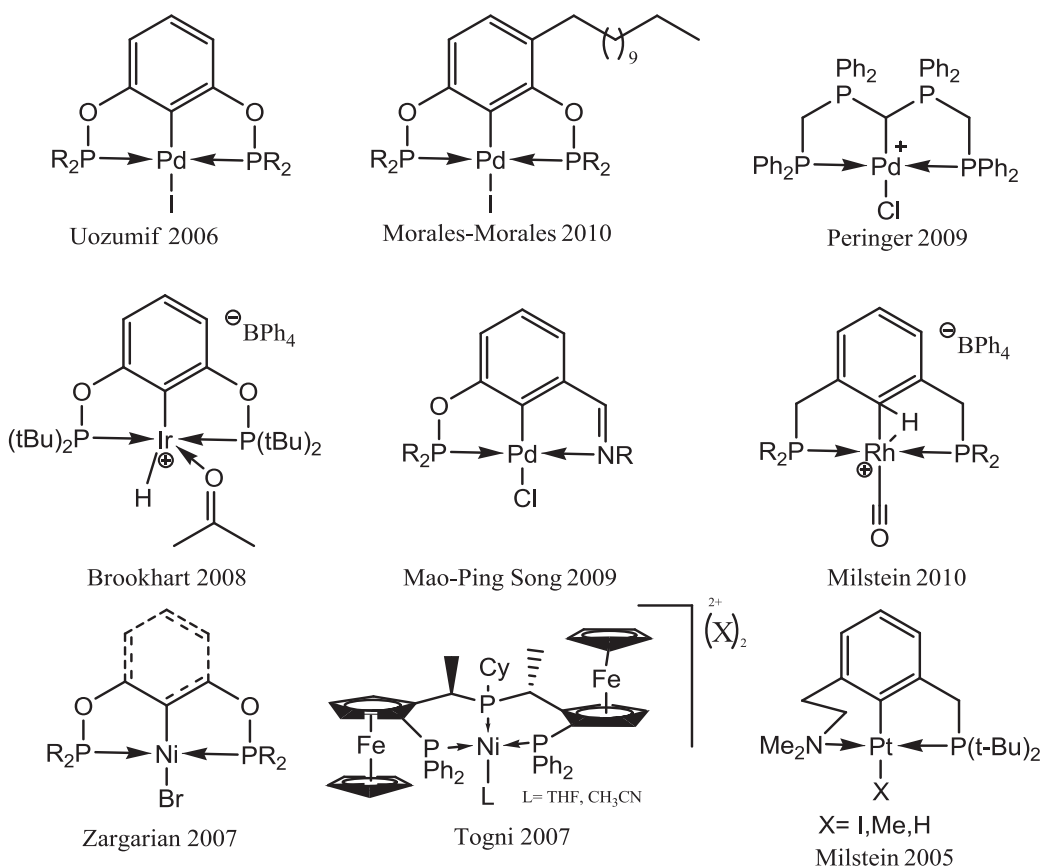
Figure 1.1 : Structure générale de complexes pinceurs

Grâce à leurs propriétés structurales et leur activité catalytique, les complexes pinceurs ont beaucoup attiré l'attention des chercheurs. En effet, sur la figure 1.1 est reportée la structure générale des complexes pinceurs. Il est important de noter que le squelette du ligand tridentate peut être aromatique ou aliphatique. Le métal est entouré par des groupes donneurs qui peuvent être des phosphines, des amines, des thiols, et même des carbènes-N-hétérocycliques.

Ainsi, dans la structure il y a toujours au moins un site de coordination libre qui peut être occupé par des ligands soit de type L, soit de type X. Généralement c'est dans ce site où il y aura coordination de substrat lors des cycles catalytiques.

La géométrie adoptée par les complexes pinceurs est plan carré et parfaitement symétrique pour les métaux de configuration électroniques d^8 au sein des complexes et pyramidale à base carrée pour ceux de configuration d^6 : ceci est dû à la disposition des groupes donneurs.

D'autre part il existe des complexes pinceurs non symétriques du point de vue de taille de métallacycles. En effet il existe des complexes pinceurs formant des cycles 5-5 et 5-6. Cette géométrie peut jouer un rôle dans les réactions catalytiques en permettant la libération d'un site de coordination supplémentaire par ouverture du métallacycle le plus grand tout en stabilisant les intermédiaires réactionnels³ (Figure 1.2).

**Figure 1.2:** Exemples de complexes pinceurs

1.2 Ligands pinceurs de type POCOP

Il existe une méthode standard de synthèse des ligands pinceurs de type POCOP, mais les différences majeures entre une voie et une autre se situent au niveau des conditions de réaction de synthèse (solvants et bases utilisés). La méthode générale consiste à ajouter la chlorophosphine ClPR_2 à un mélange de diol en présence de base (figure 1.3) en chauffant ou non.

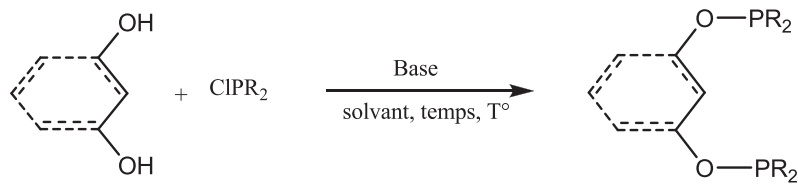


Figure 1.3 : Schéma général de synthèses de ligand POCOP

Parmi les méthodes les plus citées pour la synthèse de ligand POCOP figure celle qui a été développé par Jensen et *al*^{7a} dans les années 2000. Cette méthode consiste à ajouter la chlorodiisopropylphosphine à un mélange de base et de résorcinol dans le THF à basse température puis à laisser le mélange revenir à température ambiante (figure 1.4).

Une deuxième approche proposée par Brookhart et *al*¹⁰ repose sur l'addition de diterbutylchlorophosphine sur le résorcinol : dans ce cas la base utilisée est l'hydrure de sodium. Cette réaction nécessite un chauffage sous reflux pendant 2 h (figure 1.4). Des phosphines moins réactives ont été utilisées par Bedford et *al*¹¹ avec le résorcinol dans le THF mais sous reflux pendant 18 h (figure 1.4). Toutes ces méthodes sont très efficaces et conduisent au ligand avec de très bons rendements; ainsi tous les ligands montrent une sensibilité à l'oxydation, incluant le ligand {1,3-(Ph₂PO)₂C₆H₄} ce qui est contraire à la littérature¹¹

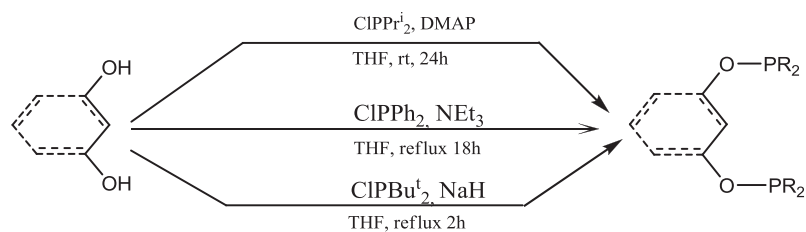


Figure 1.4 : les voies les plus citées dans la littérature de la synthèse de POCOP ligand

1.3 Les complexes pinceurs de type POCOP

La synthèse des complexes pinceurs se fait en faisant réagir le ligand POCOP avec un précurseur métallique. La plupart des travaux rapportent que la préparation de ces complexes se fait en deux étapes. La première est la coordination des groupements donneurs (dans ce cas les phosphines) au centre métallique, ce qui place le lien C-H dans une position favorable pour être activé dans une deuxième étape. Divers intermédiaires^{3a,12} des complexes du type POCOP et PCP ont été isolés et caractérisés auparavant (figure 1.5).

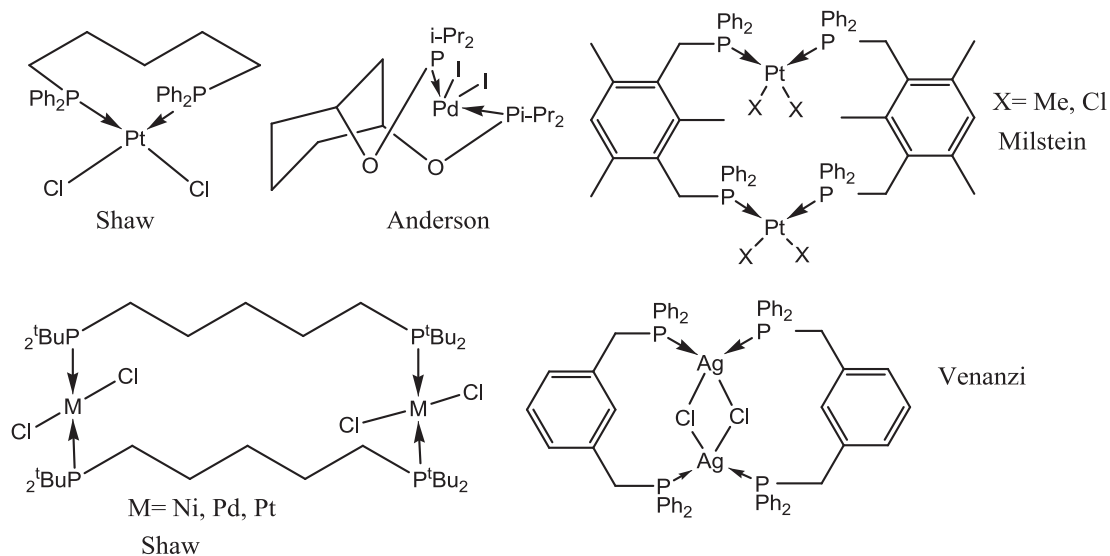


Figure 1.5 : Intermédiaires de réaction durant la formation de complexes pinceurs

En générale, les complexes pinceurs peuvent être synthétisés soit à partir de précurseur métallique à faible degré d'oxydation (D.O.), soit à fort degré d'oxydation. Parmi les métaux de faible D.O., la littérature présente des complexes d'Ir(0, + I), de Rh(0, +I), d'Os(+II), de Pd(0), de Pt(0) mais rarement de Co. Van Koten¹³, Grove¹⁴ et Ozerov¹⁵ ont démontré que la formation de complexe est due à une addition oxydante du

lien C-H ou du lien N-H dans le cas du ligand PNP après avoir pré-coordonné les phosphines au centre métallique : ce mécanisme a été bien étudié par Milstein¹⁶ qui a également montré l'addition oxydante du lien C-C.

La majorité des complexes des métaux d⁹ admettent une géométrie pyramidale à base carrée tandis que ceux avec des métaux d¹⁰ préfèrent une géométrie plane carrée (figure 1.6).

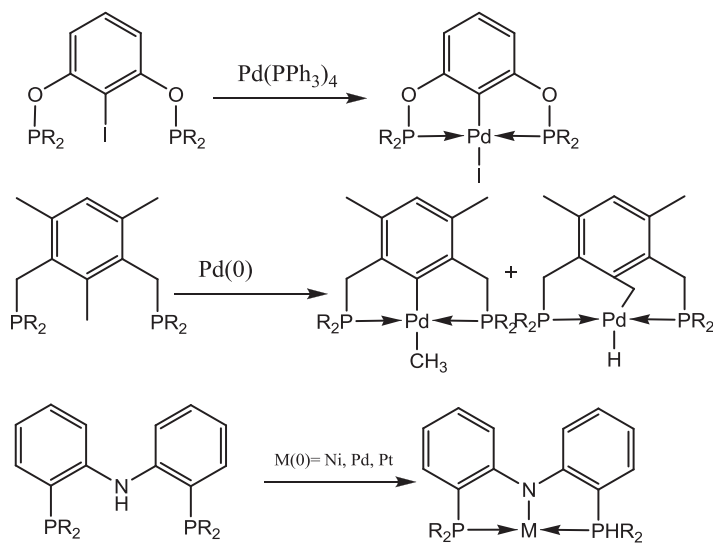


Figure 1.6 : Exemples de réactions de formation des complexes pinceurs avec des précurseurs de faible D.O.

L'utilisation de précurseurs à fort D.O. pour la synthèse des complexes pinceurs reste un défi car le mécanisme de formation des complexes est moins exploré. Dans le cas des métaux d¹⁰, beaucoup de travaux ont été publiés sur le palladium. Toutefois, le mécanisme d'activation du lien C-H d'un ligand POCOP aliphatique n'est pas encore élucidé. Dans le cas de nickel, notre groupe (travaux non publiés de Boris Vabre) a étudié la formation de complexe Ni(POC_{sp}²OP) et suggère que la formation des complexes se fait via une addition électrophile, c'est-à-dire que le précurseur métallique est pauvre en

électrons ce qui va pousser le métal à faire une interaction avec le carbone central du ligand POCOP. Cette réaction donne des meilleurs rendements en présence d'une base dans le milieu.

Un cas intéressant a été rapporté par White¹⁷ : le groupe a montré l'insertion du métal dans un lien C-X en utilisant un précurseur de Pd à fort D.O. (figure 1.7).

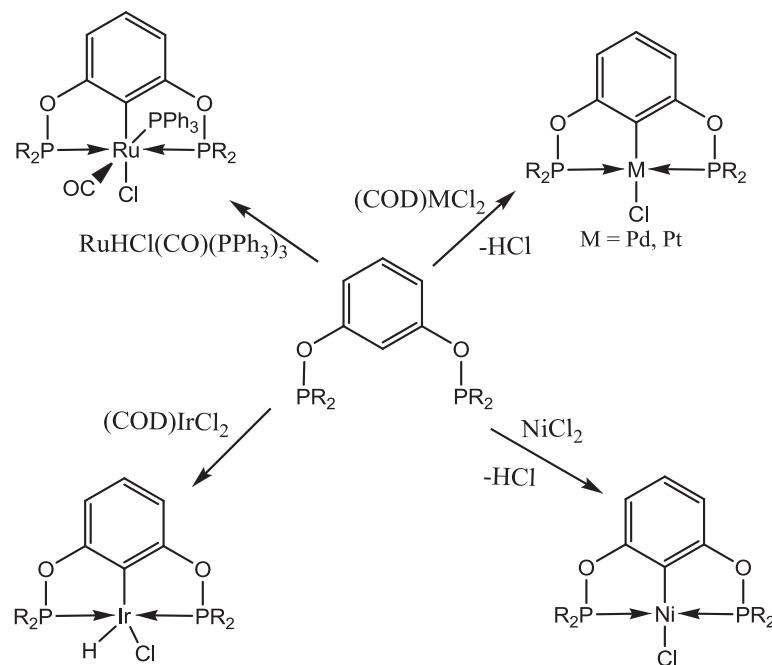


Figure 1.7: Exemples de réactions de formation des complexes pinceurs avec des précurseurs métalliques à fort D.O

1.4 Activité catalytique des complexes pinceurs de type POCOP vs PCP

Les complexes pinceurs présentent une activité catalytique intéressante dans de nombreuses réactions organiques simples, et permettent d'accéder à des composés difficiles à obtenir avec des méthodes purement organiques. Les réactions catalytiques les

plus connues des complexes pinceurs sont les réactions de couplages de Heck, de Suzuki et de Kumada, ou encore l'hydroamination des oléfines activées et l'activation de petites molécules ainsi que des liens C-C et C-H. Généralement, les métaux des deuxième et troisième périodes sont les plus utilisés. Mais à cause de leur coût élevé la recherche s'oriente maintenant vers les métaux de la première période

1.4.1 Réactions de couplages

Depuis les années 1960, les réactions de couplage ont été bien explorées. Dans cette introduction, nous nous limiterons aux réactions de Heck et Suzuki.

Le couplage de Heck est basé sur la réaction d'un iodure ou d'un bromure d'aryle avec une oléfine activée généralement par un groupe CN ou CO₂R (Figure 1.8). Le métal le plus étudié dans ce couplage est le Pd. L'introduction du système pinceur dans ce couplage (sa stabilité et sa rigidité) a été faite pour la première fois par Milstein et *al*¹⁸ pour les PCP, et plus tard par Jensen et *al*¹⁹ pour les POCOP.

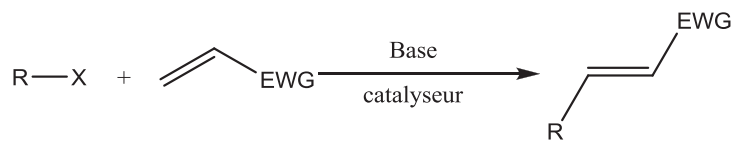


Figure 1.8 : Schéma général du couplage du Heck

Le mécanisme de couplage de Heck n'est pas encore très bien établi. Les deux mécanismes proposés diffèrent lors de la première étape. Certains chercheurs²⁰ pensent que le mécanisme peut être initié par une addition oxydante de R-X ce qui conduit à un complexe stable à 18 électrons. D'autres pensent que c'est la coordination de l'oléfine

suivie par l'addition oxydante du lien activé de l'oléfine, qui est suivie par l'élimination réductrice du HX. En tout cas, le mécanisme classique du Pd(0)/Pd(II) ne peut pas être appliqué dans ce cas, car initialement le métal est au degré d'oxydation +II.

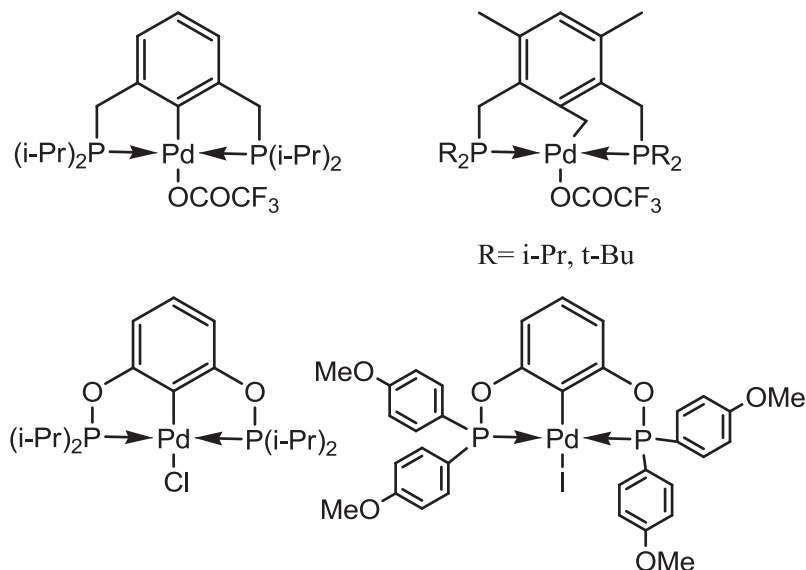


Figure 1.9 : Premiers complexes pinceurs de palladium utilisés dans le couplage de Heck

Les complexes PCP montrent une bonne activité catalytique surtout avec l'iodure d'aryle, ainsi qu'une réactivité modérée avec le bromure d'aryle. Enfin, ce système est complètement inactif avec le chlorure d'aryle. Par contre le système POCOP développé par Jensen est très efficace pour les chlorures d'aryles et même avec le styrène^{7b} comme oléfine. Le groupe de Shibasaki²¹ a étudié l'effet de changement de substituant des phosphines dans le système POCOP de palladium, et a bien montré que l'installation des groupements méthoxy sur les phosphines (figure 1.9) augmente l'activité du catalyseur. Les détails du mécanisme constituent le défi majeur pour ce type de couplage.

Suite au succès des complexes pinceurs dans la réaction de couplage de Heck, d'autres groupes ont commencé l'étude d'autres réactions de couplages. Le couplage de

Suzuki est une des meilleures méthodes pour aboutir à la formation des liaisons carbone-carbone. Ce couplage est basé sur la réaction d'un organoboronate avec un halogénure d'aryle dans des conditions basiques (figure 1.10); la différence majeure avec le couplage de Heck est l'étape de la transmétallation du palladium avec le bore ce qui n'implique pas l'activité redox du métal.

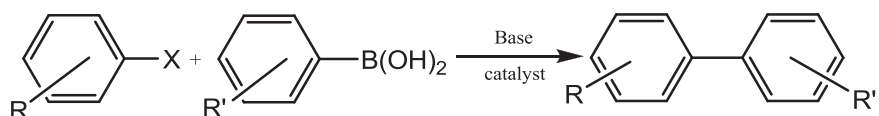


Figure 1.10 : Schéma général de la réaction de couplage de Suzuki

Des complexes POCOP de palladium ont été synthétisés et étudiés par Bedford et al²² (Figure 1.11) dans le couplage de Suzuki. Les auteurs ont bien montré que ces complexes sont stables à l'air et à haute température en solution contrairement au système PCP. Leurs études ont montré que les complexes POCOP de palladium sont bien plus actifs que les complexes PCP avec des TON pouvant aller jusqu'à 190 000, ce qui est beaucoup supérieur par rapport à leur homologue PCP.

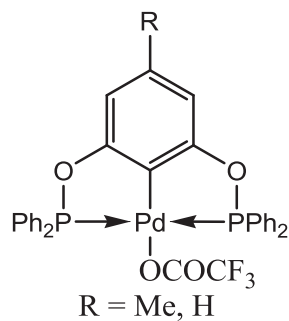


Figure 1.11 : Complexes catalyseurs de palladium utilisés en couplage de Suzuki

Le mécanisme général du couplage de Suzuki selon Milstein²³ est une addition oxydante de l'halogénure d'aryle, suivie d'une transmétallation avec l'acide boronique en

finissant par une élimination réductrice. Ce mécanisme montre les états d'oxydation +II et +IV du palladium. Nishiyama et Wendt²⁴ ont rapporté la réaction de couplage de Suzuki en utilisant des époxydes et ils ont montré que le complexe Pd (PCP) reste dans un D.O. +II durant le cycle catalytique. Le mécanisme suggère une ouverture nucléophile de cycle après la transmétallation Pd-bore (figure 1.12).

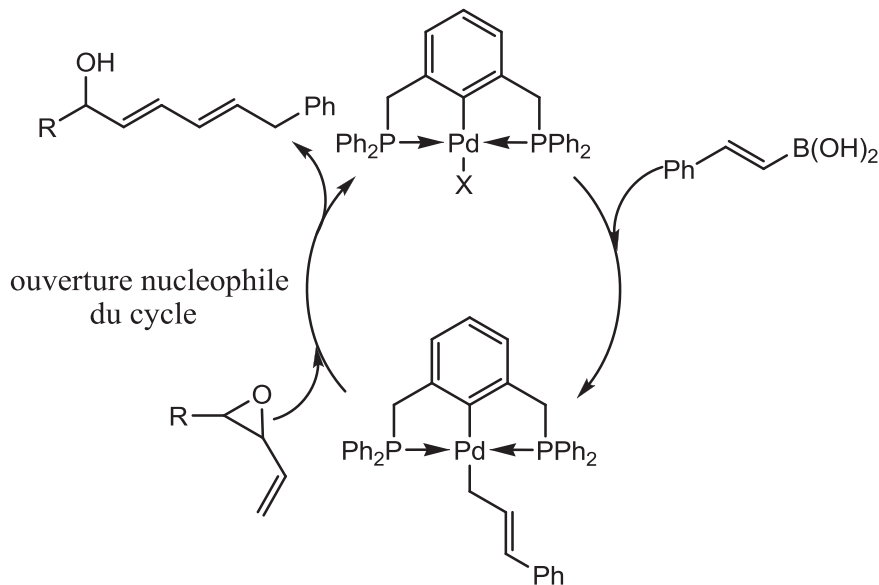


Figure 1.12 : Complex pinceur de Pd pour la réaction de couplage de Suzuki

La réactivité et la régiosélectivité dépendent des propriétés électroniques du complexe. Par exemple Van Koten a démontré que la réaction donne de très bonnes conversions en utilisant un complexe plus riche en électrons. Il existe des systèmes POCOP plus riches en électrons (figure 1.9 en bas à droite) que d'autres; c'est pourquoi nous pensons qu'utiliser les systèmes POCOP pourrait être intéressant. Les complexes pinceurs peuvent aussi catalyser d'autres types de couplages comme celui de Kumada et de Nigishi qui sont très connus dans la littérature.

1.4.2 Coordination et activation des petites molécules

Les complexes à ligand PCP de Rh, Ir et Ru ont été les espèces les plus étudiées. Les travaux sur les POCOP sont très rares. La plupart des complexes coordonnent les molécules de petite masse comme N₂, CO₂, CO, H₂ et l'éthylène. La coordination de ces molécules inhibe l'activité catalytique des complexes. Par contre d'un point de vue environnemental, la coordination des gaz toxiques peut s'avérer être une propriété intéressante.

En effet, Milstein²⁵, van Koten²⁶ et Jensen²⁷ ont présenté des complexes pinceurs de Rh(I), Ir(I) et Os(II) capables de coordonner des petites molécules. De plus les études de Milstein ont montré que les conditions favorables pour la coordination de ce genre de molécules sont de faibles coordinances et un bas D.O. du métal.

Quelques complexes PCP des métaux déjà cités ont été déjà publiés (figure 1.13) dans la dernière décennie; en effet, il existe des espèces métalliques monomériques et dimériques où des molécules d'azote sont coordonnées. L'exposition de ces complexes à d'autres gaz donne naissance à d'autres complexes en substituant le ligand diazote. Le mécanisme d'échange de ligand n'est pas associatif. Leurs études montrent aussi le rôle important des effets électroniques et stériques des phosphines qui sont à l'origine de la coordination de N₂ en protégeant ce dernier de la substitution, par exemple par l'éthylène, qui pourtant est un meilleur σ-donneur et π-accepteur que l'azote. C'est le cas quand il s'agit des groupes 'Bu sur les phosphines du complexe PCP aliphatique du rhodium, où le site de coordination est protégé par l'effet stérique de ses groupements.

Dans le même contexte les complexes PCP d'iridium et de rhodium ont été trouvés très efficaces dans la réduction de CO_2 , comme a démontré Kaska et *al.*²⁸, où le CO_2 réagit avec un complexe dihydrogène de Rh(I), qui donne les complexes hydroxo et carbonyle.

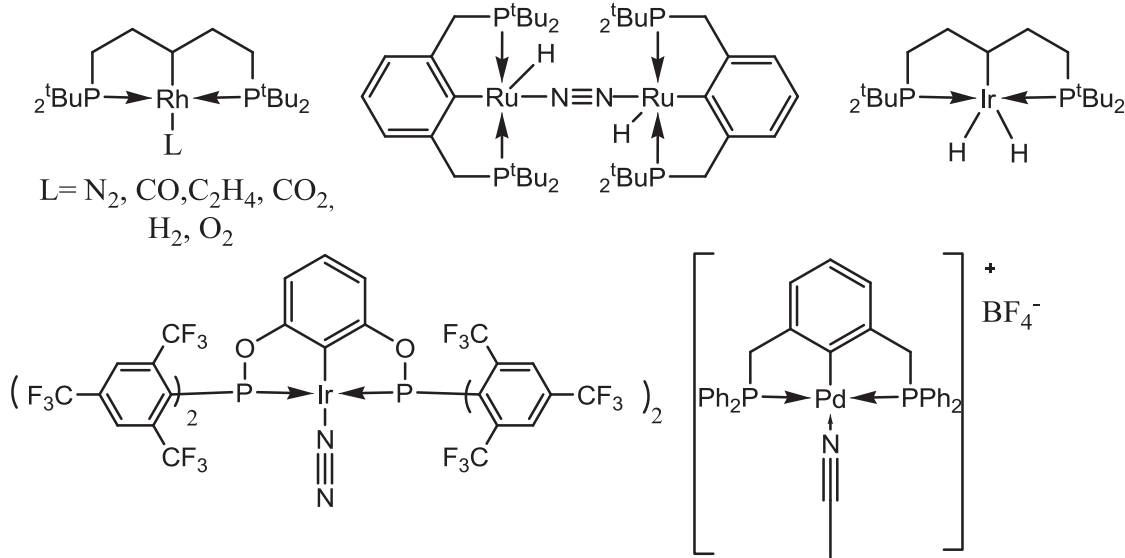


Figure 1.13 : Exemples de complexes PCP et POCOP coordonnant divers petites molécules

Récemment, Brookhart et *al.*²⁹ ont publié un complexe de type POCOP d'Ir(I) (figure 1.13) qui coordonne des molécules gazeuses de petite taille; en effet, il a observé la transformation SC-SC (``*Single Crystal to Single Crystal*``) dans laquelle il a noté un échange rapide des ligands N_2 , C_2H_2 , CO , H_2 , NH_3 et O_2 . Il a également démontré que le déplacement de ligand N_2 se fait en premier temps par coordination du nouveau ligand et non pas par la dissociation spontanée de N_2 . Selon leur étude, l'échange du ligand se fait à travers des canaux qui ont été formés par le toluène désordonné donnant ainsi l'accès à des molécules gazeuses. En fait, le complexe POCOP d'iridium (figure 1.13) sert même à

catalyser la réaction d'hydrogénéation des alcènes, en choisissant sélectivement l'éthylène versus le propylène.

1.4.3 Activation des liens C-C et C-H

L'activation du lien C-H a été intensivement étudiée, en particulier avec les complexes pinceurs à ligand PCP. Goldman et *al*³⁰ ont observé que le complexe pinceur d'iridium permet d'activer des liens vinyliques et aromatiques via une addition oxydante. Cette réaction nécessite la présence d'une oléfine sacrificielle comme un accepteur de proton, comme déjà observé dans des réactions de déshydrogénéation des alcanes avec ce complexe (figure 1.14).

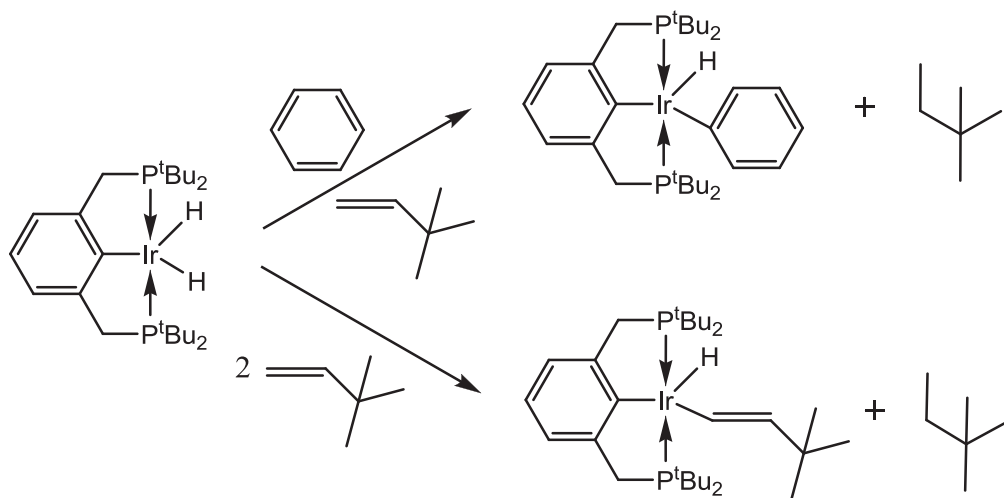


Figure 1.14 : Travaux de Goldman

Après la découverte d'interaction agostique des liens C-H et C-C avec les complexes pinceurs PCP de Rh, les chercheurs³¹ ont multiplié les efforts pour bien comprendre le mécanisme de l'activation de ces liens, où l'interaction agostique pourrait être une des étapes. Trois mécanismes ont été proposés pour l'activation du lien C-H aromatique (figure 1.15) : (i) addition oxydante avec la formation d'un complexe métal

hydrure; (ii) métallation électrophile : dans ce cas le métal est pauvre en électrons dans le complexe de départ, et fait une interaction avec le carbone suivie par d'une perte de proton; (iii) interaction agostique avec le lien C-H proposé par Gusev³², Van Koten³³ et Milstein³⁴ avec les complexes pinceurs PCP de Ru.

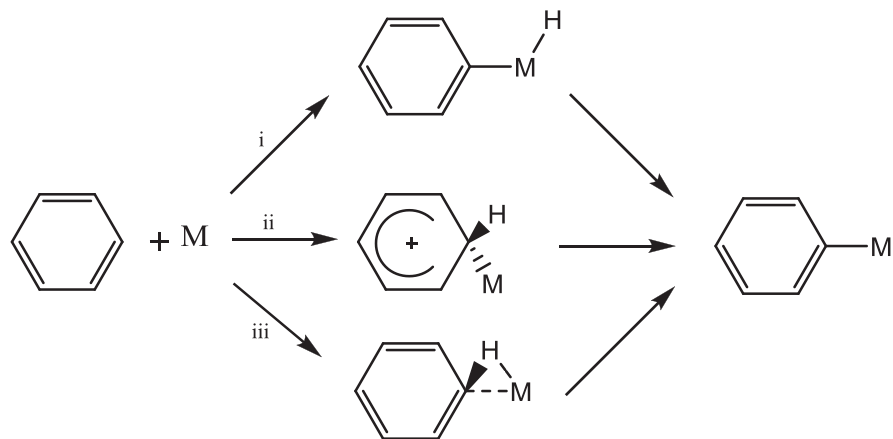
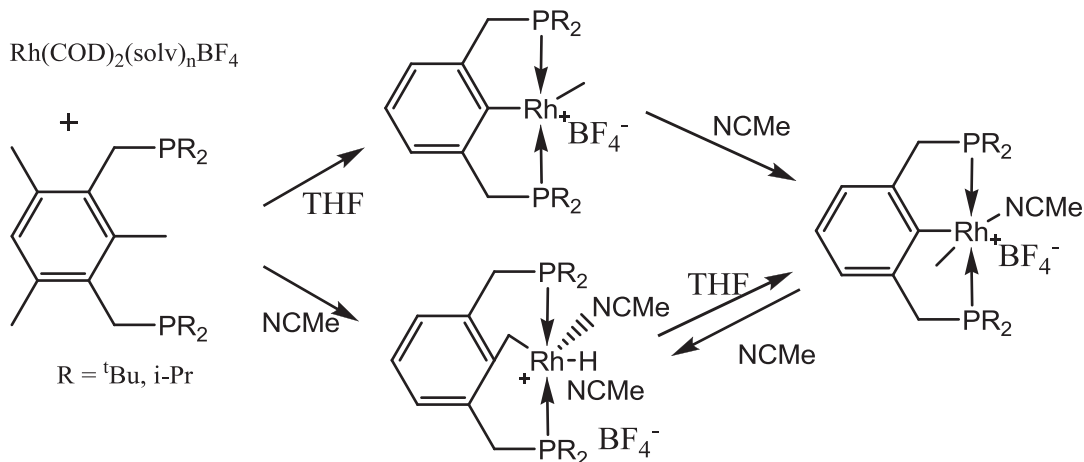


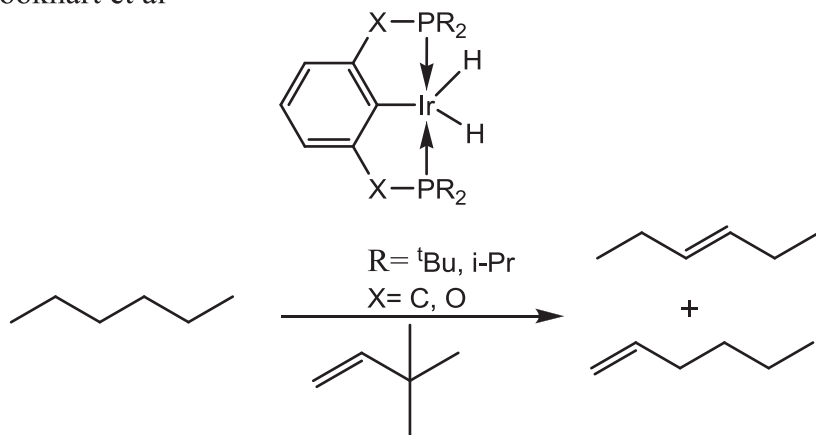
Figure 1.15: Trois mécanismes d'activation de lien C-H aromatique

En revanche, les complexes qui montrent une interaction agostique du lien C-C avec le métal sont très rares. Quelques exemples ont été présentés par Milstein³⁵ notamment avec le PCP de Rh(I) qui aboutit à une addition oxydante de ce lien et donne naissance à un complexe de Rh(III). Milstein a trouvé que l'effet donneur des phosphines a des conséquences importantes sur la cinétique de l'activation des liens C-H et C-C. En effet, l'augmentation de la densité électronique du métal central favorise l'activation de ces liens. Il a également montré que les solvants polaires favorisent l'activation du lien C-H (figure 1.16).

Milstein et al



Brookhart et al

**Figure 1.16 :** Travaux de Milstein avec PCP de Rh et de Brookhart avec ses complexes PCP et POCOP d'iridium

PCP et POCOP d'iridium

D'autre part les travaux de Brookhart³⁶ avec les deux systèmes de complexes PCP et POCOP d'iridium ont démontré que l'activation du lien C-H dans la déshydrogénéation des alcanes est plus sélective avec les PCP. Par contre, l'addition oxydante de lien C-H est plus rapide avec le POCOP. D'un point de vue stérique, selon Brookhart l'activation C-H est favorisée avec des phosphines encombrées (figure 1.16).

Szabo³⁷ a également étudié la réaction catalytique d'allylation des imines avec les complexes pinceurs de type POCOP de palladium. Dans cette réaction, le mécanisme

commence par une activation du lien C-H situé en position 3 du cyanure d'allyle ou de benzyle pour former le complexe Pd-alkyle qui va réagir avec les imines électrophiles (figure 1.17).

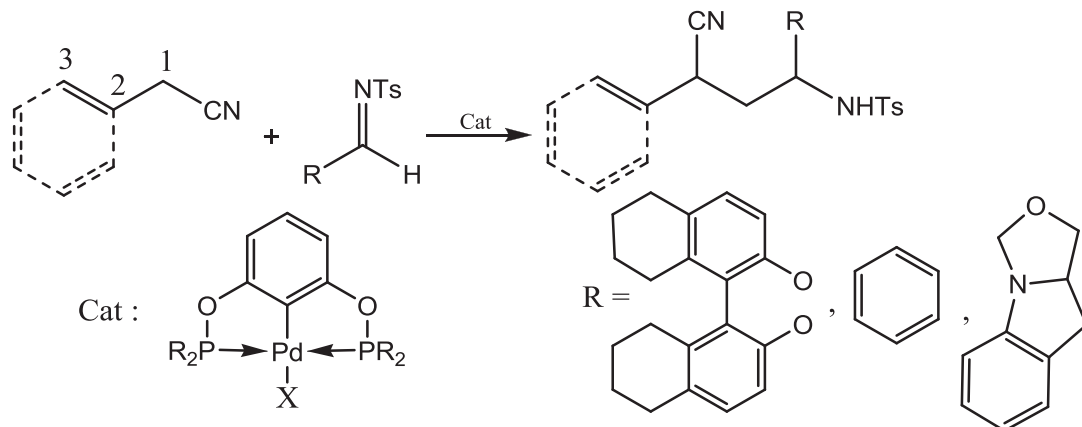


Figure 1.17: Travaux de Szabo avec ces complexes POCOP du Pd

1.4.4 Hydroamination des oléfines activées

La réaction catalytique d'hydroamination d'oléfines (figure 1.18) est une voie intéressante pour la synthèse des amines secondaires ou tertiaires. De nombreuses études ont été faites à ce sujet et montrent que le processus d'hydroamination des oléfines peut être catalysé par divers complexes de métaux du type d^9 et d^{10} (et même dans certains cas par des acides tels que HOTf^{38} ou même HCl).

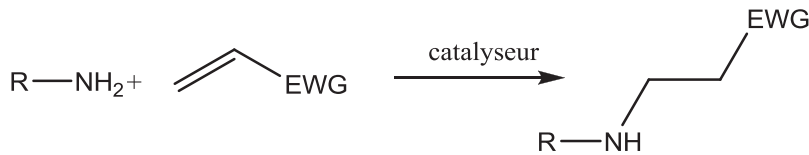


Figure 1.18 : Schéma général de la réaction d'hydroamination

Le mécanisme proposé par Milstein³⁹ de l'hydroamination des norbornylènes pour les complexes d'iridium(I) se décompose en 3 étapes : une addition oxydante du lien N-H suivie par insertion de l'oléfine dans le lien Ir-N, et finalement une élimination réductrice de C-H.

Trogler⁴⁰ a étudié cette même réaction avec du palladium(II) avec un ligand PCP aliphatique et a montré une faible activité de ce type de complexes (avec des faibles TON). Toutefois, la partie intéressante de ses résultats relève de l'observation d'un complexe cationique aliphatique PCP en coordonnant le solvant. Milstein a étudié l'homologue aromatique (figure 1.19) : ce dernier montre une meilleure activité. Ceci s'explique par le fait que les propriétés électroniques du complexe à squelette aromatique jouent un rôle important dans le mécanisme réactionnel et rendent la coordination de l'oléfine encore plus facile. En revanche, Zargarian et *al.*⁵ ont étudié des complexes cationiques du nickel avec des ligands PCP et POCOP et ont montré que le complexe POCOP est plus réactif que le complexe PCP.

La bonne activité catalytique s'explique par la même raison (propriété électroniques) : en effet, le mécanisme proposé pour le nickel et le palladium est différent de celui pour l'iridium; le mécanisme implique une coordination de l'oléfine au métal suivie par une attaque nucléophile de l'amine.

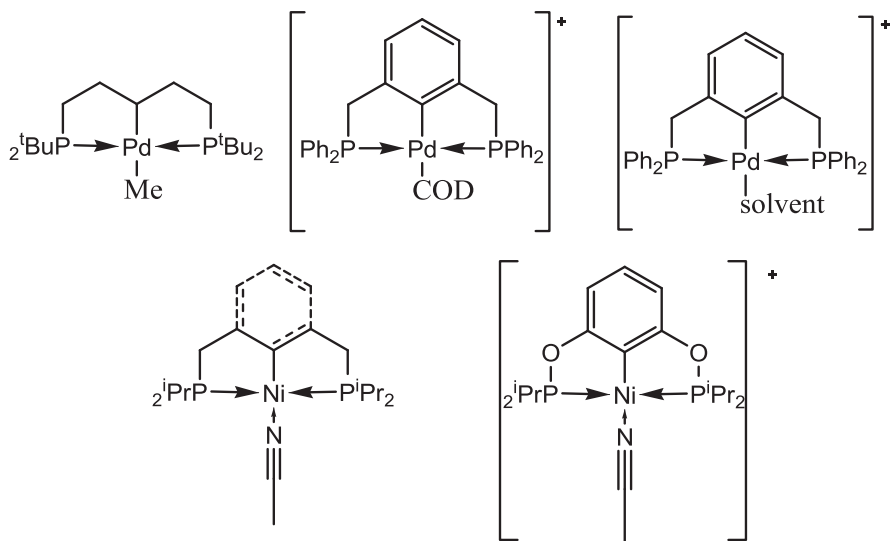


Figure 1.19 : Exemples des complexes PCP et POCOP étudiés en hydroamination

1.5 Description des travaux

Dans le deuxième chapitre nous présenterons la synthèse d'une série de complexes pinceurs de type POCOP tout en investiguant leurs propriétés structurales et électroniques. Nous allons également discuter de l'effet des phosphines sur ces propriétés. Pour cela, nous décrirons un nouveau procédé de synthèse du ligand POCOP^{Ph} , ensuite nous parlerons de synthèses de complexes en commençant par le complexe $\text{POCOP}^{\text{Ph}}\text{Ni-Br}$. Ce dernier sera le précurseur pour la synthèse des autres complexes étudiés. Différentes techniques de caractérisation, à savoir la spectroscopie (RMN, IR, UV-Vis), diffraction des rayons X et l'électrochimique (voltampérométrie cyclique) seront également l'objectif de ce chapitre. Des tests de réactivité seront également exposés. Ce chapitre sera la reproduction de manuscrit accepté à Dalton Transactions.

Dans le troisième chapitre nous décrirons la synthèse, la caractérisation structurale et électronique de nouveaux dérivés de complexes de type POCOP du nickel ainsi que leurs réactivités catalytiques. En effet, ce chapitre se concentre sur les résultats obtenus en catalyse lors de l'addition de type Michael des nucléophiles comme les amines ou alcools sur les oléfines activées, comme l'acrylonitrile. Ces réactions catalytiques sont appelées hydroamination et hydroalkoxylation. L'effet des phosphines ainsi que des additifs comme les bases et l'eau sera également étudié en détail. Malgré le fait que le mécanisme catalytique de l'hydroamination est très bien connu dans la littérature, le mécanisme de l'hydroalkoxylation avec les complexes pinceurs de type POCOP n'est pas connu jusqu'à aujourd'hui, ce qui nous conduit à l'étudier dans ce chapitre qui sera la reproduction du manuscrit soumis à *Organometallics*.

Le quatrième chapitre est une conclusion générale qui rassemble les différents résultats et résume les difficultés rencontrées. Les objectifs du projet seront discutés au vu de ces résultats, et enfin, les limitations de ce projet ainsi que quelques perspectives seront également présentées.

1.6 Références

¹ Clark, J. H. *Green Chem.* **1999**, 1.

² Johnson, J. A.; Sames, N.; Li, D. *J. Am. Chem. Soc.* **2002**, 124, 6900.

³ (a) Al-Salem, N. A.; Empsall, H. D.; Markham, R.; Shaw, B. L.; Weeks, Brian. *Dalton Trans.* **1979**, 12, 1972. (b) Moulton, C. J.; Shaw, B. L.; *Dalton Trans.* **1976**, 11, 1020.

⁴ (a) Pandarus, V.; Zargarian, D. *Organometallics* **2007**, 26, 4321. (b) Castonguay, A.; Beauchamp A. L.; Zargarian, D. *Organometallics* **2008**, 27, 5723. (d) Lefèvre, X.;

Durieux, G.; Lesturgez, S.; Zargarian, D.; *J. Mol. Catal. A.* **2010**, 335, 1. (e) Lefèvre, X.; Spasyuk, D. M.; Zargarian, D. *J. Organomet. Chem.* **2010**, 696, 864.

⁵ (a) Gossage, R. A.; van de Kuil, L. A.; van Koten, G. *Chem. Research* **1998**, 31, 423. (b) Pandarus, V.; Zargarian, D. *Chem. Com* **2007**, 9, 978. (c) Singleton, J. T. *Tetrahedron* **2003**, 59, 1837.

⁶ (a) Bergbreiter, D. E.; Osburn, P. L.; Liu, Y.-S. *J. Am. Chem. Soc.* **1999**, 121, 9531. (b) Bergbreiter, D. E.; Osburn, P. L.; Wilson, A.; Sink, E. M. *J. Am. Chem. Soc.* **2000**, 122, 9058. (c) Kiewel, K.; Liu, Y. S.; Bergbreiter, D. E.; Sulikowski, G. A. *Tetrahedron Lett.* **1999**, 40, 8945. (d) Beletskaya, I. P.; Chuchurjukin, A. V.; Dijkstra, H. P.; van Klink, G. P. M.; van Koten, G. *Tetrahedron Lett.* **2000**, 41, 1075. (e) Sjovall, S.; Wendt, O. F.; Andersson, C. *Dalton Trans.* **2002**, 1396. (f) Miyazaki, F.; Yamaguchi, K.; Shibasaki, M. *Tetrahedron Lett.* **1999**, 40, 7379. (g) Beletskaya, I. P.; Cheprakov, A. V. *Chem. Rev.* **2000**, 100, 3009. (h) Crisp, G. T. *Chem. Soc. Rev.* **1998**, 27, 427.

⁷ (a) Morales-Morales, D.; Grause, C.; Kasaoka, K.; Redon, R.; Cramer, R. E.; Jensen, C. M. *Inorg. Chim. Acta* **2000**, 958, 300. (b) Morales-Morales, D.; Redon, R.; Yung, C.; Jensen, C. M. *Chem. Commun.* **2000**, 1619. (c) Gruber, A. S.; Zim, D.; Ebeling, G.; Monteiro, A. L.; Dupont, J. *Org. Lett.* **2000**, 2, 1287. (d) Herrmann, W. A.; Bohm, V. P. W.; Reisinger, C.-P. *J. Organomet. Chem.* **1999**, 576, 23. (e) Beller, M.; Fisher, H.; Herrmann, W. A.; Ofele, K.; Bromssmer, C. *Angew. Chem. Int. Ed. Engl.* **1995**, 34, 1847.

⁸ (a) Crabtree, R. H.; Michelcic, J. M.; Quirk, J. M. *J. Am. Chem. Soc.* **1979**, 101, 7738. (b). Crabtree, R. H.; Parnell, C. P.; Uriarte, R. *Organometallics* **1987**, 6, 696. (c) Gupta, M.; Hagen, C.; Flesher, R. J.; Kaska, W. C.; Jensen, C. M. *Chem. Commun.* **1996**, 2083. (d) Wang, K.; Goldman, M. E.; Emge, T. J.; Goldman, A. S. *J. Organomet. Chem.* **1996**,

518, 55. (e) Leitner, W.; Six, C. *Chem. Ber. Recueil.* **1997**, *130*, 555. (f) Lee, D. W.; Kaska, W. C.; Jensen, C. M. *Organometallics* **1998**, *17*, 1.

⁹ (a) Dijkstra, H. P.; Slagt, M. Q.; McDonald, A.; Kruithof, C. A.; Kreiter, R.; Mills, A. M.; Lutz, M.; Spek, A. L.; Klopper, W.; van Klink, G. P. M.; van Koten, G. *Eur. J. Inorg. Chem.* **2003**, 830. (b) McDonald, A. R.; Dijkstra, H. P.; Suijkerbuijk, B. M. J. M.; van Klink, G. P. M.; van Koten, G. *Organometallics* **2009**, *28*, 4689. (c) Takenaka, K.; Uozumi, Y. *Org. Lett.* **2004**, *6*, 1833. (d) Takenaka, K.; Minakawa, M.; Uozumi, Y. *J. Am. Chem. Soc.* **2005**, *127*, 12273.

¹⁰ (a) Gottker-Schnetmann, I.; White, P.S.; Brookhart, M. *J. Am. Chem. Soc.* **2004**, *126*, 1804-1811. (b) Gottker-Schnetmann, I.; White, P.S.; Brookhart, M. *Organometallics* **2004**, *23*, 1766.

¹¹ Draper S. M.; Welch , S. L.; Bedford, R. B. *New J. Chem.* **2000**, *24*, 745.

¹² (a) Crocker, C; Errington, R. J.; Markham, R.; Moulton, C. J.; Odell, K. J.; Shaw, B. L.; *J. Am. Chem. Soc.* **1980**, *102*, 4373. (b) Sjovall, S; Johansson, M. H.; Andersson, C. ; *Eur. J. Inorg. Chem.* **2000**, *11*, 2907. (c) van der Boom, M. E.; Gozin, M.; Ben-David, Y.; Shimon, L. J. W.; Frolov, F.; Kraatz, H. B; Milstein, D. *Inorg. Chem.* **1996**, *35*, 7068. (d) Caruso, F.; Camalli, M.; Rimml, H.; Venanzi, L. M. *Inorg. Chem.* **1995**, *34*, 673.

¹³ Meijer, M. D; Ronde, N.; Vogot, D.; van Klink, G. P. M.; van Koten, G. *Organometallics* **2001**, *20*, 3993.

¹⁴ Grove, D. M.; van Koten, G.; Ubble, H. J. C.; zoet, R.; Spek, A. L. *Organometallics* **1984**, *3*, 1003.

¹⁵ Ozerov, O. V.; Guo, C.; Fan, L.; Foxman, B. M. *Organometallics* **2004**, *23*, 5573.

¹⁶ Rybtchinski, B.; Vigalok, A.; Ben David, Y. Milstein, D. *J. Am. Chem. Soc.* **1996**, *118*, 12406.

¹⁷ Canty, A. J.; Patel, J.; Skelton, B. W.; White, A. H. *J. Organomet. Chem.* **2000**, *599*, 195.

¹⁸ Ohff, M.; Ohff, A.; van der Boom, M. E.; Milstein, D. *J. Am. Chem. Soc.* **1997**, *119*, 11687.

¹⁹ (a) Morales-Morales, D.; Grause, C.; Kasaoka, K.; Redon, R.; Cramer, R. E.; Jensen, C. M. *Inorg. Chim. Acta* **2000**, *300-302*, 958. (b) Morales-Morales, D.; Redon, R.; Yung, C.; Jensen, C. M. *Chem. Commun.* **2000**, 1619.

²⁰ (a) Herrmann, W. A.; Bohm, V. P. W.; Reisinger, C.-P. *J. Organomet. Chem.* **1999**, *576*, 23. (b) Collman, J. P.; Hegedus, L. S.; Norton, J. R.; Finke, R. G. *Principles and Applications of Organometallic Chemistry*, University Science Books, 2nd ed.; **1987**. (c) Canty, A. J. *Handbook of Organopalladium Chemistry for Organic Synthesis*; John Wiley & Sons: Hoboken, NJ, **2002**.

²¹ Miyazaki, F.; Yamaguchi, K.; Shibasaki, M. *Tetrahedron Lett.* **1999**, *40*, 7379.

²² Bedford, R. B.; Draper, S. M.; Scully, P. N.; Welch, S. L. *New J. Chem.* **2000**, *24*, 745.

²³ (a) Ohff, M.; Ohff, A.; Milstein, D. *Chem. Commun.* **1999**, *4*, 357. (b) Weissman, H.; Milstein, D. *Chem. Commun.* **1999**, *18*, 1901.

²⁴ Olsson, D.; Wendt, O. F. *J. Organomet. Chem.* **2009**, *694*, 3112. (b) Takemoto, T.; Iwasa, S.; Hamada, H.; Shibatomi, K.; Kameyama, M.; Motoyama, Y.; Nishiyama, H. *Tetrahedron Lett.* **2007**, *48*, 3397.

²⁵ Cohen, R.; van der Boom, M. E.; Shimon, L. J. W.; Rozenberg, H.; Milstein, D. *J. Am. Chem. Soc.* **2000**, *122*, 7723. (b) Gandelman, M.; Vigalok, A.; Konstantinovsky, L;

Milstein, D. *J. Am. Chem. Soc.* **2000**, *122*, 9848. (c) Cohen, R.; Rybtchinski, B.; Gandelman, M.; Rozenberg, H.; Martin, J. M. L.; Milstein, D. *J. Am. Chem. Soc.* **2003**, *125*, 6532.

²⁶ Abbenhuis, R. A. T. M.; del Rio I.; Bergshoef, M. M.; Boersman, J.; Veldman, N.; Spek, A. L.; van Koten, G. *Inorg. Chem.* **1998**, *37*, 1749.

²⁷ (a) Jensen, C. M. *Chem. Commun.* **1999**, 2443. (b) Lee, D. W.; Kaska, W. C.; Jensen, C. M. *Organometallics* **1998**, *17*, 1.

²⁸ (a) Kaska, W. C.; Nemeh, S.; Shirazi, A.; Potuznik, S. *Organometallics* **1988**, *7*, 13. (b) McLoughlin, M. A.; Keder, N. L.; Harrison, W. T. A.; Flesher, R. J.; Mayer, H. A.; Kaska, W. C. *Inorg. Chem.* **1999**, *38*, 3223.

²⁹ Zheng, H.; Peter, S. W.; Brookhart, M. *Nature*, **2010**, *465*, 598.

³⁰ (a) Kanzelberger, M.; Singh, B.; Czerw, M.; Krogh-Jespersen, K.; Goldman, A. S. *J. Am. Chem. Soc.* **2000**, *122*, 11017. (b) Krogh-Jespersen, K.; Czerw, M.; Kanzelberger, M.; Goldman, A. S. *J. Chem. Inf. Comput. Sci.* **2001**, *41*, 56.

³¹ (a) Vigalok, A.; Uzan, O.; Shimon, L. J. W.; Ben-David, Y.; Martin, J. M. L.; Milstein, D. *J. Am. Chem. Soc.* **1998**, *120*, 12539. (b) Albrecht, M.; Dani, P.; Lutz, M.; Spek, A. L.; van Koten, G. *J. Am. Chem. Soc.* **2000**, *122*, 11822. (c) Dani, P.; Karlen, T.; Gossage, R. A.; Smeets, W. J. J.; Spek, A. L.; van Koten, G. *J. Am. Chem. Soc.* **1997**, *119*, 11317.

³² Gusev, D. G.; Madott, M.; Dolgushin, F. M.; Lyssenko, K. A.; Antipin, M. Y. *Organometallics* **2000**, *19*, 1734.

³³ (a) Dani, P.; Toorneman, M. A. M.; van Klink, G. P. M.; van Koten, G. *Organometallics* **2000**, *19*, 5287. (b) Steenwinkel, P.; Kolmschot, S.; Gossage, R. A.; Dani, P.; Veldman, N.; Spek, A. L.; van Koten, G. *Eur. J. Inorg. Chem.* **1998**, 477.

(c) del Rio, I.; Gossage, R. A.; Lutz, M.; Spek, A. L.; van Koten, G. *J. Organomet. Chem.* **1999**, *583*, 69.

³⁴ Vigalok, A.; Uzan, O.; Shimon, L. J. W.; Ben-David, Y.; Martin, J. M. L.; Milstein, D. *J. Am. Chem. Soc.* **1998**, *120*, 12539.

³⁵ (a) Rybtchinski, B.; Vigalok, A.; Ben-David, Y.; Milstein, D. *J. Am. Chem. Soc.* **1996**, *118*, 12406. (b) Gandelman, M.; Vigalok, A.; Shimon, L. J. W.; Milstein, D. *Organometallics* **1997**, *16*, 3981. (c) Gandelman, M.; Vigalok, A.; Konstantinovsky, L.; Milstein, D. *J. Am. Chem. Soc.* **2000**, *122*, 9848. (d) Rybtchinski, B.; Oevers, S.; Montag, M.; Vigalok, A.; Rozenberg, H.; Martin, J. M. L.; Milstein, D. *J. Am. Chem. Soc.* **2001**, *123*, 9064.

³⁶ Biswas, S.; Ahuja, R.; Ray, A.; Choliy, Y.; Krogh-Jespersen, K.; Brookhart, M.; Goldman, A. S. 17-21, **2008**, 236th ACS National Meeting, Philadelphia, PA, United States INOR-125.

³⁷ (a) Wallner, O. A.; Olsson, V. J.; Eriksson, L.; Szabo, K. *J. Inorg. Chim. Acta* **2006**, *359*, 1767. (b) Aydin, J.; Kumar, K. S.; Sayah, M. J.; Wallner, O. A.; Szabo, K. *J. Org. Chem.* **2007**, *72*, 4689.

³⁸ (a) Noyce, D. S.; DeBruin, K. E *J. Am. Chem. Soc.* **1968**, *90*, 372. (b) Fedor, L. R.; De, N. C.; Gurwara, S. K. *J. Am. Chem. Soc.* **1973**, *95*, 2905. (c) Jensen, J. L.; Carré, D. J. *J. Org. Chem.* **1974**, *39*, 2103. (d) Bell, R. P.; Preston, J.; Whitney, R. B. *J. Chem. Soc.* **1962**, *1166*. (e) Lemechko, P.; Grau, F.; Antoniotti, S.; Dunach, E. *Tet. Lett.* **2007**, *48*, 5731.

³⁹ Casalnuovo, A. L.; Calabrese, J. C.; Milstein, D. *J. Am. Chem. Soc.* **1988**, *110*, 6738.

⁴⁰ Seligson, A. L.; Troglar, W. C. *Organometallics* **1993**, *12*, 738.

**Chapitre 2: The Impact of P-Substituents on the Structures,
Spectroscopic Properties, and Reactivities of POCOP-Type
Pincer Complexes of Nickel (II)**

Abderrahmen B. Salah and Davit Zargarian*

Département de chimie, Université de Montréal, Montréal (Québec), Canada H3C 3J7

Accepté à Dalton Transactions, mars 2011

2.1 Abstract

The room temperature reaction of $\text{NiBr}_2(\text{NCCH}_3)_x$ with the pincer-type ligand $\text{POCHOP}^{\text{Ph}}$ gave the new pincer complex $(\text{POCOP}^{\text{Ph}})\text{NiBr}$ (**1**, $\text{POCOP}^{\text{Ph}} = \kappa^P, \kappa^C, \kappa^P$ -2,6-{ Ph_2PO }₂ C_6H_3). Complex **1** reacts with AgX to give the analogous Ni-X derivatives ($\text{X} = \text{CN}$, **2**; OSO_2CF_3 , **3**; OC(O)CH_3 , **4**; ONO_2 , **5**), whereas complex **3** reacts with phenylacetylene and NEt_3 to give the Ni-CCPh derivative **6**. On the other hand, reaction of **1** or **3** with RLi or RMgI did not afford the desired Ni-R derivatives, giving instead the corresponding iodo and hydroxo derivatives. Complexes **1-6** have been characterized by NMR, IR, and UV-Vis spectroscopy and X-ray crystallography. The solid state structural and IR data indicate that Ni-C_{sp} interaction is dominated by ligand-to-metal σ -donation in **2** and **6**. Cyclic voltammetry measurements indicate that complexes **3** and **4** display reversible redox behaviour ($\text{Ni}^{\text{II}}/\text{Ni}^{\text{III}}$); comparison of the $E^0_{1/2}$ values for these complexes and their $\text{POCOP}^{i\text{-Pr}}$ analogues shows that both the X ligands and the *P*-substituent have a considerable impact on the ease of oxidation in this family of complexes.

Keywords: nickel pincer complexes, synthesis, UV-vis spectra, cyclic voltammetry, Kumada coupling, homocoupling and cross-coupling

2.2 Introduction

The well-documented capacity of pincer complexes¹ to act as efficient catalysts for diverse transformations² and their potential applications as advanced materials³ have attracted intense scrutiny from many researchers. The meridional chelation of metal atoms by pincer ligands generally results in strong M-ligand bonds and fairly robust structures, both of which confer considerable thermal stability to pincer complexes. Moreover, the chemical reactivities and physical properties of these complexes can be modulated by systematic variations of donor atoms and the steric and electronic properties of pincer ligand substituents.⁴

Our group has studied the chemistry of organonickel complexes based on PCP-POCOP-, and POCN-type pincer ligands.⁵ In the case of nickel complexes based on PCP- and POCN-type ligands, we have explored the influence of *P*- and *N*-substituents on structures and reactivities (Figure 2.1). In contrast, our investigations of the corresponding POCOP-type complexes have been limited to the OP(*i*-Pr)₂ analogues only, but different analogues have been scrutinized by other groups. For instance, Guan's group has reported on the chemistry of (POCOP^t-Bu)₂NiX (POCOP^t-Bu = $\kappa^P, \kappa^C, \kappa^P$ -2,6-{*t*-Bu₂PO}₂C₆H₃),⁶ and Morales-Morales' group has described the structure and activities of (POCOP^{Ph})NiCl in catalytic coupling of PhS-SPh and aryl halides.⁷

As a follow-up to our previous studies on the catalytic activities of (POCOP^{*i*-Pr})NiX in alcoholysis and aminolysis of acrylonitrile derivatives (Michael-type hydroamination and hydroalkoxylation,^{5d,f,g,j,l,m} Kharasch addition,^{5f,g} and Kumada-Corriu coupling,^{5j}) we sought to prepare new series of POCOP-type complexes bearing different *P*-substituents and explore their structures and reactivities. This report describes the synthesis and

characterization of the complexes $(\text{POCOP}^{\text{Ph}})\text{NiX}$ (X : Br, **1**; CN, **2**; OSO_2CF_3 , **3**; OC(O)CH_2 , **4**; ONO_2 , **5**; $\text{C}\equiv\text{CPh}$, **6**). All complexes were characterized by UV-Vis, IR, and NMR spectroscopy, single crystal X-ray diffraction studies, and cyclic voltammetry studies were conducted to determine the effect of P -substituents and X ligands on redox potentials, as described below.

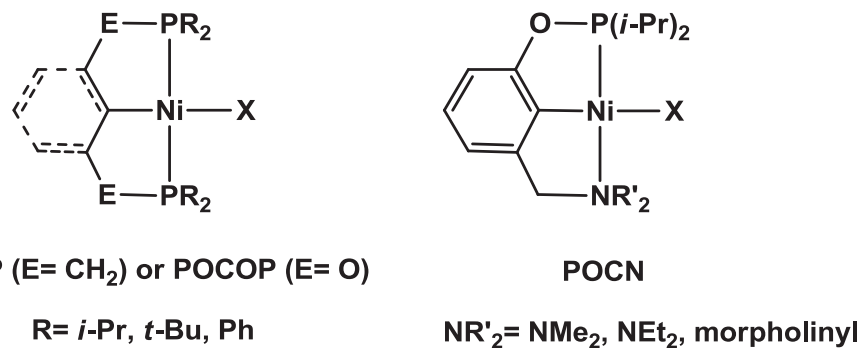


Figure 2.1: PCP, POCOP and POCN pincer type complexes of Nickel

2.3 Results and Discussion

2.3.1. Synthesis.

The previously reported procedure for preparing the POCOP-type ligand 1,3-{Ph₂PO}₂C₆H₄, **a**, required refluxing a mixture of resorcinol, ClPPh₂, and NEt₃ in toluene for 18 h, followed by filtration of the reaction mixture through a column of celite.⁸ Our optimization studies showed, however, that comparable results can be obtained under less demanding conditions (THF, r.t., 30 min), and the desired product can be isolated conveniently by evaporation of the reaction mixture, extraction of the residual white solid into hexane, followed by drying. Ligand **a** was thus obtained in 86% yield as a colorless

oil that solidifies over a few min (Figure 2.2). It is worth noting that while ligand **a** has been described in the literature as being stable to ambient atmosphere,⁹ in our experience it is fairly sensitive to hydrolysis and should be protected from ambient atmosphere.

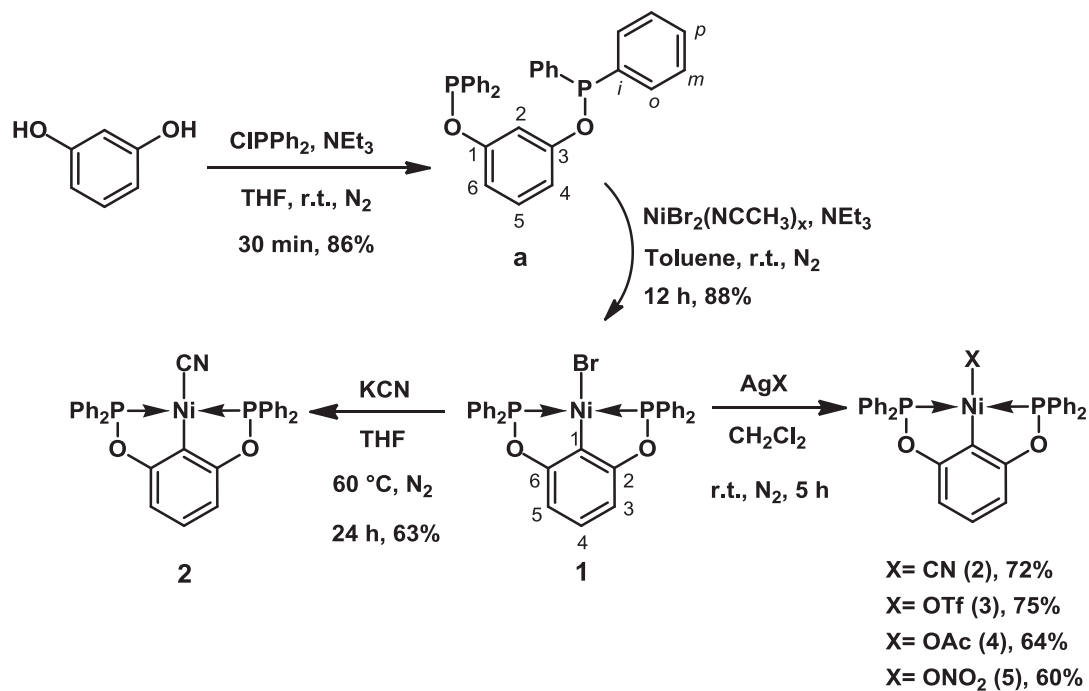


Figure 2.2: Synthesis of ligand and complexes

Reacting ligand **a** with NiBr₂(NCCH₃)_x in the presence of NEt₃ (toluene, 12 h, r.t.) gave complex **1** in 88 % yield (Figure 2.2). The base, which serves to quench the HBr generated during the cyclometallation step, is needed for ensuring a good yield. Complex **1** then served as a precursor to Ni-X derivatives via ambient temperature reactions with AgX that proceeded to give the cyano, triflate, acetate, and nitrate analogues. The cyano derivative **2** could also be obtained from KCN, but this approach required extensive heating and gave a lower yield (60 °C for 24 h, 63%, Figure 2.2). We also succeeded in preparing the alkynyl derivative (POCOP^{Ph})Ni(C≡CPh), **6**, but the Ni-Br precursor proved too inert for this synthesis and so the triflate derivative, complex **3**, had to be used as precursor (Figure 2.3).

In contrast to the successful isolation of the alkynyl derivative **6**, we did not succeed in the preparation of the corresponding alkyl derivatives, regardless of whether we used the Ni-Br or Ni-triflate precursors. Thus, attempts at methylation of **3** gave instead the Ni-I (**7**) and Ni-OH (**8**) derivatives (Figure 2.3), which presumably arise from a Schlenk equilibrium with IMgMe/XMgI (**7**) or hydrolysis (**8**). To be sure, the alkyl derivatives do form during the course of the reaction, but their isolation proved difficult. For instance, monitoring the reactions of **3** with MeLi, MeMgX, or *i*-BuMgX by NMR showed evidence of formation of the desired Ni-R species. The ^1H NMR spectrum of the mixture of **1** and MeMgI, for example, displayed a triplet at 0.47 ppm ($^3J_{\text{P}-\text{H}} = 8$ Hz) while its $^{31}\text{P}\{\text{H}\}$ NMR spectrum showed a peak downfield of the corresponding signal for **1** (153 ppm); these observations are consistent with the formation of the anticipated Ni-Me derivative.¹⁰ However, the product isolated after work-up in all cases proved to be the corresponding iodo, bromo or hydroxo derivatives. It should be noted that following the same protocol and using the same batches of RLi/RMgX and solvent allowed us to isolate the previously reported alkyl derivative (POCOP^{*i*-Pr})NiMe,^{5g} which suggests that the analogous (POCOP^{Ph})Ni(alkyl) complexes are inherently less robust.

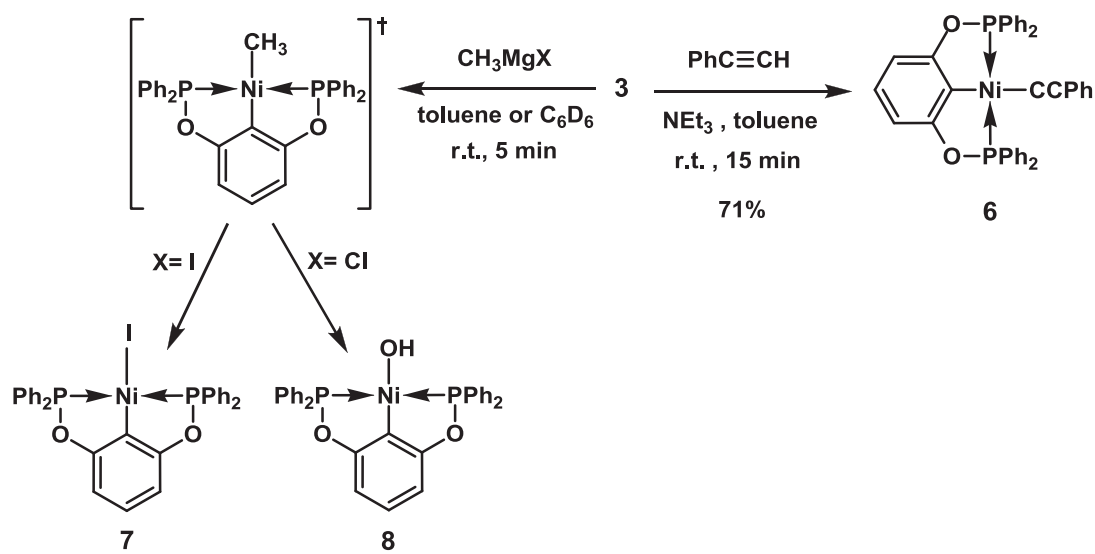


Figure 2.3: Attempts of synthesis of alkyl derivetives

The new complexes showed unusually high thermal stabilities, some decomposing as solids at ca. 209 ± 2 °C (4) or 218 ± 2 °C (3 and 5) while the rest did not melt or decompose up to 220 °C. The bromo, cyano, acetate, and phenylacetylide derivatives are air-stable indefinitely in the solid state. These derivatives also appear to be fairly air-stable in CH_2Cl_2 and toluene solutions over minutes, but addition of a small amount of water to these solutions accelerated the decomposition (presumably by hydrolysis of the ligand), especially in the case of the acetate derivative. The triflate and nitrate derivatives, on the other hand, were found to decompose in ambient air, both in solution and in the solid state.

2.3.2. Spectroscopic characterization.

The Ni-Br complex 1 displays a ${}^{31}\text{P}\{{}^1\text{H}\}$ NMR signal at δ 146, downfield of the signals for ligand **a** (112) and the Ni-Cl analogue (142);⁹ the corresponding signals for

the other Ni-X derivatives appeared at δ 135 (Ni-OAc and Ni-OH), 141 (Ni-OTf), 142 (Ni-ONO₂), 147 (Ni-I), and 154 (Ni-CN and Ni-CCPh). Evidently, the ³¹P chemical shifts for this family of complexes appear to correlate with the electronegativity of the ligating atom (or its polarizability): Ni-O < Ni-Cl < Ni-Br < Ni-I < Ni-C. The ¹⁹F{¹H} NMR of complex **3** displayed a singlet at ca. δ -78.

The proton and ¹³C nuclei of the central aromatic moiety in the title complexes were readily identified from the characteristic signals found in the corresponding spectra: doublets for H3/H5, triplets for H4, virtual triplets for C2/C6 and C3/C5, triplets for C1 and singlets for C4; the protons of the *P*-Ph substituents did not show distinct signals, but distinct virtual triplets were detected for their *ipso* and *ortho* ¹³C nuclei. (N.B. The atom labeling scheme is shown in Figure 2.2; tabulated ¹H and ¹³C NMR data are provided in Supporting Information.) The pair-wise equivalence of the symmetry-related nuclei (H3/H5, C3/C5; C2/C6; *o*-H and *o*-C; *m*-H and *m*-C; *p*-H and *p*-C; and *i*-C) confirm that these complexes possess C_{2v} symmetry in solution. As anticipated, the quaternary carbons are represented by very weak signals, especially those that are coupled to the P nuclei. For instance, weak triplets were observed for Ni-CCPh at ca. δ 129 (²J_{P-C}= 4 Hz) and Ni-CN at ca. δ 133 (²J_{P-C}= 4 Hz); the latter resonance can be compared to the corresponding signal for (POCOP^{*i*-Pr})Ni(CN): δ 133.7 (²J_{P-C}= 19 Hz)⁵ⁿ.

The IR spectra showed some of the absorptions characteristic of the X ligands, including ν (C≡N) in **2** (2116 cm⁻¹), ν (S=O) and ν (C-F) in **3** (1020 and 1105 cm⁻¹), ν (C=O) in **4** (1581 cm⁻¹), ν (N=O) in **5** (1362 cm⁻¹), and ν (C≡C) in **6** (2105 cm⁻¹). Comparison of the IR data for complexes **2** and **6** to those of related compounds (Table 1) offer an insight into the nature of Ni-C_{sp} interactions in these complexes. Thus, we find

that the $\nu(\text{C}\equiv\text{N})$ value of 2116 cm^{-1} in **2** is similar to the corresponding frequency in $(\text{POCOP}^{i\text{-Pr}})\text{Ni}(\text{CN})$ (2109 cm^{-1})⁵ⁿ and intermediate between that of organic nitriles (e.g., 2253 cm^{-1} in MeCN) and the corresponding frequencies in the alkali salts (e.g., 2070 cm^{-1} in KCN and 2080 cm^{-1} in NaCN). Similarly, the $\nu(\text{C}\equiv\text{C})$ value of 2105 cm^{-1} in **6** is very close to that of phenylacetylene (2115 cm^{-1}) and greater than the corresponding absorption frequencies in $\text{MC}\equiv\text{CPh}$ (2030 cm^{-1} for M= Li; 2005 cm^{-1} for M= Na; 1998 cm^{-1} for M= K). We conclude that the Ni-C interactions in these complexes comprise contributions from covalent and electrostatic attractions. That $\text{Ni}\rightarrow\text{C}$ π -backdonation does not make important contributions to the Ni-C interaction in complexes **2** and **6** is implied from the observation that $\nu(\text{C}\equiv\text{N})$ and $\nu(\text{C}\equiv\text{C})$ values in these d⁸ compounds are similar to the corresponding frequencies in the d⁰ complexes listed in Table 2.1.

Table 2.1. IR data for complexes 2 and 6 and related compounds

Complex	$\nu(\text{C}\equiv\text{N})$ or $\nu(\text{C}\equiv\text{C})$ (cm ⁻¹)	Reference
(POCOP ^{Ph})Ni(CN) (2)	2116	This work
MeCN	2253	This work
KCN	2070	¹¹
NaCN	2080	¹¹
(POCOP ^{i-Pr})Ni(CN)	2109	⁵ⁿ
Cp ₃ Zr(CN)	2130	¹²
[Cp ₂ Ti(CN)] ₂ (μ-O)	2123	¹³
(POCOP ^{Ph})Ni(CCPh) (6)	2105	This work
HCCPh	2115	This work
KCCPh	1998	¹⁴
NaCCPh	2005	¹⁴
LiCCPh	2030	¹⁴
Cp ₂ Ti(C≡CPh) ₂	2065	¹⁵
Cp ₂ Zr(C≡CPh) ₂	2075	¹⁶
Cp ₂ Hf(C≡CPh) ₂	2098	¹⁶
Cp ₂ Zr(C≡CPh)Cl	2098	¹⁶

The lowest energy absorption band in the UV-Vis spectra of this family of complexes can provide information about the size of the HOMO-LUMO gap in each case. Inspection of their UV spectra showed a significantly lower energy band for complex **1** compared to its $P(i\text{-Pr})_2$ analogue (Figure 2.4). Similar observations were made for the triflate and acetate derivatives **3** and **4** and their $P(i\text{-Pr})_2$ counterparts, but in the case of these derivatives the impact of the *P*-substituent is less dramatic (Table 2.2). We conclude that the more nucleophilic phosphinite moiety $\text{OP}(i\text{-Pr})_2$ gives rise to larger HOMO-LUMO gaps. Within the family of complexes $(\text{POCOP}^{\text{Ph}})\text{NiX}$, the absorption frequency for the lowest energy band also varies as a function of the X ligand: CN > CCPH > ONO₂ > OAc > OTf > Br. In accord with this observation, the Ni-CN derivative is a faint yellow in the solid state, giving nearly colorless solutions, whereas the Ni-Br complex is deep red.

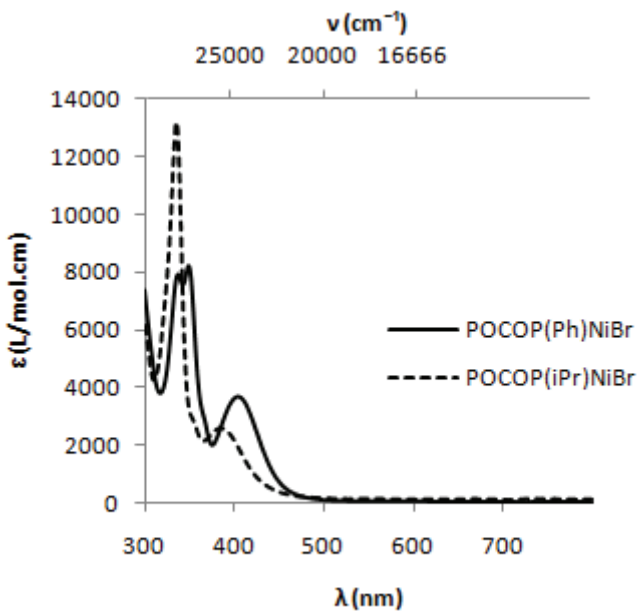


Figure 2.4. UV-Vis spectra for complexes **1** and $(\text{POCOP}^{i\text{-Pr}})\text{NiBr}$, recorded using CH_2Cl_2 solutions (1.11×10^{-4} M).

Table 2.2. Lowest energy electronic transitions for the complexes (POCOP)^RNiX

(POCOP ^R)NiX		λ (nm)	ν (cm ⁻¹)	ε (L.mol ⁻¹ .cm ⁻¹)
X	R			
Br	Ph	415	24 100	3560
	<i>i</i> -Pr	392	25 500	2370
OTf	Ph	396	25 300	5008
	<i>i</i> -Pr	388	25 800	1796
OAc	Ph	393	25 400	2059
	<i>i</i> -Pr	381	26 200	2804
ONO ₂	Ph	388	25 800	4694
C≡CPh	Ph	385	26 000	5248
C≡N	Ph	372	26 900	1354

2.3.3. Solid state characterization.

Single crystals were grown for all complexes and subjected to crystallography in order to determine their solid state structures. The structures of the iodo and hydroxo derivatives have been reported earlier.¹⁷ All the structures were refined to a high degree of confidence in spite of the disorders that were found in the triflate derivative **3** (due to the rotation of the CF₃ group about the S-C bond), the acetate derivative **4** and the nitrate derivative **5** (due to rotation about the Ni-O axes; crystal also severely twinned), and the alkynyl derivative **6** (due to displacement of the CCP_h group). Crystal and data collection details for complexes **1-6** are presented in Table 2.3, selected structural parameters are listed in Table 2.4, and ORTEP diagrams are shown in Figure 2.5

Table 2.3. Crystal Data Collection and Refinement Parameters for Complexes 1-6.

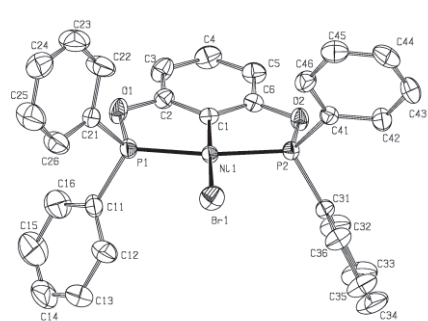
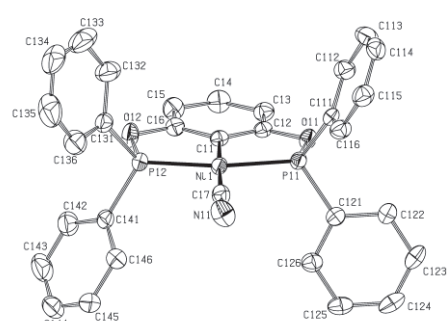
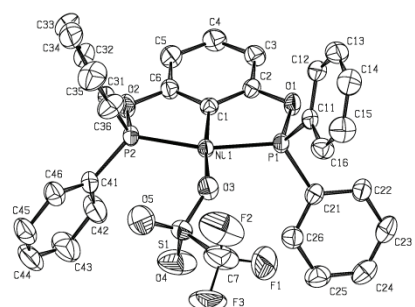
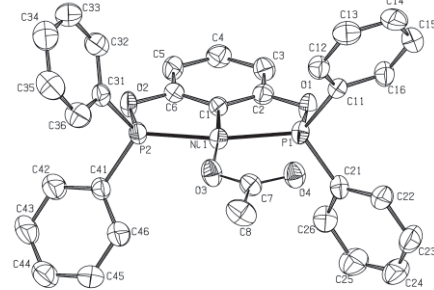
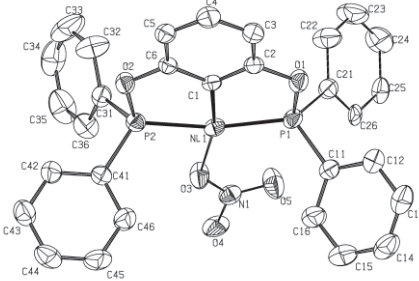
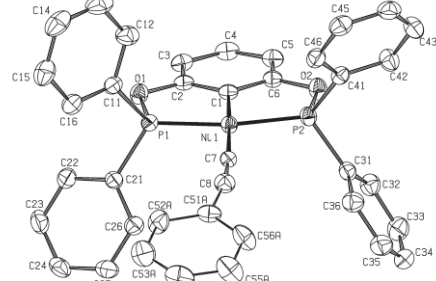
	1	2	3	4	5	6
Chem. Formula	C ₃₀ H ₂₃ BrO ₂ P ₂ Ni	C ₃₁ H ₂₃ NO ₂ P ₂ Ni	C ₃₁ H ₂₃ O ₅ F ₃ P ₂ SNi	C ₃₂ H ₂₆ O ₄ P ₂ Ni	C ₃₀ H ₂₃ NO ₅ P ₂ Ni	C ₃₈ H ₂₈ O ₂ P ₂ Ni
Cryst. colour	Yellow	Yellow	Yellow	Yellow	Yellow	Yellow
Fw	616.04	562.15	685.2	595.18	598.14	637.25
T (K)	200(2)	150(2)	200(2)	150(2)	200(2)	150(2)
λ (Å)	0.71073	1.54178	0.71073	1.54178	0.71073	0.71073
Space Group	P2 ₁ /c	P2 ₁ /c	P $\bar{1}$	P $\bar{1}$	P2 ₁ /c	Pna2 ₁
a (Å)	15.058(3)	28.9769(4)	8.8415(13)	8.7434(3)	16.548(2)	19.587(1)
b (Å)	10.004(2)	10.4287(2)	12.5965(19)	9.9182(4)	11.3201(15)	14.6211(7)
c (Å)	17.392(4)	17.1986(3)	13.563(2)	16.1169(6)	16.655(2)	10.5024(5)
α (deg)	90	90	95.864(2)	92.699(2)	90	90
β (deg)	90.397(3)	90.305(10)	91.903(2)	97.355(2)	119.769(2)	90
γ (deg)	90	90	92.098(2)	98.210(2)	90	90
Z	4	8	2	2	4	4
V(Å ³)	2619.7(9)	5197.20(15)	1500.6(4)	1368.89(9)	2708.3(6)	3007.7(3)
ρ _{calcd}	1.562	1.437	1.516	1.444	1.467	1.407
μ (cm ⁻¹)	24.15	24.79	8.81	24.30	8.76	7.86
θ range (deg)	1.35-27.50	1.52-72.71	1.51-27.49	4.51-69.26	1.42-27.51	1.74-31.54
N° of all ref.	53391	70201	30583	19890	6235	74930
N° of uniq. ref.	6016	9992	6898	4937	6235	9574
Flack Parameter	-	-	-	-	-	0.002(6)
Rint	0.035	0.068	0.037	0.1134	0	0.045
R1 ^a [I>2σ]	0.0384	0.0475	0.0348	0.0646	0.0319	0.0283
wR2 ^b [I>2σ]	0.1248	0.1198	0.0892	0.1772	0.0771	0.0575
R1[all data]	0.0479	0.0660	0.0472	0.0738	0.0369	0.0378

WR2[all data]	0.1296	0.1271	0.0940	0.1866	0.0800	0.0600
GOF	1.086	0.937	1.024	1.065	1.060	0.955
N° of restraints	0	0	51	1	1	173

^a R₁=Σ(||F_o|-|F_c|)/Σ|F_o|^bwR₂= {Σ[w(F_o²-F_c²)²]/Σ[w(F_o²)²]}½**Table 2.4. Selected Bond Distances (Å) and Angles (deg) for Complexes 1-6.**

	1	2	3	4	5	6
Ni1-C1	1.874(3)	1.891(3)	1.870(2)	1.866(3)	1.875(2)	1.893(2)
Ni1-P1	2.1550 (9)	2.1444(8)	2.1667(6)	2.1876(9)	2.1797(7)	2.1343(4)
Ni1-P2	2.1544 (9)	2.1455(8)	2.1860(6)	2.1612(9)	2.1755(7)	2.1283(4)
Ni1-X	2.3002 (6)	1.877(3)	1.934(2)	1.886(3)	1.937(3)	1.878(2)
C1-Ni1-P1	82.3(1)	81.87(9)	82.02 (6)	83.4(1)	82.41(7)	82.56(5)
C1-Ni1-P2	82.3(1)	82.05(9)	81.61 (6)	81.7(1)	81.73(7)	82.03(5)
C1-Ni1-X	177.62 (9)	177.9(1)	173.63 (7)	174.0(1)	165.0(1)	177.72(7)
P1-Ni1-P2	164.39 (4)	163.92(3)	163.24 (2)	165.10(4)	164.14(3)	164.58(2)
P1-Ni1-X	98.39 (3)	96.64 (9)	92.74 (5)	102.3(1)	112.16(8)	96.01(5)
P2-Ni1-X	97.16 (3)	99.45 (9)	103.35 (5)	92.6(1)	83.64(8)	99.40(5)

Figure 2.5. ORTEP diagrams for complexes **1-6**. Thermal ellipsoids are set at the 50% probability level for all complexes. Calculated hydrogen atoms and disordered molecules are omitted for clarity.

1**2****3****4****5****6**

The overall geometry around the Ni in all complexes is a somewhat distorted square plane. This distortion arises primarily from the bite angle of the POCOP ligand that results in a tightening of all C1-Ni-P and P-Ni-P angles (82-83° and 163-165°, respectively), whereas most C1-Ni-X angles are fairly linear (174-178°) except the C1-Ni-O angle in complex **5** (165°). Nearly linear angles were observed for the Ni-C-N moiety in **2** (178°) and the Ni-C-C moiety in **6** (175°), whereas some deviation from linearity was found in the C-C-C moiety in the alkynyl derivative (168°).

The S=O distances in **3** are ca. 1.402(2) and 1.411(2) Å, while the unique S-O distance is 1.452(2) Å. The longest Ni-C1 distances are found in **2** and **6**, 1.89 Å vs. 1.87-1.88 Å for the remaining derivatives, which is consistent with the greater trans influence of the CN and CC-Ph ligands. The Ni-C_{sp} distance in the alkynyl derivative is fairly short (1.88 Å), as expected, but the Ni-O distance is surprisingly short in the acetate derivative compared to the triflate and nitrate analogues (1.89 vs. 1.93 Å), implying perhaps a much stronger Ni-X interaction for the acetate ligand. The shortest Ni-P bonds are seen in **6** (~2.13 Å) and the longest in **3**, **4** and **5** (2.16-2.19 Å), the derivatives with the very polarized Ni-O bonds.

A comparison of Ni-P_{av} distances in the analogous complexes (POCOP^R)NiX for which structural data are available is instructive as it allows us to ascertain the influence of *P*-substituents on Ni-P distances. Thus, we find that Ni-P_{av} distances are virtually identical in the two bromo derivatives (2.1554(8) for R= *i*-Pr^{5f} vs. 2.1547(9) Å for R= Ph), but somewhat different in the cyano complexes (2.1450(8) for R= Ph vs. 2.1555(5) Å for R= *i*-Pr⁵ⁿ). The slightly shorter Ni-P_{av} distances in (POCOP^{Ph})Ni(CN) might be attributed to the smaller steric bulk of the OPPh₂ vs. OP(*i*-Pr)₂ moieties.

Comparing other structural parameters for the complexes (POCOP^R)Ni(CN) (R=Ph and *i*-Pr) reveals that the PPh₂ analogue has a much shorter Ni-C_{sp} distance (1.88 vs. 1.94 Å) and a much longer C≡N distance (1.15 vs. 1.06 Å).⁵ⁿ Moreover, the C≡N distance in **2** is similar to the corresponding distances in Ti(CN)₄ (1.165(2) Å),¹⁸ and the C≡C distance in **6** is comparable to that in Cp₂Zr(CC-Ph)₂ (1.204(2) vs. 1.206(3) and 1.211(3) Å);¹⁹ these observations are consistent with the above-cited conclusion that Ni→C π-backdonation does not appear to make important contributions to the Ni-C interaction in **6**.

2.3.4. Cyclic voltammetry measurements.

The redox properties of the title complexes were investigated by cyclic voltammetry measurements and, where possible, compared to their POCOP^{*i*-Pr} analogues, the main objective being to determine how the redox potentials for the Ni^{II}/Ni^{III} couple are influenced by the *P*-substituents and X ligands. Unfortunately, only the triflate and acetate derivatives underwent quasi-reversible redox cycles (Figure 2.6), the remaining compounds showing nearly irreversible oxidations. The E⁰_{1/2} values listed in Table 2.5 indicate that oxidation is somewhat more facile in the POCOP^{*i*-Pr} analogue for the acetate derivatives, which is consistent with the greater nucleophilicity of the OP(*i*-Pr)₂ moieties. On the other hand, the opposite seems to be the case in the triflate derivatives; we speculate that this observation might arise from the weaker binding of the triflate moiety in the bulkier POCOP^{*i*-Pr} analogue.

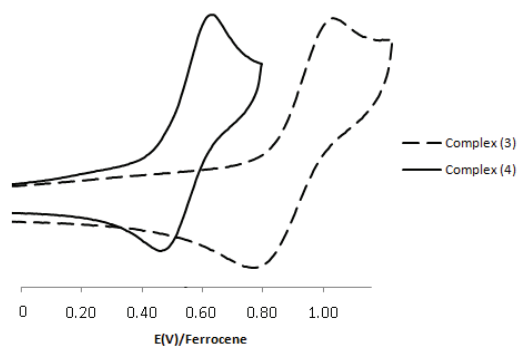


Figure 2.6. Cyclic voltammograms of complexes **3** and **4** (1 mM solutions in CH_2Cl_2) containing 0.1 M $[\text{NBu}_4][\text{PF}_6]$. The measurements were made at 25 °C using a glassy carbon working electrode and a scan rate of 100mV/s. All $E^0_{1/2}$ values are referenced to the $\text{Fe}^{\text{II}}/\text{Fe}^{\text{III}}$ redox couple of Ferrocene

Table 2.5. Redox potentials*

Complex	$E^0_{1/2}$ (V)
$(\text{POCOP}^{i-\text{Pr}})\text{Ni}(\text{OSO}_2\text{CF}_3)$	0.98
3	0.81
$(\text{POCOP}^{i-\text{Pr}})\text{Ni}(\text{OCOCH}_3)$	0.43
4	0.55

*For details on the experimental conditions see the caption for Figure 2.6

Another noteworthy observation is that the acetate derivatives (in both POCOP^{Ph} and $\text{POCOP}^{i-\text{Pr}}$ cases) appear to be much easier to oxidize than their triflate counterparts (Table 2.5). We attribute this observation to the greater tendency of an acetate ligand to adopt a bidentate binding mode, which might provide additional stabilization for an oxidized species (*cf.* $[(\text{POCOP})\text{Ni}(\eta^2\text{-OAc})][\text{PF}_6]$). Unfortunately, we did not succeed in generating isolable trivalent species $(\text{POCOP}^{\text{Ph}})\text{Ni}(\text{X})\text{Br}$ by bromination reactions, regardless of which divalent precursor was used (X= Br, OAc, etc.).

2.3.5. Reactivity tests.

Notwithstanding the disappointing observation that stable and isolable alkyl derivatives $(\text{POCOP}^{\text{Ph}})\text{NiR}$ cannot be obtained, we carried out multiple tests to effect

Corriu-Kumada type coupling reactions catalyzed by in-situ generated alkyl species. Thus, refluxing THF mixtures of Grignard reagents, ArBr (Ar= Ph, 3-CF₃-C₆H₄, 2-Et-C₆H₄, 4-OMe-C₆H₄) and (POCOP^{Ph})NiBr (1% loading) gave low and variable yields of the desired coupling products R-Ar (5-40%) in addition to other by-products; control experiments established that both the Grignard reagent and the nickel precursor are essential for these reactions. Some of the by-products detected in these reactions could not be identified precisely, but we suspect that most arise from ring-opening oligomerization of THF. The main by-product that was often present in 50% or higher yields and could be identified readily on the basis of GC/MS analyses was the biaryl Ar-Ar formed from the catalytic homocoupling or the ArBr substrate. Interestingly, reaction mixtures containing different substrates, ArBr and Ar'Br, gave variable ratios of products arising from both homocoupling (Ar-Ar) and cross-coupling (Ar-Ar'). We speculate that these coupling reactions arise from the generation of aryl radicals through a single electron transfer to the substrates from the in-situ generated Ni-alkyl species. However, no trivalent derivatives could be isolated from these reactions, nor through deliberate attempts to oxidize the bromo or acetate precursors with Br₂ and *N*-bromosuccinimide: the initially yellow reaction mixtures turned dark-green and then black, and no ³¹P NMR signals were detected.

The above results implied that the thermal decomposition and other side reactions of the in-situ generated alkyl intermediates are competitive with the coupling reaction. We then tested the reactivity of isolated samples of the cyano or alkynyl derivative with PhBr (60 °C, THF or C₆D₆), but no coupling product was observed in either case. The alkynyl derivative **6** also failed to undergo hydrogenolysis and form the target hydride species,

and no C-H substitution was induced by thermal reactions of the acetate and nitrate derivatives with benzene.

2.4. Conclusion

This study has shed some light on the influence of *P*-substituents R and X ligands on the pincer-type complexes (POCOP^R)NiX. Perhaps the most definitive conclusion to draw from our observations pertains to the dramatically lower stability of (POCOP^{Ph})Ni(alkyl) complexes compared to their *i*-Pr counterparts; this limitation prevented us from isolating alkyl derivatives and investigating their reactivities. The influence of the *P*-substituents on other properties of the title complexes is less clear cut. For instance, the redox potentials measured for the acetate derivatives support the contention that the POCOP^{Ph} ligand is a less effective donor of electron density to the Ni center relative to its *i*-Pr counterpart, but this conclusion is not supported by the measurements made for the triflate derivatives. The results of the cyclic voltammetry studies do show that the acetate derivatives can be oxidized much more readily than their triflate analogues; unfortunately, however, this comparison could not be extended to the other derivatives for which the redox behaviour is not sufficiently reversible.

We conclude, therefore, that neutral Ni complexes based on POCOP^{*i*-Pr} and POCOP^{*t*-Bu} ligands should be considered more promising candidates for promoting coupling and insertion reactivities.⁶ On the other hand, there are preliminary indications that the reactivities of the cationic adducts [(POCOP^{Ph})Ni(L)]⁺ as Lewis acid type promoters are comparable and complementary to those of their better studied *i*-Pr analogues; a full account of these studies will be reported in due course.

2.5. Experimental Section

2.5.1. General.

All manipulations were carried out using standard Schlenk and glove box techniques under nitrogen atmosphere. All solvents used for experiments were dried to water contents of less than 10 ppm (determined using a Mettler Toledo C20 coulometric Karl Fischer titrator) by passage through activated aluminum oxide columns (MBraun SPS) and freeze-thaw degassed. C₆D₆ was dried over 4 Å molecular sieves and then freeze-thaw degassed. The precursor compound NiBr₂(NCCH₃)_x was prepared according to published method ²⁰ The following were purchased from Aldrich and, unless otherwise noted, used without further purification: Ni (metal), bromine, resorcinol, chlorodiphenylphosphine, triethylamine, KCN and all silver salts.

A Bruker AV 700 spectrometer was used for recording the ¹H and ¹³C{¹H} (176 MHz) NMR spectra for the ligand, and a Bruker AV 300 was used for recording the ¹⁹F{¹H} NMR spectra. A Bruker AV 400 spectrometer was used for recording all the other NMR spectra: ¹H, ¹³C{¹H} (101 MHz), and ³¹P{¹H} (162 MHz). ¹H and ¹³C chemical shifts are reported in ppm downfield of TMS and referenced against the residual C₆D₆ signals (7.15 ppm for ¹H and 128.02 ppm for ¹³C); ³¹P chemical shifts are reported in ppm and referenced against the signal for 85% H₃PO₄ (external standard, 0 ppm). Coupling constants are reported in Hz. ¹⁹F NMR chemical shifts are referenced to CFCl₃ (0 ppm), which results in a single resonance for C₆F₆ at -164.9 ppm.

2.5.2. Synthesis of 1,3-(OPPh₂)₂C₆H₄ (ligand a).

To a solution of resorcinol (500 mg, 4.50 mmol) and NEt₃ (1.25 mL, 9.00 mmol) in 30 mL of THF inside a Schlenk flask was added slowly Ph₂PCl (1.70 mL, 9.00 mmol) at 25 °C. Stirring this mixture over 30 min led to precipitation of a white solid. Evaporation of the solvent under vacuum and extraction of the solid residue with hexane (3×25 mL), followed by evaporation under vacuum gave an air-sensitive pale yellow oil (1.84 mg, 86%). A few mg of this oil was dissolved in C₆D₆ for NMR characterization.

¹H NMR (700 MHz, C₆D₆): δ 7.68 (^vt, ³J_{HH} = 8, 8H, *o*-H in PPh₂), 7.16 (td, ³J_{HH} = 8, 8H, *m*-H in PPh₂), 7.13 (t, ³J_{HH} = 7, 4H, *p*-H in PPh₂), 7.50 (t, J_{HP} = 1, 1H, ArH²), 7.03 (d, ³J_{HH} = 8, 2H, ArH⁴), 6.98 (t, J_{HH} = 7, 1H, ArH⁵). ¹³C{¹H} NMR (176 MHz, C₆D₆): δ 158.77 (d, ²J_{CP} = 15, 2C, ArC¹), 113.08 (d, J_{CP} = 10, 2C, ArC⁴), 141.14 (1C, ArC⁵), 110.17 (t, J_{CP} = 12, 1C ArC²), 130.80 (d, J_{CP} = 22, 4C, *i*-C in PPh₂), 128.54 (d, J_{CP} = 4, 8C, *o*-C in PPh₂), 129.66 (8C, *m*-C in PPh₂), 130.26 (4C, *p*-C in PPh₂). ³¹P{¹H} NMR (162 MHz, C₆D₆): δ 112(2P). This data matched the literature values.^{8,9}

2.5.3. Synthesis of (POCOP^{Ph})NiBr (1).

NiBr₂(NCCH₃)_x (1.36 g, 5.23 mmol) and NEt₃ (0.6 mL, 4.0 mmol) were added to the stirred solution of ligand a (2.00 g, 4.50 mmol) in 25 mL of Toluene. The resulting deep yellow mixture was stirred at 25 °C for 12 h. Vacuum evaporation of the solvent followed by extraction of the residual solid with 50 mL of anhydrous chloroform and filtration through a short column of silica gel gave a yellow filtrate that was evaporated under vacuum to give 1 as a yellow powder (2.44 g, 88%).

¹H NMR (400 MHz, CDCl₃): δ 6.68 (d, ³J_{HH} = 8, 2H, ArH³), 7.13 (t, ³J_{HH} = 8, 1H, ArH⁴), 7.49 (t, ³J_{HH} = 8, 4H, *p*-H in PPh₂), 7.54 (t, ³J_{HH} = 8, 8H, *m*-H in PPh₂), 8.02 (td, *J*_{HH/HP} = 8 ; 1, 8H, *o*-H in PPh₂). ¹³C{¹H} NMR (176 MHz, C₆D₆): δ 167.05 (t, ²J_{CP} = 11, 2C, ArC^{2/6}), 132.50 (d, *J*_{CP} = 35, 4C, *i*-C in PPh₂), 132.2 (t, ³J_{CP} = 10, 8C, *o*-C in PPh₂), 131.8 (4C, *o*-C in PPh₂), 129.8 (2C, ArC^{3/5}), 129.4 (1C, ArC⁴), 128.80 (t, *J*_{CP} = 7, 8C, *m*-C in PPh₂), 106.60 (t, ²J_{cp} = 7, 1C, ArC¹), ³¹P{¹H} NMR (162 MHz, C₆D₆): δ 146(s), UV-Vis (CH₂Cl₂, 1.18 × 10⁻⁴) [λ_{max}, nm (ε, L·mol⁻¹·cm⁻¹)]: 415(3560), 369(3127), 353(8330), 338(7788). Elemental Anal. for C₃₀H₂₃BrO₂P₂Ni Calc. (found): C, 58.49 (58.51); H, 3.76 (3.67) %.

2.5.4. Synthesis of (POCOP^{Ph})NiCN (2).

Method 1. KCN (53 mg, 0.81 mmol) was added to a Schlenk tube containing a solution of **1** (100 mg, 0.16 mmol) in 3 mL of THF. The mixture was stirred at 60 °C for 24 h, and the solvent was removed under vacuum to give a pale yellow solid. Filtration through a short column of silica gel gave a pale yellow filtrate that was evaporated to give the desired product. (57 mg, 63%). **Method 2.** AgCN (70 mg, 0.52 mmol) was added to a Schlenk tube containing a solution of **1** (200 mg, 0.325 mmol) in 10 mL of CH₂Cl₂ protected from ambient light with aluminum foil. The resulting mixture was stirred at RT for 5h, filtered, and evaporated under vacuum to give a clear yellow solid. This was passed through a short column of silica gel, and the resulting filtrate was evaporated to furnish the desired product (144 mg, 77%).

¹H NMR (400 MHz, C₆D₆): δ 6.92 (d, ³J_{HH} = 8, 2H, ArH⁴), 7.04 (m, 12H, *m+p*-H in PPh₂), 7.10 (t, ³J_{HH} = 8, 1H, ArH⁵), 8.25 (m, 8H, *o*-H in PPh₂). ¹³C NMR (101 MHz,

C_6D_6): δ 132.53 (1C, CN), 132.27 (2C, ArC^{2/6}), 132.0 (1C, ArC⁴) 131.33 (t, $J_{cp} = 5$, 8C, *o*-C in PPh₂), 131.3 (4C, *i*-C in PPh₂), 131.26 (4C, *p*-C in PPh₂), 130.8 (2C, ArC^{3/5}) 129.4 (t, $J_{cp} = 5$, 1C, ArC¹) 128.6 (t, $J_{cp} = 4$, 8C, *m*-C in PPh₂). ³¹P{¹H} NMR (160 MHz, C_6D_6): δ 154 (2P). IR (solid state, cm⁻¹): ν (C=C^{Ar})= 1436, 1483, 1558, 1582, ν (C≡N)= 2116. UV-Vis (CH₂Cl₂, 1.11×10^{-4}) [λ_{max} , nm (ϵ , L.mol⁻¹.cm⁻¹)]: 372(1354), 337(7585). Elemental Anal. for C₃₁H₂₃O₂N₁P₂Ni Calc. (found) % : C, 66.23 (65.93); H, 4.12 (4.44); N, 2.49 (2.42).

2.5.5. Synthesis of (POCOP^{Ph})Ni(OSO₂CF₃) (3).

AgOTf (74 mg, 0.325 mmol) was added to a Schlenk containing a solution of **1** (200 mg, 0.32 mmol) in 15 mL of CH₂Cl₂ and protected from ambient light with aluminum foil. The resulting mixture was stirred at 25 °C for 5 h and then evaporated under vacuum to give a yellow powder (crude yield 157 mg, 75%). A small portion of this solid was purified by filtration through a short column of silica gel.

¹H NMR (400 MHz, C₆D₆): δ 6.66 (d, $^3J_{HH} = 8$, 2H, ArH³), 6.93 (t, $^3J_{HH} = 12$, 1H ArH⁴), 7.13 (m, 12H *m+p*-H in PPh₂), 8.10 (m, 8H, *o*-H in PPh₂). ¹³C {¹H} NMR (101 MHz, C₆D₆): δ 132.74 (m, $^3J_{cp} = 6$, 12C, *m+p*-C in PPh₂), 107.66 (t, $^2J_{cp} = 7$, 1C, ArC¹), 131.62 (1C, CF₃), 131.38 (4C, *i*-C in PPh₂), 131.31 (1C, ArC⁴), 129.30 (8C, *o*-C in PPh₂), 131.88 (2C, ArC^{3/5}), 168.6 (^vt, $J_{cp} = 11$, 2C, ArC^{2/6}). ³¹P{¹H} NMR (160 MHz, C₆D₆): δ 141(s,2P). ¹⁹F NMR (179 MHz, C₆D₆): δ -77.93 (s,3F). IR (toluene, cm⁻¹): ν (SO₃)= 1020, 1240; ν (CF₃)= 1105¹, ν (C=C^{Ar})= 1438, 1481, ν =1556, 1583. UV-Vis (CH₂Cl₂, 1.27×10^{-4}) [λ_{max} , nm (ϵ , L.mol⁻¹.cm⁻¹)]: 396(5008), 327(9553). Elemental

Anal. for $C_{31}H_{23}O_5P_2F_3Ni$ Calc.(found) % : C, 54.34 (54.55); H, 3.38 (3.22); S, 4.65 (4.68).

2.5.6. Synthesis of $(POCOP^{Ph})Ni(OCOCH_3)$ (4).

$AgOAc$ (81 mg, 0.50 mmol) was added to a Schlenk flask containing a solution of **1** (200 mg, 0.32 mmol) in 15 mL of CH_2Cl_2 and protected from ambient light with aluminum foil. The mixture was stirred at 25 °C for 1 h, filtered, and evaporated under vacuum to give and the desired product as a yellow powder (crude yield 122 mg, 64%). A small portion of this solid was purified by filtration through a short column of silica gel.

1H NMR (400 MHz, C_6D_6): δ 7.04 (t, $^3J_{HH} = 8$, 1H, ArH⁴), 6.79 (d, $^3J_{HH} = 8$, 2H, ArH³), 7.16 (m, 12H, *m*+*p*-H in PPh₂), 8.2 (m, 8H, *o*-H in PPh₂), 1.97 (s, 3H, CH_3CO). ^{13}C NMR (101 MHz, C_6D_6): δ 128.77 (t, $J_{cp} = 5$, 12C, *m*-C in PPh₂), 128.94 (d, 4C, $J = 4$, *i*-C in PPh₂), 130.4 (4C, CH_3), 131.30 (4C, *p*-C in PPh₂), 129.78 (t, $J = 7$, 1C, CO), 132.70 (t, $J_{cp} = 7$, 8C, *o*-C in PPh₂), 106.57 (t, $J_{cp} = 4$, 2C, ArC^{3/5}), 135.37 (2C, ArC^{2/6}), 134.8 (1C, ArC⁴) 130.97 (t, $J_{CP} = 6$, 1C, ArC¹) $^{31}P\{^1H\}$ NMR (160 MHz, C_6D_6): δ 135 (s, 2P). IR (solid state, cm⁻¹): v(C=O)= 1581, v(C-O)= 1128. UV-Vis (CH_2Cl_2 , 5.6×10^{-5}) [λ_{max} , nm (ϵ , mol⁻¹ cm²)]: 393(2059), 367(4965), 338(5565). Elemental Anal. for $C_{32}H_{26}O_4P_2Ni$ Calc.(found) % : C, 64.58 (64.52); H, 4.40 (4.40).

2.5.7. Synthesis of $(POCOP^{Ph})Ni(ONO_2)$ (5).

$AgNO_3$ (87 mg, 0.51 mmol) was added to a Schlenk flask containing a solution of **1** (200 mg, 0.325 mmol) in 15 mL of CH_2Cl_2 and protected from ambient light with aluminum foil. The mixture was stirred at 25 °C for 4 h, filtered, and evaporated under vacuum to give the desired product as a yellow powder (crude yield 115 mg, 60%). A small portion of this solid was purified by filtration through a short column of silica gel.

¹H NMR (300 MHz, C₆D₆): δ 6.86 (t, ³J_{HH} = 12, 1H, ArH⁴), 6.62 (d, ³J_{HH} = 5 Hz, 2H, ArH³), 6.97 (m, 12H, *m+p*-H in PPh₂), 7.91 (m, 8H, *o*-H in PPh₂). ¹³C NMR (75 MHz, C₆D₆, C₆D₆): δ 132.45 (t, J_{cp} = 8, 8C, *m*-C in PPh₂), 133.1 (1C, ArC⁴), 132.8 (4C, *p*-C in PPh₂), 131.1 (4C, *i*-C in PPh₂), 129.5 (t, J_{cp} = 5, 8C, *o*-C in PPh₂), 129.8 (t, J_{cp} = 4, 1C, ArC¹), 107.5 (t, J_{cp} = 6, 2C, ArC^{3/5}), 168.7 (t, J_{cp} = 11, 2C, ArC^{2/6}). ³¹P{¹H} NMR (160 MHz, C₆D₆): δ 142 (s, 2P). IR (solid state, cm⁻¹) : ν(NO₂) = 1362, 814. UV-Vis (CH₂Cl₂, 5.8 × 10⁻⁵) [λ_{max}, nm (ε, L·mol⁻¹·cm²)]: 388(4694), 334(11034). Elemental Anal. for C₃₀H₂₃O₅N₁P₂Ni Calc. (found) % : C, 60.24 (60.29); H, 3.88 (3.92); N, 2.34 (2.23).

2.5.8. Synthesis of (POCOP^{Ph})Ni(C≡CPh) (6).

To a Schlenk flask containing a solution of **3** (500 mg, 0.73 mmol) in 15 mL of toluene was added NEt₃ (213 μl, 1.533 mmol) and phenylacetylene (160 μl, 1.46 mmol) and the resulting mixture was stirred at 25 °C for 15 min. Vacuum evaporation followed by extraction of the residual solid with 25 mL of diethyl ether gave a pale yellow mixture that was filtered through a short column of silica gel and evaporated to give the desired product as a yellow pale powder (355 mg, 71%).

¹H NMR (400 MHz, C₆D₆): δ 7.14 (t, ³J_{HH} = 8, 1H, ArH⁴), 7.21 (t, ³J_{HH} = 8, 2H, *m*-H in C≡CPh), 7.65 (d, ³J_{HH} = 7, 2H, ArH³), 8.40 (q, ³J_{HH} = 6, 8H, *o*-H in PPh₂), 7.00 (d, ³J_{HH} = 8, 2H, *o*-H in C≡CPh), 7.07 (m, 13H *m+p*-H in PPh₂ & *o*-H in C≡CPh). ¹³C{¹H} NMR (101 MHz, C₆D₆): δ 130.84 (4C, *p*-C in PPh₂), 128.24 (m, J_{cp} = 5, 8C, *m*-C in PPh₂), 125.19 (1C, Ni-C≡C), 126.80 (1C, Ni-C≡C), 129.9 (4C, *i*-C in PPh₂), 130.6 (1C, ArC⁴), 131.60 (t, J_{cp} = 8, 8C, *o*-C in PPh₂), 134.00 (1C, *o*-C in C≡CPh), 133.7 (1C, *p*-C in C≡CPh), 133.47 (1C, *m*-C in C≡CPh), 128.80 (1C, ArC¹), 113.93 (1C, *i*-C in C≡CPh), 106.00 (t, J_{cp} = 4, 2C, ArC^{3/5}), 167.00 (^vt, J_{cp} = 10, 2C, ArC^{2/6}). ³¹P{¹H} NMR (160 MHz

C_6D_6): δ 154 (2P). IR (solid state, cm^{-1}): $\nu(\text{C}=\text{C}^{\text{Ar}})=$ 1434, 1480), 1555), $\nu(\text{C}\equiv\text{C})=$ 2105. UV-Vis (CH_2Cl_2 , $7.85 \cdot 10^{-5}$) [λ_{max} , nm (ε , $\text{L} \cdot \text{mol}^{-1} \cdot \text{cm}^{-1}$)]: 385(5248), 363(7363), 308(5528). Elemental Anal. for $\text{C}_{38}\text{H}_{28}\text{O}_2\text{P}_2\text{Ni}$ Calc. (found) %: C, 71.62 (71.21); H, 4.67 (4.43).

2.5.9 Crystal Structure Determinations.

Single crystals of all complexes were grown by slow diffusion of hexanes into a saturated toluene solution of each complex. The crystallographic data for complexes **1**, **3**, **5** and **6** were collected on Kristalloflex 760 generator equipped with a Mo sealed tube and a graphite monochromator and a Platform goniometer from Bruker and a APEX II detector. The crystallographic data for complex **2** was collected on a FR591 generator from Nonius equipped with a Helios optics, a Kappa rotating anode, and a CCD 6K detector. The crystallographic data for complex **4** was collected on a Bruker Microstar generator (micro source) equipped with a Helios optics, a Kappa Nonius goniometer and a Platinum135 detector.

Cell refinement and data reduction were done using SAINT²¹. An empirical absorption correction, based on the multiple measurements of equivalent reflections, was applied using the program SADABS.²² The space group was confirmed by XPREP routine²³ in the program SHELXTL.²⁴ The structures were solved by direct-methods and refined by full-matrix least squares and difference Fourier techniques with SHELX-97.²⁵ All non-hydrogen atoms were refined with anisotropic displacement parameters. Hydrogen atoms were set in calculated positions and refined as riding atoms with a common thermal parameter.

2.6. Acknowledgements.

The authors gratefully acknowledge financial support received from Université de Montréal, Universities Mission of Tunisia in Montreal (MUT) (fellowships to A.B.S.), and NSERC of Canada (Research Tools and Instruments and Discovery grants to D.Z.).

The authors have benefited from valuable discussions with their colleagues Profs. F. Schaper, G. S. Hanan, and C. Reber.

2.7. References

¹ For a few general reviews on chemistry of pincer complexes see: (a) M. E. van der Boom and D. Milstein, *Chem. Rev.*, 2003, **103**, 1759; (b) L.-C. Liang, *Coord. Chem. Rev.* 2006, **250**, 1152; (c) H. Nishiyama, *Chem. Soc. Rev.*, 2007, **36**, 1133; (d) W. Leis, H. A. Mayer and W. C. Kaska, *Coord. Chem. Rev.*, 2008, **252**, 1787; (e) D. Benito-Garagorri and K. Kirchner, *Acc. Chem. Res.*, 2008, **41**, 201; (f) D. Morales-Morales, *Mini-Rev. Org. Chem.*, 2008, **5**, 141; (g) M. Q. lagt, D. A. P.van Zwieten, A. J. C. M. Moerkerk, R. J. M. K. Gebbink, and G.van Koten, *Coord. Chem. Rev.*, 2004, **248**, 2275.

² For reports on catalytic activities of pincer complexes see: (a) M. Albrecht and G. van Koten, *Angew. Chem., Int. Ed.*, 2001, **40**, 375; (b) A. S. Goldman, A. H. Roy, Z. Huang, R. Ahuja, W. Schinski, M. Brookhart, *Science* 2006, **312**, 257. (c) T. Zweifel, J.-V. Naubron and H. Grützmacher, *Angew. Chem., Int. Ed.*, 2009, **48**, 559; (d) M. Ohff, A. Ohff, M. E. van der Boom and D. Milstein, *J. Am. Chem. Soc.*, 1997, **119**, 11687; (e) F. Miyazaki, K. Yamaguchi and M. Shibasaki, *Tetrahedron Lett.*, 1999, **40**, 7379; (f) A. Naghipour, S. J. Sabounchei, D. Morales-Morales, D. Canseco-González and C. M. Jensen, *Polyhedron*, 2007, **26**, 1445; (g) C. Gunanathan, Y. Ben-David and D. Milstein, *Science*, 2007, **317**, 790; (h) S. Sebelius, V. J. Olsson and K. J. Szabo, *J. Am. Chem. Soc.*,

2005, **127**, 10478; (i) W. H. Bernskoetter and M. Brookhart, *Organometallics*, 2008, **27**, 2036. For reviews on catalytic applications of pincer complexes see: (j) J. T. Singleton, *Tetrahedron*, 2003, **59**, 1837; (k) N. Selander, and K. J. Szabo, *Chem. Rev.*, 2010, DOI: 10.1021/cr1002112.

³ For reports on potential applications of pincer complexes as functional materials see: (a) (b) G. D. Batema, M. Lutz, A. L. Spek, C. A. van Walree, C. d. M. Donegá, A. Meijerink, R. W. A. Havenith, J. Pérez-Moreno, K. Clays, M. Büchel, A. van Dijken, D. L. Bryce, G. P. M. van Klink and G. van Koten, *Organometallics*, 2008, **27**, 1690; (c) A. F. M. J. van der Ploeg, G. van Koten and C. Brevard, *Inorg. Chem.*, 1982, **21**, 2878; (d) H. P. Dijkstra, M. D. Meijer, J. Patel, R. Kreiter, G. P. M. van Klink, M. Lutz, A. L. Spek, A. J. Carty and G. van Koten, *Organometallics*, 2001, **20**, 3159; (e) M. Albrecht, M. Lutz, A. L. Spek, G. van Koten, *Nature London* 2000, **406**, 970; (f) E. J. Rivera, C. Figueroa, J. L. Colon, L. Grove, W. B. Connick, *Inorg. Chem.*, 2007, **46**, 8569; (g) Tastan, Seher; Krause, Jeanette A.; Connick, William B. *Inorg. Chim. Acta*, 2006, **359**, 1889; (h) D. V. Aleksanyan, V. A. Kozlov, Y. V. Nelyubina, K. A. Lyssenko, L. N. Puntus, E. I. Gutsul, N. E. Shepel, A. A. Vasil'ev, P. V. Petrovskii, I. L. Odintsev, *Dalton Trans.*, 2011, **40**, 1535.

⁴ (a) D. G. Gusev, F.-G. Fontaine, A. J. Lough and D. Zargarian, *Angew. Chemie Int. Ed. Eng.*, 2003, **42**, 216; (b) M. J. Ingleson, B. C. Fullmer, D. T. Buschhorn, H. Fan, M. Pink, J. C. Huffman, and K. G. Caulton, *Inorg. Chem.*, 2008, **47**, 407; (c) M. Gozin, M. Aizenberg, S.-Y. Liou, A. Weisman, Y. Ben-David, and D. Milstein, *Nature*, 1994, **370**, 42; (d) D. M. Grove, G. van Koten, P. Mul, A. A. H. van der Zeijden, J. Terheijden, M. C. Zoutberg and C. H. Stam, *Organometallics*, 1986, **5**, 322; (e) D. G. Gusev, T.

Maxwell, F. M. Dolgushin, M. Lyssenko and A. J. Lough, *Organometallics*, 2002, **21**, 1095; (f) M. Albrecht and G. van Koten. *Angew Chem. Int. Ed.*, 2001, **40**, 3750.

⁵ (a) L.F. Groux, F. Bélanger-Gariépy and D. Zargarian, *Can. J. Chem.*, 2005, **83**, 634; (b) A. Castonguay, F. Charbonneau, A. L. Beauchamp and D. Zargarian, *Acta Cryst.*, 2005, **E61**, m224; (c) A. Castonguay, C. Sui-Seng, A. L. Beauchamp and D. Zargarian, *Organometallics*, 2006, **25**, 602; (d) C. Sui-Seng, A. Castonguay, Y. Chen, D. Gareau, L. F. Groux and D. Zargarian, *Top. in Cata.*, 2006, **37**, 81; (e) A. Castonguay, A. L. Beauchamp and D. Zargarian, *Acta Cryst.*, 2007, **E63**, 2134; (f) V. Pandarus, D. Zargarian, *Chem. Commun.* 2007, 978; (g) V. Pandarus and D. Zargarian, *Organometallics*, 2007, **26**, 4321; (h) A. Castonguay, A. L. Beauchamp and D. Zargarian, *Organometallics*, 2008, **27**, 5723; (i) A. Castonguay, A. L. Beauchamp and D. Zargarian, *Inorg. Chem.*, 2009, **48**, 3177; (j) A. Castonguay, D. M. Spasyuk, N. Madern, A. L. Beauchamp and D. Zargarian, *Organometallics*, 2009, **28**, 196; (k) D. M. Spasyuk, A. van der Est, and D. Zargarian, *Organometallics*, 2009, **28**, 6531; (l) D. M. Spasyuk and D. Zargarian, *Inorg. Chem.*, 2010, **49**, 6203; (m) X. Lefèvre, G. Durieux, S. Lesturgez, and D. Zargarian *J. Mol. Catal. A.*, 2010, **335**, 1; (n) X. Lefèvre, D. M. Spasyuk, and D. Zargarian *J. Organomet. Chem.*, 2010, **696**, 864; (o) D. M. Spasyuk, S. Gorelsky, A. van der Est and D. Zargarian, *Inorg. Chem.*, 2011, **50**, 2661.

⁶ (a) J. Zhang, C. Medley, J. A. Krause and H. Guan, *Organometallics*, 2010, **29**, 6393; (b) S. Chakraborty, J. A. Krause and H. Guan, *Organometallics*, 2009, **28**, 582; (c) S. Chakraborty, J. Zhang, J. A. Krause and H. Guan, *J. Am. Chem. Soc.*, 2010, **132**, 8872.

⁷ G. B. Valente, B. P. Oscar, H.-A. Cesar, R. A. Toscano and D. Morales-Morales, *Tetrahedron lett.* 2006, **47**, 5059.

⁸ R. B. Bedford, S. M. Draper, P. N. Scully and S. L. Welch, *New J. Chem.* 2000, **24**, 745.

⁹ D. Morales-Morales, C. Grause, K. Kasaoka, R. Redon, R. E. Cramer and C. M. Jensen, *Inorg. Chim. Acta*, 2000 **300–302** 958.

¹⁰ For comparison: ¹H NMR of the analogous complex (POCOPⁱ-Pr)NiMe^{5g} shows a triplet at -0.63 ppm (³J_{P-H}= 9 Hz) while the ³¹P{¹H} NMR signal for this species was similarly found to be downfield of that of its Ni-Br precursor (ca. 192 vs 186 ppm).

¹¹ F. A. Miller, C. H. Wilkins, *Analytical Chem.* 1952, **24**, 1253.

¹² W. Wayne, J. Lukens, R. A. Andersen. *Organometallics* 1996, **14**, 3435.

¹³ (a) N. Klouras, V. Nastopoulos, and N. Tzavellas, *Z. anorg. allg. Chem.*, 1995, **621** 1767-1770. (b) U. Thewalt, W. Nuding, *J. Organomet. Chem.* 1996, **512**, 127.

¹⁴ A.N. Rodionov, G. V. Timofeyuk, T.V. Talalaeva, D. N. Shigorin, K. A. L. Kocheshkov, *Ya. Karpov Inst. Phys.-Chem., Moscow, Izvestiya Akademii Nauk SSSR, Seriya Khimicheskaya* 1965, **1**, 42.

¹⁵ J. H. Teuben, H. J. De Lief de Meijer, *J. Organomet. Chem.* 1969, **17**, 87.

¹⁶ Erker, G.; Frömberg ,W.; Benn , R.; Mynott, R.; Angermund, K.; Krüger ,C. *Organometallics* 1989, **8**, 911.

¹⁷ (a) A. Salah, D. Zargarian, *Acta Cryst. 2011, E67*, m437. (b) A. Salah, D. Zargarian, *Acta Cryst. E* 2011, in press.

¹⁸ V. M. Rayón, P. Redondo, C. Barrientos, A. Largo, *J. Chem. Phys.* 2009, **131**, 9.

¹⁹ R. Choukroun, B. Donnadieu, J.-S. Zhao, P. Cassoux, C. Lepetit, B. Silvi *Organometallics* 2000, **12**, 1901.

²⁰ B. J. Hathaway, D. G. Holah, *J. Chem. Soc.* 1964, **8**, 2400.

²¹ SAINT (**1999**) Release 6.06; Integration Software for Single Crystal Data. Bruker AXS Inc., Madison, Wisconsin, USA.

²² G.M. Sheldrick, (**1999**). SADABS, Bruker Area Detector Absorption Corrections. Bruker AXS Inc., Madison, Wisconsin, USA.

²³ XPREP (**1997**) Release 5.10; X-ray data Preparation and Reciprocal space Exploration Program. Bruker AXS Inc., Madison, Wisconsin, USA.

²⁴ SHELXTL (**1997**) Release 5.10; The Complete Software Package for Single Crystal Structure Determination. Bruker AXS Inc., Madison, Wisconsin, USA.

²⁵ (a) G.M. Sheldrick, (**1997**). SHELXS97, Program for the Solution of Crystal Structures. Univ. of Gottingen, Germany. (b) G.M. Sheldrick, (**1997**). SHELXL97, Program for the Refinement of Crystal Structures. University of Gottingen, Germany.

2.8. Supporting Information.

Tables of ¹H, ¹³C NMR, and UV-vis data. X-ray analyses for all complexes have been deposited at The Cambridge Crystallographic Data Centre (CCDC) and can be retrieved with the reference numbers 814530 (**1**), 814531 (**5**), 814532 (**3**), 814533 (**4**), 814534 (**2**), and 814535 (**6**).

These data can be obtained free of charge via www.ccdc.cam.ac.uk/data_request/cif, or by emailing data_request@ccdc.cam.ac.uk, or by contacting The Cambridge Crystallographic Data Centre, 12, Union Road, Cambridge CB2 1EZ, UK; fax: +44 1223 336033.

Supporting Information**For****The Impact of P-Substituents on the Structures, Spectroscopic Properties, and Reactivities of POCOP-Type Pincer Complexes of Nickel(II)**

Abderrahmen B. Salah and Davit Zargarian

Département de chimie, Université de Montréal, Montréal (Québec), Canada H3C 3J7

List of items :

1. Table of ^1H NMR data for complexes **1-6**
2. Table of ^{13}C NMR data for complexes
3. UV-Vis curves for complexes $(\text{POCOP}^{i\text{-Pr}})\text{Ni}-\text{OCOCH}_3$, $(\text{POCOP}^{i\text{-Pr}})\text{Ni}-\text{OSO}_2\text{CF}_3$ and complexes **1-6**

Table 2.6. ^1H NMR data for complexes **1-6**

	<i>o</i> -H (qq)*	<i>m</i> -H (qt)	<i>p</i> -H (t)	H3/H5 (d)	H4 (t)
A	7.68 (8H)	7.16 (8H)	7.13 (8H)	6.98 (8H)	7.03 (8H)
Ni-Br	8.25 (8H)	7.07 (m, 12H) p+m		6.68 (8H)	7.13 (8H)
Ni-CN	8.22 (m)	7.04 (m, 12H) p+m		6.92(8)	7.10(8)
Ni-Otf	8.10(m)	7.13(m, 12H) p+m		6.66(8)	6.94(8)
Ni-Oac	8.2 (m)	7.15(m, 12H) p+m		6.78(8)	7.08(8)
Ni-ONO₂	7.91(m)	6.97(m, 12H) p+m		6.78(8)	6.88(8)
Ni-CCPh	8.40 (qq, 10)	7.07 (m,15H) p+m-H of CCPh		6.99(8)	7.14(8)

* qq= quasi quartet; qt= quasi triplet

Table 2.7. $^{13}\text{C}\{\text{H}\}$ NMR data for complexes **1-6**.

	<i>i</i> -C ^vt , 4C ($^v\text{J}_{\text{P-C}}$)	<i>o</i> -C ^vt , 8C ($^v\text{J}_{\text{P-C}}$)	<i>m</i> -C ^vt , 8C ($^v\text{J}_{\text{P-C}}$)	<i>p</i> -C ^vt , 4C ($^v\text{J}_{\text{C-P}}$)	C2/C6 ^vt , 2C ($^v\text{J}_{\text{P-C}}$)	C3/C5 ^vt , 2C ($^v\text{J}_{\text{P-C}}$)	C1* t, 1C ($^2\text{J}_{\text{C-P}}$)	C4 s, 1C
1	132.0 (15.5)	128.39 (5.3)	131.8 (7)	131.41 (8)	167.05 (11.0)	106.60 (6.8)	128.7 (8.3)	129.4
2	132.27 (28.98)	128.55 (5)	131.33 (4)		167.08 (11.3)	106.29 (7.1)	129.37 (24.4)	130.81
3	131.61 (25.2)	129.3 (7)	132.74 (7)		168.6 (10.8)	107.6 (6.8)	130.48 (4.2)	131.31
4	135.2 (11)	131.37 (9.4)	132.75 (7)		168.71 (10.8)	107.6 (6.8)	130.97 (3.3)	130.4
5	131.23 (9.7)	129.45 (4.8)	132.45 (6.8)		168.72 (2.0)	107.5 (3.0)	129.23 (4.1)	132.8
6	133.7 (24.9)	128.24 (5)	131.6 (7.2)	130.84	167.0	106.0 (6.7)	128.76 (6.2)	130.6

* The signals of the quaternary carbons are very weak.

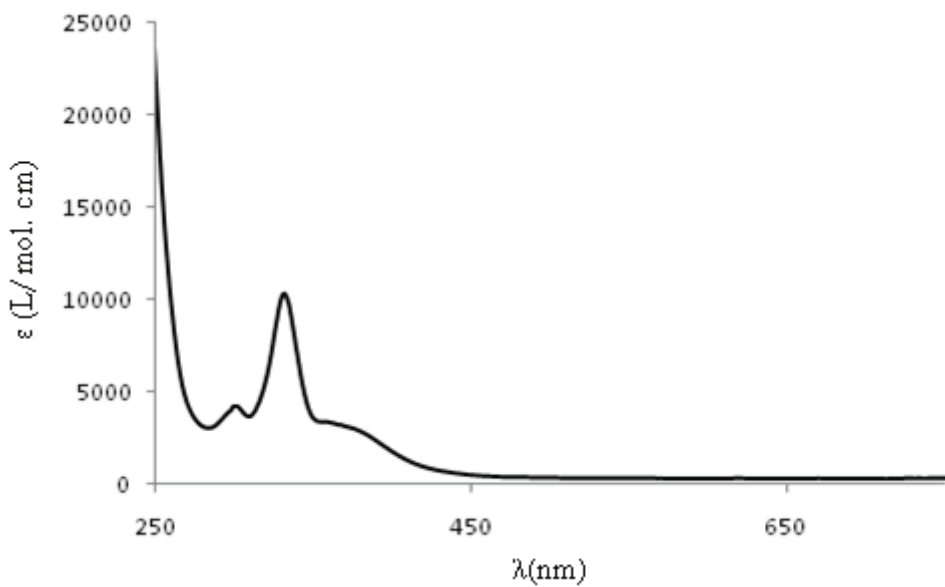


Figure 2.7. UV-Vis of $(\text{POCOP}^{i\text{-Pr}})\text{Ni}-\text{OCOCH}_3$ in CH_2Cl_2 .
Concentration = 1.054×10^{-4} mol/L

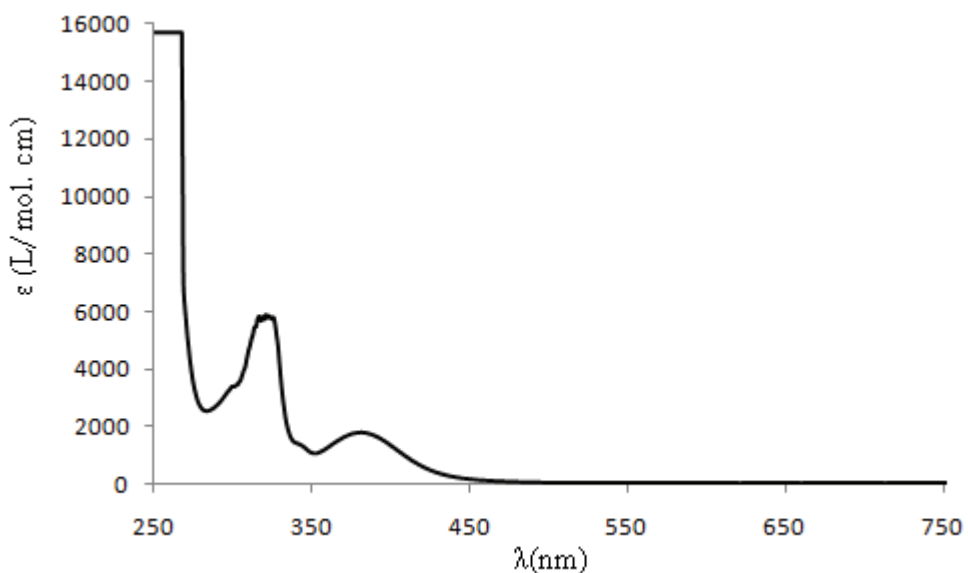


Figure 2.8. UV-Vis of $(\text{POCOP}^{i\text{-Pr}})\text{Ni}-\text{OSO}_2\text{CF}_3$ in CH_2Cl_2 .
Concentration = 1.054×10^{-4} mol/L

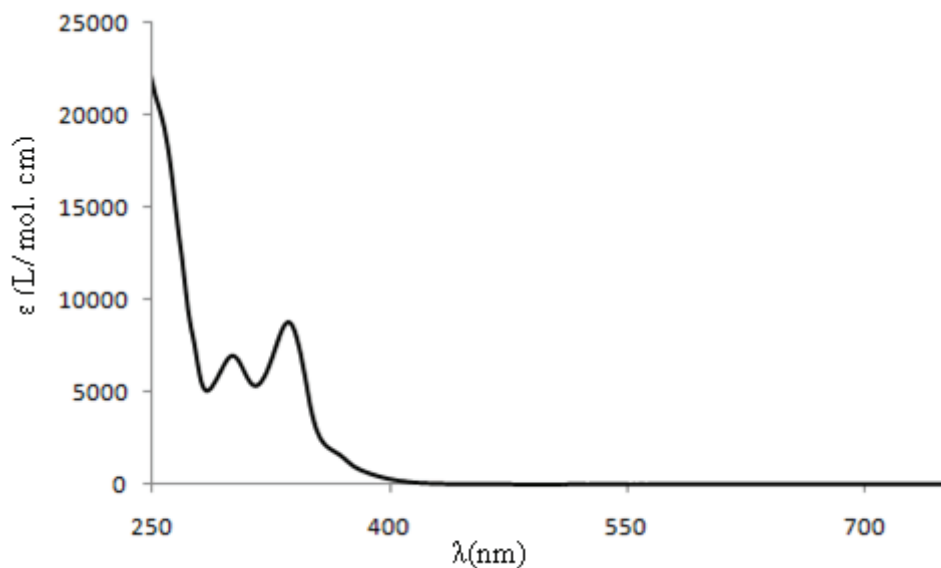


Figure 2.9. UV-Vis of complex **2** in CH_2Cl_2 . Concentration = $1.11 \cdot 10^{-4}\text{ mol/L}$

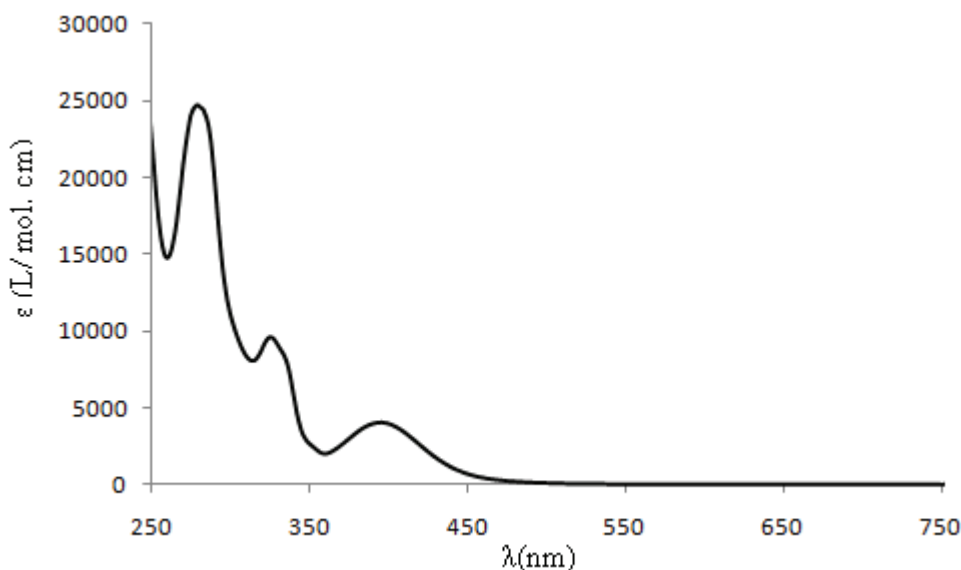


Figure 2.10. UV-Vis of complex **3** in CH_2Cl_2 . Concentration = $1.27 \cdot 10^{-4}\text{ mol/L}$

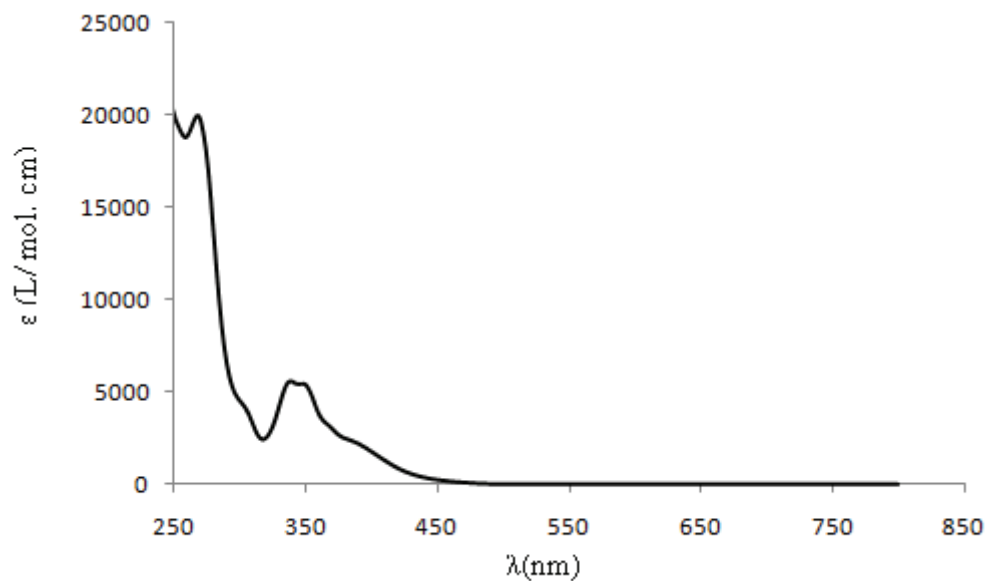


Figure 2.11. UV-Vis of complex **4** in CH_2Cl_2 . Concentration = $5.60 \cdot 10^{-5} \text{ mol/L}$

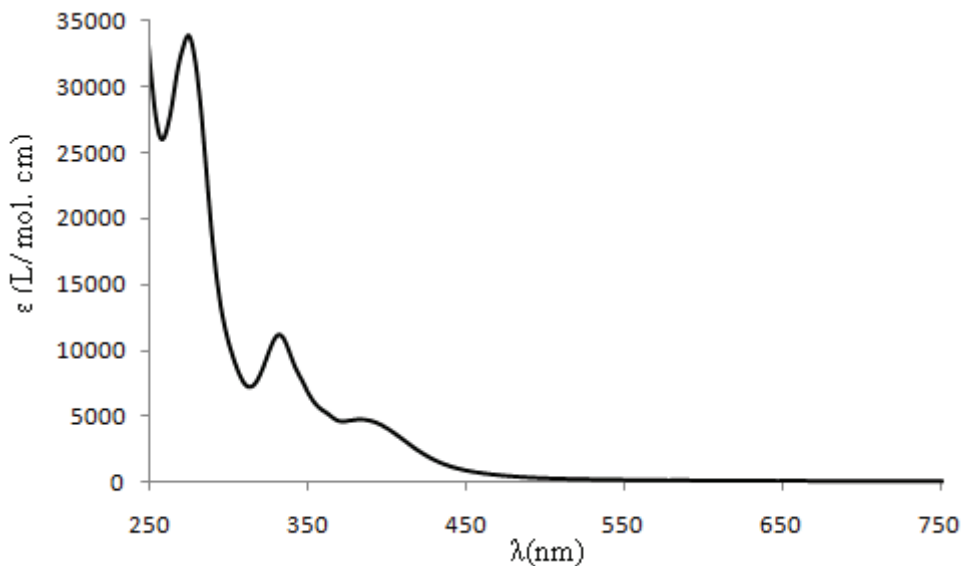


Figure 2.12. UV-Vis of complex **5** in CH_2Cl_2 . Concentration = $5.80 \cdot 10^{-4} \text{ mol/L}$

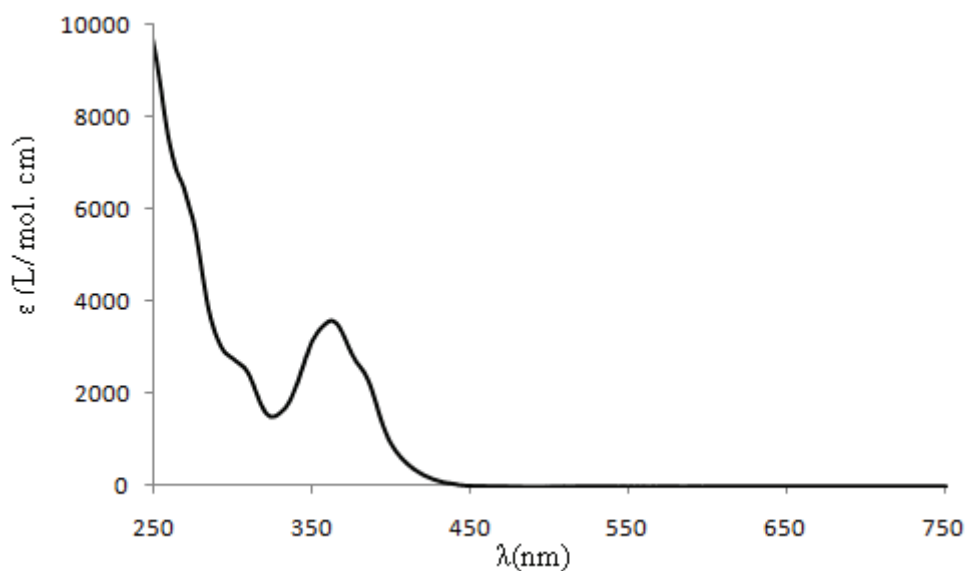


Figure 2.13. UV-Vis of complex **6** in CH_2Cl_2 . Concentration = 7.85×10^{-5} mol/L

Chapitre 3: Hydroamination and Alcoholytic of Acrylonitrile**Promoted by the Pincer Complex { $\kappa^P, \kappa^C, \kappa^P$ -2,6-**

Abderrahmen B. Salah, Caroline Offenstein, and Davit Zargarian*

Département de chimie, Université de Montréal, Montréal (Québec), Canada H3C 3J7

Soumis à Organometallics Juin 2011

3.1. Abstract

This report describes catalytic activities of the pincer-type complex $\{\kappa^P,\kappa^C,\kappa^P\text{-}2,6\text{-}(\text{Ph}_2\text{PO})_2\text{C}_6\text{H}_3\}\text{Ni}(\text{OSO}_2\text{CF}_3)$ (**1**) in the anti-Markovnikov addition of aliphatic and aromatic amines and alcohols to acrylonitrile, crotonitrile, and methacrylonitrile. The influence of additives on the catalytic activities was investigated and it was found that sub-stoichiometric quantities of water promoted the C-N bond forming reactions catalyzed by **1**, especially the reactions involving aromatic amines; in comparison, NET_3 had a less dramatic impact. The opposite pattern was observed for the alcoholysis of acrylonitrile promoted by **1**: water had no beneficial effect on these reactions, while NET_3 proved to be a potent promoter. Another important difference between these reactions is that hydroamination works better with more nucleophilic amines, whereas the alcoholysis reactions work well with ArCH_2OH , $\text{CF}_3\text{CH}_2\text{OH}$, and ArOH , but not at all with the more nucleophilic aliphatic alcohols methanol, ethanol, and isopropanol. Both hydroamination and alcoholysis proceed much better with acrylonitrile compared to its Me-substituted derivatives crotonitrile and methacrylonitrile. Under optimized conditions, precatalyst **1** promotes conjugate additions to acrylonitrile with catalytic turnover numbers of up to 100 (hydroamination) or higher (alcoholysis). Spectroscopic studies have established that the main Ni-containing species in the hydroamination reactions is a cationic adduct in which the olefinic substrate is bound to the Ni center via its nitrile moiety; this binding activates the double bond toward an outer sphere nucleophilic attack by the amine (Michael addition). The solid state structures of the cationic nitrile adducts $[\{\kappa^P,\kappa^C,\kappa^P\text{-}2,6\text{-}(\text{Ph}_2\text{PO})_2\text{C}_6\text{H}_3\}\text{Ni}(\text{NCR})][\text{OSO}_2\text{CF}_3]$ ($\text{R= Me, } \mathbf{2a}; \text{CH}_2\text{CH}_2\text{N(H)Ph, } \mathbf{2e}$), which can be regarded as model complexes for the species involved in the hydroamination catalysis,

have been elucidated. Also reported are the solid state structures of the charge-neutral compound $\{\kappa^P,\kappa^C,\kappa^P\text{-}2,6-(i\text{-Pr}_2\text{PO})_2\text{C}_6\text{H}_3\}\text{Ni}(\text{OSO}_2\text{CF}_3)$ and an octahedral Ni(II) species obtained from the aerobic/hydrolytic oxidation of **1**.

3.2. Introduction

The past two decades have witnessed spectacular advances in transition metal-catalyzed organic transformations as many different families of complexes have been shown to catalyze a diverse array of reactions involving C-C and C-heteroatom bond formation. Pincer complexes¹ have been at the forefront of advances in catalytic hydrogenation, dehydrogenation, coupling, addition and other transformations.² The tridentate, meridional ligation of a metal center by pincer ligands gives rise to structurally robust complexes that facilitate useful reactivities thanks primarily to their thermal stability and stabilization of unusual oxidation states. These important characteristics and the relative ease with which it is possible to generate new pincer ligands featuring variable electronic and steric properties have fuelled the growth of pincer chemistry and expanded their applications.^{3,4}

One of the earliest applications of pincer complexes in catalysis was described in Trogler's reports on direct addition of amine N-H bonds to activated olefins.⁵ These reports showed that the complex $[\{\kappa^P,\kappa^C,\kappa^P\text{-(}t\text{-Bu}_2\text{P)}(\text{CH}_2)_5(\text{P}(t\text{-Bu})_2)\}\text{PdX}]$ ($\text{X} = \text{Me}$, BF_4^-) can bind the nitrile moiety of acrylonitrile, thus activating the double bond towards nucleophilic attack by aniline. The catalytic activities afforded by this system were shown to be greater than those obtained by the non-pincer species $(\text{PMe}_3)_2\text{PdMe}_2$, $(\text{dmpe})\text{PdR}_2$, and $(\text{dppe})\text{PdR}_2$ ($\text{dmpe} = \text{Me}_2\text{PCH}_2\text{CH}_2\text{PMe}_2$; $\text{dppe} = \text{Ph}_2\text{PCH}_2\text{CH}_2\text{PPh}_2$; $\text{R} =$

CH_2SiMe_3 , Me). Given the importance of olefin hydroamination as an attractive, atom-efficient approach for the preparation of new amines,⁶ many other reagents have been developed for promoting this reaction, including complexes of lanthanides,⁷ group 4 metals,⁸ Rh,⁹ Ir,¹⁰ Ni,¹¹ Pd,¹² Pt,¹³ and Cu.¹⁴ The analogous addition of alcohol O-H bonds to olefins (alcoholysis), which is an equally attractive approach for making new ethers, can be promoted by catalysts based on Cu¹⁴, Ag,¹⁵ Au,¹⁶ Ru,¹⁷ Rh,¹⁸ Pd,¹⁹ and Pt,²⁰ and also by some Lewis and Bronsted acids²¹ and bases.²²

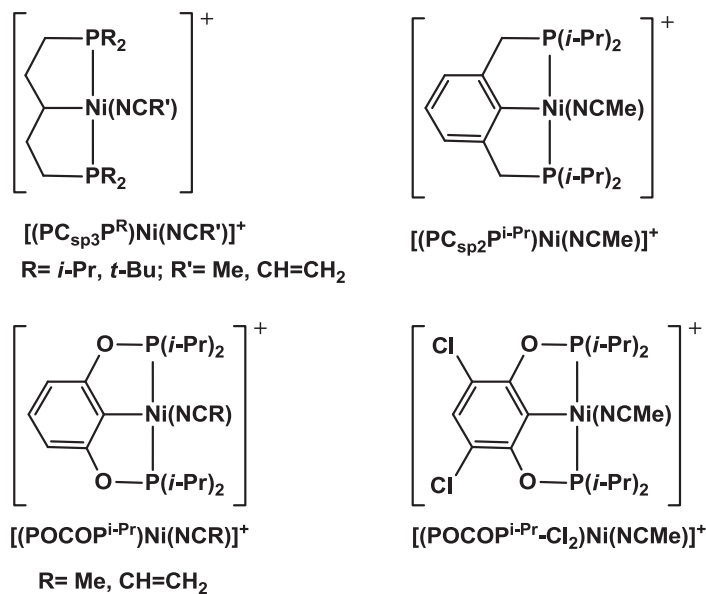


Figure 3.1. PCP and POCOP type pincer complexes

Our group has been interested in developing synthetic routes to pincer complexes of nickel and exploring their reactivities as pre-catalysts for a variety of reactions, including the hydroamination and alcoholysis of olefins.^{23,24} We have shown that cationic Ni(II) complexes based on PCP- and POCOP-type pincer ligands (Figure 3.1) serve as competent pre-catalysts for the addition of aliphatic and aromatic amines to acrylonitrile and its derivatives (Michael additions). For example, the cationic complexes

$[(PC_{sp^3}P^{i-Bu})-Ni(NCCH=CH_2)]^+$,^{23d} $[(PC_{sp^3}P^{i-Pr})Ni(NCMe)]^+$,²³ⁱ $[(PC_{sp^2}P^{i-Pr})Ni(NCMe)]^+$,²³ⁱ $[(POCOP^{i-Pr})Ni(NCR)]^+$ (R= Me, ^{23i,m} CH=CH₂^{23g}), and $[(POCOP^{i-Pr}-Cl_2)Ni(NCMe)]^+$,²³ⁱ promote the anti-Markovnikov addition of amines to acrylonitrile. Catalytic turnover numbers (TON) of up to 100 have been achieved for the addition of poorly nucleophilic aromatic amines at 60 °C and in the presence of NEt₃,^{23m} whereas much greater TON are attainable with more nucleophilic aliphatic amines.^{23g} Very recently, $[(POCOP^{i-Pr})-Ni(NCMe)]^+$ was also found to catalyze the addition of substituted phenols to acrylonitrile.^{23m}

As alluded to above, Michael-type addition of amines to cyano olefins catalyzed by cationic precatalysts are believed to proceed via a Lewis acid mechanism involving coordination of the nitrile moiety, which serves to enhance the electrophilicity of the C=C moiety. We reasoned that Ni precatalysts based on a less nucleophilic pincer ligand should generate more strongly electrophilic cationic intermediates wherein the coordinated cyano olefins should experience greater activation towards nucleophiles. To test the validity of this supposition, we have studied the relative efficacies of precatalysts based on POCOP^{Ph} and POCOP^{i-Pr} ligands for Michael additions on acrylonitrile and its derivatives. The present report describes the catalytic activities of the in-situ generated cations $[(POCOP^R)Ni(NCR')][OTf]$ (R= Ph, *i*-Pr; OTf= OSO₂CF₃) in the hydroamination and alcoholysis of acrylonitrile, crotonitrile, and methacrylonitrile. Also described are the preparation and spectroscopic characterization of the cationic complexes $[(POCOP^{Ph})Ni(NCR)][OTf]$ (R= Me, **2a**; CH=CH₂, **2b**; CH=CHMe, **2c**; C(Me)=CH₂, **2d**; CH₂CH₂N(H)Ph, **2e**) as well as the solid state structures of the cationic adducts **2a**

and **2e**, the precatalyst $(POCOP^{i-Pr})Ni(OTf)$, and a new octahedral complex obtained from the aerobic/hydrolytic decomposition of the precatalyst $(POCOP^{Ph})Ni(OTf)$, **1**.

3.3. Results and Discussion

The proposed catalytic investigations can be conducted by using the pre-formed cationic adducts $[(POCOP)Ni(NCR)]^+$ as well-defined precatalysts. Alternatively, the requisite cationic species can be generated in-situ using the charge-neutral triflate derivatives $(POCOP)Ni(OTf)$ as precursors, because the triflate moiety is displaced readily by the cyano olefin that is present in excess in catalytic reaction mixtures. One advantage of using pre-formed cations is that they are often quite robust under ambient conditions and can be stored over relatively long periods without decomposition; on the other hand, the isolation of analytically pure samples of such cationic complexes is sometimes problematic, and so the composition of precatalysts can vary from one batch to another. The advantage of using triflate derivatives as catalyst precursors is that they are usually easier to prepare and isolate in pure form, but they are also more susceptible to hydrolysis under ambient conditions, which can compromise the purity of aged samples. To determine which species, the charge-neutral triflate derivative or a cationic nitrile adduct, should be regarded as the more practical $POCOP^{Ph}$ -based catalyst precursor for the envisaged catalytic reactions, we prepared samples of these derivatives and tested their sensitivity to ambient atmosphere and catalytic activities.

Table 3.1. UV-Vis data for the cationic adducts $[(\text{POCOP}^{\text{Ph}})\text{Ni}(\text{NCR})][\text{OTf}]$

NCR	$\lambda(\text{nm})$	$\nu (\text{cm}^{-1})$	$\epsilon (\text{L/mol.cm})$
NCMe	386	25 907	993
NCCH=CH ₂	390	25 641	2266
NCCH=CH(Me)	395	25 316	963
NCC(Me)=CH ₂	390	25 641	659

3.3.1. Synthesis and characterization of cationic precursors.

Initial tests showed that the previously reported triflate derivative ($\text{POCOP}^{\text{Ph}}\text{Ni}(\text{OTf})$, **1**, ^{23r}) is a suitable precursor for the synthesis of the cationic adducts $[(\text{POCOP}^{\text{Ph}})\text{Ni}(\text{NCR})][\text{OTf}]$. For instance, monitoring C₆D₆ solutions of **1** ($\sim 2.9 \times 10^{-2}$ M) by ³¹P{¹H} NMR spectroscopy showed that addition of one or more equiv of RCN caused the immediate disappearance of the precursor signal at ca. 143 ppm and new signals appeared at δ 149.7 (acetonitrile), 150.5 (acrylonitrile), and 150.8 (crotonitrile and methacrylonitrile). Monitoring these substitution reactions by UV-Vis spectroscopy showed that reaction of **1** with acetonitrile resulted in bathochromic displacement of an MLCT band (396 nm to 386 nm, Figure 3.15-SI in Supporting Information), consistent with the somewhat paler color of the new species. Similar observations were made for the reactions with acrylonitrile and its Me-substituted derivatives ($\lambda_{\text{max}} \sim 385\text{-}395$ nm, Table 3.1).

The above observations suggested that the triflate moiety in **1** can be displaced by RCN, and encouraged us to attempt the synthesis of the cationic adducts $[(\text{POCOP}^{\text{Ph}})\text{Ni}(\text{NCR})][\text{OTf}]$. The acetonitrile adduct $[(\text{POCOP}^{\text{Ph}})\text{Ni}(\text{NCMe})][\text{OTf}]$, **2a**,

was prepared by stirring **1** in acetonitrile for 30 min at room temperature, and isolated in ca. 80% yield by evaporation of the mixture and recrystallization of the crude product from toluene/hexane. This complex could also be obtained, albeit in a somewhat lower yield, by reacting the bromo precursor with AgOTf in acetonitrile (Figure 3.2). Using similar procedures, we also generated and spectroscopically characterized analogous cationic adducts with acrylonitrile (**2b**), crotonitrile (**2c**), and methacrylonitrile (**2d**); unfortunately, however, we did not succeed in obtaining analytically pure samples of these adducts for complete characterization and study. On the other hand, complex **2a** has been characterized fully, including its solid state structure, as described below.

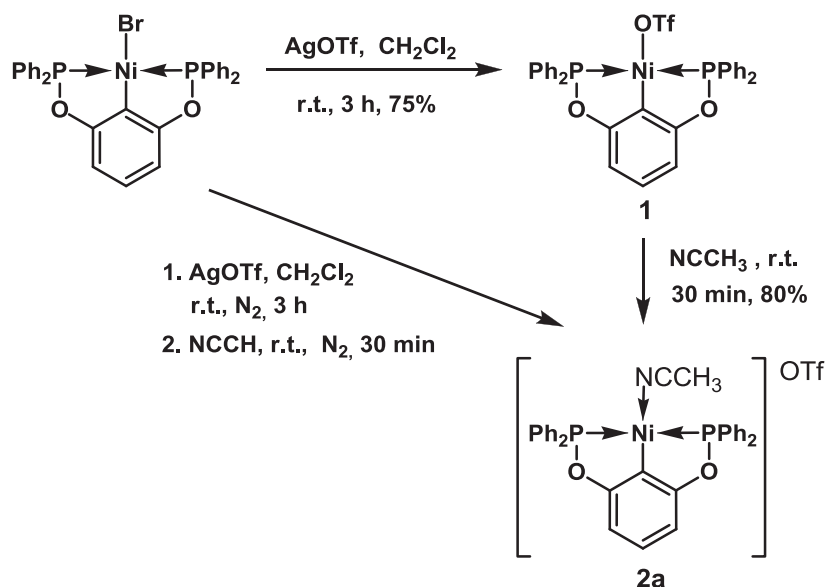


Figure 3.2. Synthesis path of complex **2a**

Analysis of the ^1H NMR spectra showed relatively minor differences between the new cationic adducts **2** and the charge-neutral triflate complex **1**. For instance, the aromatic resonances for H4 on the central ring and the *p*- and *m*-H in PPh_2 shifted

downfield by about 0.2-0.3 ppm, whereas the *o*-H shifted upfield by about 0.36 ppm. The H3/H5 and H4 resonances of **2a** shifted downfield by about 0.3 ppm compared to its *i*-Pr₂P counterpart,^{23g} whereas the NCCH₃ resonance is shifted upfield by 0.15 ppm. The ¹³C{¹H} NMR spectrum of **2a** showed the characteristic triplet resonance for C1 and virtual triplet resonances for C2/C6 and all the PPh carbon nuclei; the resonance for C1 is shifted downfield by 8 ppm compared to [(POCOP^{*i*-Pr})Ni(NCMe)][OTf].^{23g} Interestingly, the UV-Vis spectrum of the latter was virtually identical to that of **2a** (See Figures 3.13-SI and 3.15-SI, Table 1), indicating that the *P*-substituent has little or no influence on the electronic transitions in this family of complexes. Finally, cyclic voltammetry measurements showed that the cationic complex **2a** undergoes a quasi-reversible redox process very similar to that of the charge-neutral triflate complex **1** ($E^0_{1/2}$ (Ni^{II}/Ni^{III})~0.80 V).²⁵ Observation of similar redox potentials for **1** and **2a** implies that the MeCN→Ni⁺ interaction in **2a** transfers sufficient electron density to compensate for the positive charge on Ni.

Single crystals for complex **2a** were obtained and subjected to crystallography in order to determine its solid state structural parameters. Crystal and data collection details are presented in Table 3.2, selected structural parameters are listed in Table 3.3, and the ORTEP diagram is shown in Figure 3.3. The overall geometry around the Ni atom in **2a** is square planar, but the small bite angle of the POCOP ligand gives rise to a smaller than ideal P-Ni-P angle of 163°. The Ni-C and C≡N distances and main angles are virtually identical in **2a** and its *i*-Pr analogue, but the Ni-P distances are significantly longer in **2a**, which is consistent with the weaker nucleophilicity of the PPh₂ moiety vs. P(*i*-Pr)₂.^{23g}

Table 3.2. Crystal Data Collection and Refinement Parameters for Complexes 2a, 2e, 3 and 4.

	2a	2e	3	4
Chem. Formula	C ₃₂ H ₂₆ O ₂ P ₂ Ni, 0.5(C ₆ H ₁₄), (CF ₃ O ₃ S)	C ₃₉ H ₃₃ N ₂ NiO ₂ P ₂ , C ₇ H ₈ ,CF ₃ O ₃ S	C ₁₉ H ₃₁ O ₅ F ₃ P ₂ S ₁ Ni	C ₆₀ H ₅₆ O ₁₂ P ₂ Ni, 2(C ₄ H ₁₀ O), 2(CF ₃ O ₃ S)
Cryst. colour	yellow	yellow	Yellow	yellow
Fw	769.34	923.53	549.15	1580.02
T (K)	200(2)	150(2)	200(2)	100(2)
λ (Å)	1.54178	1.54178	1.54178	1.54178
Space Group	P-1	P2 ₁ /c	P2 ₁ /n	P-1
a (Å)	8.6077(3)	12.0258(4)	9.8032(1)	11.5099(4)
b (Å)	14.2378(4)	31.2235(10)	18.4399(3)	13.1896(4)
c (Å)	15.1147(5)	12.5921(4)	14.8955(2)	14.4315(5)
α (deg)	96.3850(10)	90	90	66.105(2)
β (deg)	105.1370(10)	113.407(1)	109.198(1)	83.163(2)
γ (deg)	93.290(2)	90	90	66.897(2)
Z	2	4	4	1
V(Å ³)	1769.79(10)	4339.1(2)	2542.92(6)	1840.36(11)
ρ _{calcd}	1.444	1.414	1.434	1.442
μ (cm ⁻¹)	27.05	23.14	34.97	24.79
θ range (deg)	3.06 -72.14	2.83- 69.74	3.95-72.49	3.35-71.09
N° of all ref.	21999	88707	32945	48543
N° of uniq. ref.	14944	8163	4960	6903
Rint	0.0781	0.045	0.035	0.057
R1 ^a [I>2σ]	0.0631	0.0425	0.0390	0.0583
wR2 ^b [I > 2σ]	0.1736	0.1149	0.1042	0.1647

R1[all data]	0.0658	0.0439	0.0406	0.0649
WR2[all data]	0.1771	0.1166	0.1061	0.1732
GOF	1.028	1.017	1.037	1.075
No. of restraints	3	28	0	4

$$^a R_1 = \sum(|F_o| - |F_c|) / \sum |F_o| \quad ^b wR_2 = \{ \sum [w(F_o^2 - F_c^2)^2] / \sum [w(F_o^2)^2] \}^{1/2}$$

Table 3.3. Selected Bond Distances (Å) and Angles (deg) for 2a, 1, and their POCOP*i*-Pr analogues

	2a	[(POCOP <i>i</i> -Pr)Ni(NCMe)][OTf]	1	3
Ni-C1	1.885(3)	1.881(2)	1.870(2)	1.875(2)
Ni-P1	2.1782(7)	2.1683(7)	2.1667(6)	2.1793(5)
Ni-P2	2.1796(7)	2.1704(7)	2.1860(6)	2.1817(5)
Ni-N or Ni-O	1.891(2)	1.874(2)	1.934(2)	1.951(1)
C1-Ni-P1	81.94(8)	81.93(7)	82.02(6)	81.97(6)
C1-Ni-P2	81.94(8)	82.46(7)	81.61(6)	82.22(6)
C1-Ni-X	178.0(1)	175.8(1)	173.63(7)	178.67(7)
P1-Ni-P2	163.28(3)	164.38(3)	163.24(2)	163.83(2)
P1-Ni-X	98.52(7)	96.67(6)	92.74(5)	96.71(5)
P2-Ni-X	98.17(7)	98.87(6)	103.35(5)	99.11(5)
C≡N	1.140(4)	1.140(3)	-----	-----

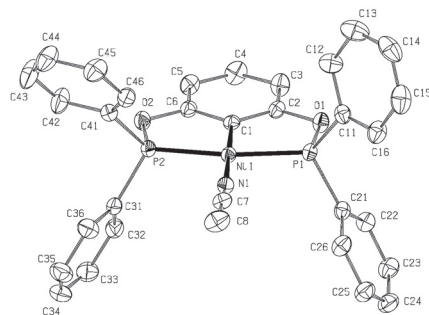


Figure 3.3. ORTEP diagram for complex **2a**. Thermal ellipsoids are set at the 50% probability level. The triflate anion, solvent and the calculated hydrogen atoms are omitted for clarity.

3.3.2. Relative stabilities of complexes **1**, **2a**, and **3**.

Having access to the charge-neutral triflate derivative **1** and the cationic adduct **2a** allowed us to examine their respective suitability for the envisaged catalytic studies. Initial tests showed that **2a** is resistant to hydrolysis/oxidation, both in the solid state and in solution, whereas **1** decomposes when exposed to ambient atmosphere; as anticipated, this decomposition is faster for solutions of **1** (ca. 20% decomposition over 1-2 h) than solid samples (over a day or more). To gain some insight into this decomposition pathway, we exposed a toluene solution of **1** to ambient atmosphere for 2 days, which resulted in the isolation of a small crop of crystals that turned out to be the dicationic, octahedral Ni(II) complex **4** (*vide infra*). Thus, aerobic/hydrolytic decomposition of **1** results in the protonation of the aryl moiety of the POCOP^{Ph} ligand, oxidation of the phosphine moieties, and coordination of four water molecules to the nickel center. It is interesting to note that complex **3**, the *i*-Pr analogue of **1**, reacts very differently when exposed to ambient air: a slow and clean displacement of the triflate moiety by water

gives the cationic aquo adduct $[(\text{POCOP}^{i\text{-Pr}}\text{Ni}(\text{OH}_2)][\text{OTf}]^{26}$ which does not react further with oxygen or water (Figure 3.4).

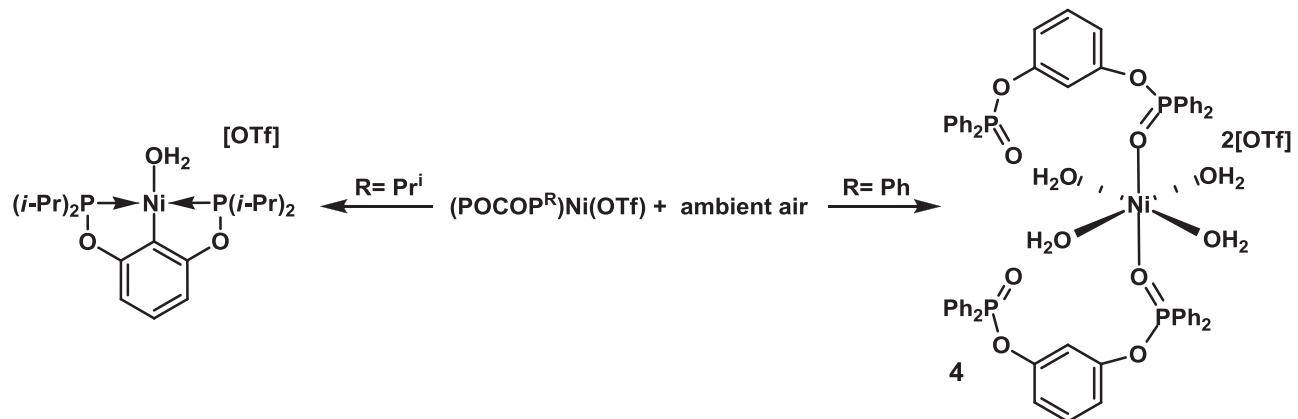


Figure 3.4. Reaction of triflate derivatives under ambient air

The observed difference between the aerobic/hydrolytic decomposition pathways traversed by these closely related complexes prompted us to revisit this issue by exposing solutions of **3** to ambient air for longer periods of time and examining the decomposition product(s). Curiously, the crystals obtained during our decomposition tests with complex **3** turned out to be those of the intact triflate derivative, which had proven elusive during several previous recrystallization attempts! The solid state structures of **3** and **4** were elucidated X-ray by means of diffraction studies and are discussed below.

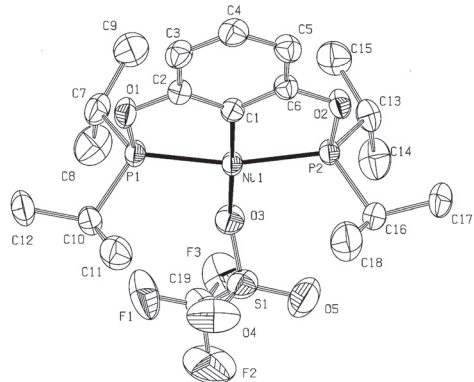


Figure 3.5. ORTEP diagram for complex **3**. Thermal ellipsoids are set at the 50% probability level. Calculated hydrogen atoms are omitted for clarity.

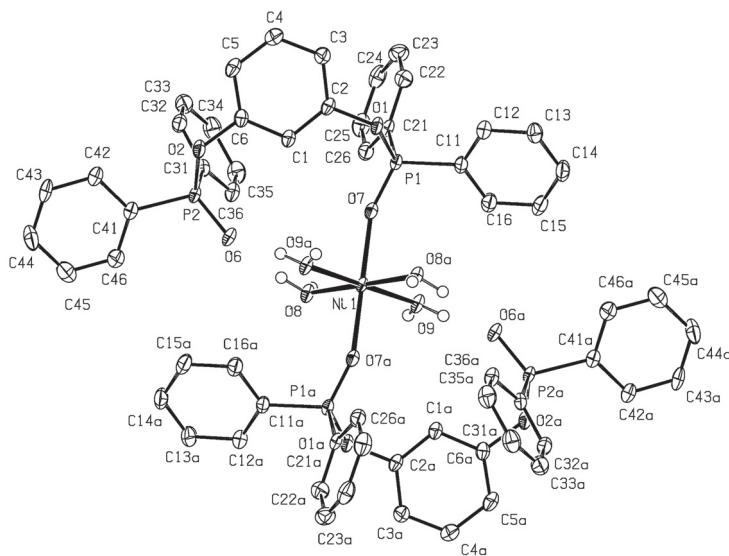


Figure 3.6. ORTEP diagram for complex **4**. Thermal ellipsoids are set at the 50% probability level. Calculated hydrogen atoms, triflate anion, and solvent are omitted for clarity. Selected distances (\AA) and angles ($^\circ$): Ni-O7= 2.076(2); Ni-O8= 2.053(2); Ni-O9= 2.052(2); O7-P1= 1.479(2); O6-P2= 1.486(2); O7-Ni-O8= 90.02(7); O7-Ni-O9= 88.39(7); O8-Ni-O9= 93.08(7); P1-O7-Ni= 152.1(1).

The ORTEP diagram for complex **3** is shown in Figure 3.5, and selected structural parameters are listed in Table 3.3 along with the corresponding data for the Ph analogue **1**.^{23r} As was the case for **2a** and **1**, the coordination geometry around Ni in complex **3** is approximately square planar, but the small bite angle of the POCOP ligand results in a smaller than ideal P-Ni-P angle of ca. 164° (Table 3.3). The two Ni-P distances are fairly similar (ca. 2.18 Å) as in **2a** but unlike the case in **1** wherein the two values are fairly different (2.167 and 2.186 Å). The Ni-C distance in **3** is similar to the corresponding values in **1** and **2a** (1.875(2) vs. 1.870(2) and 1.885(3) Å), but the Ni-O(sp³) distance is somewhat longer than that in **1** (ca. 1.95 vs. 1.93 Å). The S=O distances are ca. 1.40 and 1.43 Å, while the unique S-O distance is 1.46 Å.

The ORTEP diagram for complex **4** and a selection of structural parameters are shown in Figure 3.6. The Ni atom, which resides on an inversion center, is coordinated by 6 oxygen atoms in an octahedral geometry. All four aquo ligands are engaged in H-bonding, two with the two S=O moieties of the triflate anion and the other two with the two P=O moieties. The Ni-OH₂ distance is somewhat shorter than the corresponding Ni-O=P distance (ca. 2.05 Å vs. 2.08 Å). The P-O distance in the non-coordinating P=O moiety is somewhat longer than the P=O moiety coordinated to Ni (1.486(2) vs. 1.479(2) Å).

3.3.3. Catalytic hydroamination of acrylonitrile catalyzed by the triflate derivatives **1** and **3**.

Although the results of the above decomposition tests implied that the more robust complex **2a** should be the more suitable pre-catalyst for the envisaged catalytic

reactions, tests of hydroamination efficacy showed the charge-neutral triflate derivative **1** to be a much more active precatalyst. For example, addition of aniline to acrylonitrile proceeded with higher TON when the triflate derivative was used as precursor (TON~50-75 for **1** vs. ~15 for **2a**). Even though we have not been able to identify the reason(s) for the poor effectiveness of the cationic species **2a** for the hydroamination reactions, it was concluded that the charge-neutral Ni-OTf precursor **1** would be a more promising precatalyst for the purposes of our study. Therefore, we have screened the catalytic reactivities of **1** and its *i*-Pr analogue **3** to evaluate the influence of *P*-substituents on reactivities.

Multiple optimization experiments were conducted to determine the importance of various reaction conditions on the hydroamination of acrylonitrile (Figure 3.7). A standard protocol was devised in order to evaluate systematically the catalytic competence of (POCOP^R)Ni(OTf) complexes as a function of *P*-substituents R. This protocol consisted of stirring at 50 °C for 3 h mixtures containing 100 equiv each of the amine and acrylonitrile, dodecane (as internal standard for the GC/MS analyses), and complex **1** or its POCOP^{i-Pr} analogue, **3**, as precatalyst (0.02 M solutions); the final mixtures were filtered and analyzed by GC/MS. Initial tests showed that dry toluene (ca. 1 mL) was the best solvent for these reactions: hexane or acetonitrile led to much lower yields, whereas other solvents such as THF, dichloromethane and ethyl acetate promoted double additions with primary amines. Control experiments were also conducted and showed that hydroamination of acrylonitrile proceeds in the absence of a catalyst only for addition of morpholine (ca. 25% after 24 h at r.t.), whereas no direct and uncatalyzed amination was observed with other aliphatic amines (cyclohexylamine, diethylamine, and

benzylamine: 24 h at r.t. or 12 h at 70°C) or substituted anilines (10 days at r.t. or 3 days at 60 °C).

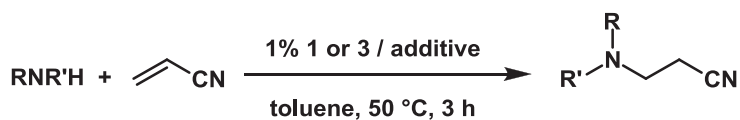


Figure 3.7. Equation of hydroamination of acrylonitrile

Table 3.4. Catalytic activities for hydroamination of acrylonitrile

Runs	Amines	Turnover numbers					
		A ^a		B ^b		C ^c	
		1	3	1	3	1	3
1	Aniline	50	42	55	100	75	53
2	3-Methylaniline	75	100	70	100	100	90
3	4-Methoxyaniline	80	100	83	100	100	95
4	N-Ethyl aniline	90	92	7	92	100	47
5	4-Chloroaniline	0	0	36	100	50	8
6	2,5-Dimethylaniline	34	26	40	100	92	74
7	2,4,6-Trimethylaniline	5	0	9	35	18	7
8	Benzylamine	78	94	69	100	100	84
9	Cyclohexylamine	100	100	58	100	100	100
10	Morpholine	100	100	100	100	100	100
11	Diethylamine	42	53	60	100	88	100

All the catalytic reactions were conducted at 50 °C for 3 h and using a 1:1 ratio of acrylonitrile : amine and 1% of complex **1** or **3**.

The reactions were monitored by ¹H and ³¹P NMR and the final mixtures were analyzed by GC/MS. Yields and TON were determined on the basis of calibration curves prepared using authentic samples of the anticipated products. ^a No additive. ^b 50 equiv of NEt₃ present. ^c 50 equiv of water present.

As can be seen from the data listed in Table 3.4, pre-catalysts **1** and **3** showed comparable activities for the addition of aniline to acrylonitrile in the absence of any additives (Runs 1A), but different patterns of reactivity emerged when the reactions were tested in the presence of additives. The influence of NEt_3 was investigated first, because previous studies had shown that sub-stoicheometric quantities of this base favor the catalytic hydroamination of acrylonitrile and its derivatives; bases are thought to play the role of H^+ -transfer agents that can facilitate the conversion of the initial intermediate of the addition into the final product (i.e., $\text{RR}'\text{HN}^+\text{CH}_2\text{C}^-\text{H}(\text{CN}) \rightarrow \text{RR}'\text{NCH}_2\text{CH}_2(\text{CN})$).^{12,23f,m} Tests conducted during the present study showed that adding 50 equiv of NEt_3 to our reaction mixtures improved substantially the addition of aniline to acrylonitrile catalyzed by **3**; in contrast, only negligible or moderate improvements were noted for many of the additions catalyzed by **1** (Runs 1, 3, 6, 7, and 11), while in some cases NEt_3 actually hindered the catalysis (Runs 2, 4, 8, and 9). We also tested other bases or protic reagents such as water for their ability to act as proton transfer agents,²⁷ and found that the presence of 50 equiv of water led to an important increase in the TON for the reaction promoted by **1**, whereas for the reactions promoted by **3** most of the Runs showed no beneficial impact from water.²⁸

Greater reactivities were obtained when electron-donating substituents were introduced on the aromatic ring of aniline (Runs 2 and 3) or its nitrogen atom (Runs 4), whereas an electron-withdrawing substituent retarded the catalysis significantly (Runs 5). On the other hand, the results of Runs 6 and 7 establish the greater sensitivity of the reaction to steric effects: *ortho*-Me substituents severely retard the addition reaction. As anticipated, Runs 8-11 showed that benzyl amine and secondary aliphatic amines are very

reactive for the addition to acrylonitrile, especially in the presence of NEt₃ (with **3**) or water (with **1**). One anomalous observation is the greater reactivity of *N*-ethylaniline (Runs 4) vs. diethyl amine (Runs 11) in the absence of additives: the more nucleophilic amine seems to be less reactive, presumably due to the side reactions engendered by the competitive binding of HNEt₂ to the cationic Ni center (*vide infra*).

In summary, the catalytic activities listed in Table 3.4 show that NEt₃ and water have different impacts on the two precatalysts studied. For instance, the presence of water is beneficial for all additions to acrylonitrile catalyzed by precatalyst **1**, whereas in the case of reactions catalyzed by **3** water can be very beneficial (Runs 6 and 11), somewhat beneficial (Runs 1, 5, 7, and 8), or even detrimental (Runs 2, 3, 4, and 8). Likewise, the presence of NEt₃ improves the catalysis significantly in all instances where the standard, additive-free reaction conditions give TON values of less than 90 with precatalyst **3** (Runs 1, 6, 7, and 11); on the other hand, the impact of NEt₃ on additions catalyzed by **1** can be quite beneficial (Runs 5), somewhat beneficial (Runs 1, 3, 6, 7, and 11), somewhat detrimental (Runs 2 and 8), or highly detrimental (Runs 4). We conclude that the best overall catalyst precursor for promoting the hydroamination of acrylonitrile is the combination of **3** and NEt₃, but the combination of **1** and water is nearly as effective.

3.3.4. Hydroamination with crotonitrile and methacrylonitrile.

Control experiments showed that in the absence of a catalyst none of the amines tested reacts with methacrylonitrile or crotonitrile (75 °C, 24 h), a testimony to the inherently lower electrophilicity of the double bond in these substrates compared to acrylonitrile. Indeed, tests showed that even the catalyzed hydroamination of these

olefins proceeds only with morpholine as the nucleophile. Thus, heating a mixture of morpholine and methacrylonitrile or crotonitrile at 60 °C in the presence of **1** gave the anti-Markovnikov hydroamination product with a TON of 100 over 3 h; interestingly, lower TON were obtained when the reaction mixture contained the additives NEt_3 (60) or water (45).

3.3.5. Catalytic alcoholysis of acrylonitrile.

Control experiments showed that acrylonitrile does not react with alcohols in the absence of a precatalyst, but with certain alcohols the alcoholysis was observed in the presence of a catalytic amount of **1** (Figure 3.8. Table 3.5), corroborating the crucial role played by this compound in promoting C-O bond forming reactions. Unfortunately, crotonitrile and methacrylonitrile failed to react, even in the presence of **1**, with any of the alcohols tested.

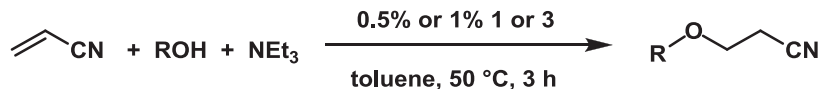


Figure 3.8. Equation of alcoholysis of acrylonitrile

Table 3.5. Catalyzed alcoholysis of acrylonitrile

Run	ROH	Ni:ACN:ROH:N _{Et} ₃	TON	
			1	3 [*]
1a	CF ₃ CH ₂ OH	1 : 200 : 200 : 0	100	0
1b		1 : 200 : 200 : 200	traces	0
2a	PhCH ₂ OH	1 : 100 : 100 : 0	30	0
2b		1 : 200 : 200 : 200	144	0
3a	3,4,5-(OMe) ₃ C ₆ H ₂ CH ₂ OH	1 : 100 : 100 : 0	63	0
3b		1 : 200 : 200 : 200	traces	0
4a	2-Methylphenol	1 : 100 : 100 : 0	17	0
4b		1 : 200 : 200 : 200	54	58
5a	3-Methylphenol	1 : 100 : 100 : 0	37	0
5b		1 : 200 : 200 : 200	182	100
6a	2,4,6-Trimethylphenol	1 : 100 : 100 : 0	9	0
6b		1 : 200 : 200 : 200	64	69
7a	4-Phenylphenol	1 : 100 : 100 : 0	40	0
7b		1 : 200 : 200 : 200	140	60

The catalytic reactions were conducted by adding a mixture of ROH and N_{Et}₃ to a toluene mixture of acrylonitrile and **1**, followed by stirring the resulting mixture at 60 °C over 3 h. The catalysis was monitored by NMR and GC/MS and the final reaction mixtures were analyzed by GC/MS to determine yields. * This column lists the results of catalytic reactions conducted at 60 °C over 24 h (except for run 1 which was allowed to go for 4 h only) in the presence of 1% **3** and using 100 equivalents each of acrylonitrile, the alcohol, and N_{Et}₃.^{23m}

Perhaps the most striking feature of the C-O bond forming reactions reported herein is that they appear to work best with ArCH₂OH (Runs 2 and 3) and the weakly nucleophilic

(and fairly acidic) $\text{CF}_3\text{CH}_2\text{OH}$ (Run 1) and ArOH (Runs 4-7), which contrasts with the hydroamination reactions that proceed most readily with the more nucleophilic amines. Indeed, the more nucleophilic aliphatic alcohols MeOH , EtOH , and $i\text{-PrOH}$ cause a rapid decomposition of complex **1** even at ambient temperature (*vide infra*). Another difference between the alcoholysis and hydroamination reactions studied here is that NEt_3 is a beneficial additive for the alcoholysis catalysis, effectively promoting all the reactions studied except the addition of $\text{CF}_3\text{CH}_2\text{OH}$. Table 3.5 also gives the previously reported results of analogous alcoholysis reactions catalyzed by $[(\text{POCOP}^{i\text{-Pr}})\text{Ni}(\text{NCMe})][\text{OTf}]$.^{23m} Comparison of these results to the analogous reactions using **3** as the precursor reveals that the alcoholysis reactions catalyzed by the precatalyst based on the POCOP^{Ph} ligand proceed either nearly as well (Runs 4b and 6b) or more readily (Runs 1-3, 4a, 5 and 7).

3.3.6. Mechanistic insights.

The most commonly proposed mechanism for Michael-type (conjugate) additions to activated olefins promoted by late transition metals involves outer-sphere attack by an uncoordinated nucleophile on the olefinic substrate that is coordinated to the electrophilic metal centre via the $\text{C}=\text{C}$ moiety or its functional moiety (COOR , CN , etc.), followed by proton transfer to generate the product. For example, in his report on the addition of aniline to acrylonitrile catalyzed by pincer complexes of Pd, Trogler showed that the main species observed in solution during the catalysis is the κ^{N} -acrylonitrile adduct, $[(\text{PCP})\text{Pd}\leftarrow\text{NC}(\text{CH}=\text{CH}_2)]^+$; it was argued, however, that the nitrile binding is fairly labile and allows the formation of minor quantities of the π -bound isomer, which is the intermediate that reacts with aniline to give the hydroamination product.^{5b} Abu-Omar has proposed a similar mechanism involving attack of nucleophiles on π -bound olefins for

the Pd-catalyzed addition of benzyl alcohol to methyl vinyl ketone.^{19b} It is interesting to note that acrylonitrile was unreactive in the latter system, presumably because it binds the Pd center via its nitrile moiety, which does not allow for sufficient activation of the double bond. A new variation of Lewis acid mechanisms was proposed recently by Yi for alcoholysis of acrylonitrile.^{17a} According to this proposal, a Ru(II)-acetamido complex acts as a bifunctional catalyst, affecting a heterolytic activation of the alcohol O-H bond through the acetamido moiety (Lewis basicity) and simultaneously promoting the κ^N -bonding of acrylonitrile to an empty coordination site (Lewis acidity). Finally, Gunnoe has proposed a different mechanism that does not require olefin pre-coordination to the metal, involving instead attack on uncoordinated olefins by nucleophilic Cu-NR₂ and Cu-OR species.^{14a,b}

A number of observations from the present study suggest that hydroamination of amines promoted by complex **1** involves attack of the amine nucleophiles on κ^N -bound cyano olefins, whereas alcoholysis of acrylonitrile likely involves a charge-neutral Ni-OR species. First, our Ni precursors do not bind unactivated olefins or activated olefins bearing functional groups other than nitrile, nor do they promote the hydroamination of these olefins, emphasizing the importance of a nitrile moiety for the success of this reaction. Second, as we have noted above, monitoring the reaction of the precursor **1** with acrylonitrile and its derivatives by $^{31}\text{P}\{^1\text{H}\}$ NMR and UV-vis spectroscopy has confirmed the facile formation of cationic pincer complexes featuring RCN→Ni binding. These observations suggest that the cationic adducts featuring κ^N -NCR are likely involved in the hydroamination catalysis. We have conducted a series of NMR tests in an effort to follow the fate of the cationic acrylonitrile adduct

$[(\text{POCOP}^{\text{Ph}})\text{Ni}(\text{NCCH}=\text{CH}_2)][\text{OTf}]$, **2b**, generated in-situ from **1** under various conditions, as described below.

Addition of a large excess of aniline to a sample of **1** (ca. 0.17 M in C_6D_6) containing 5 equiv of acrylonitrile led to gradual emergence of a new ^{31}P resonance ca. 0.6 ppm downfield of the signal for the acrylonitrile adduct **2a**, suggesting that a structurally very similar new product had formed. The following simple test allowed us to confirm the identity of this new species: to a mixture of **1** and acrylonitrile was added an authentic sample of $\text{NCCH}_2\text{CH}_2\text{N}(\text{H})\text{Ph}$, the anticipated product of the addition of aniline to acrylonitrile; this led to displacement of the coordinated acrylonitrile and produced the same ^{31}P NMR signal mentioned above. The facile formation of this new adduct prompted us to isolate it and elucidate its solid state structure. Diffusion of hexane vapors into a saturated toluene solution of **1** containing one equiv of $\text{NCCH}_2\text{CH}_2\text{N}(\text{H})\text{Ph}$ gave single crystals that were subjected to crystallography. Figure 3.9 shows the ORTEP diagram for $[(\text{POCOP}^{\text{Ph}})\text{Ni}(\text{NCCH}_2\text{CH}_2\text{NHPh})][\text{OTf}]$, **2e**. The coordination geometry of this cationic complex is very similar to that of **2a** discussed above, but **2e** displays H-bonding between the aniline N-H and one of the triflate oxygens; in addition, the triflate moiety experiences a three-fold disorder for the CF_3 group and a two-fold symmetry for the SO_2 moiety. The Ni-C distances are virtually identical in both complexes (ca. 1.88 Å) as are the C-N bond lengths (1.140(4) vs. 1.146(3) Å), but **2a** exhibits somewhat shorter bond distances for Ni-P (av. 2.172 vs. 2.179 Å) and Ni-N (ca. 1.87 vs. 1.89 Å).

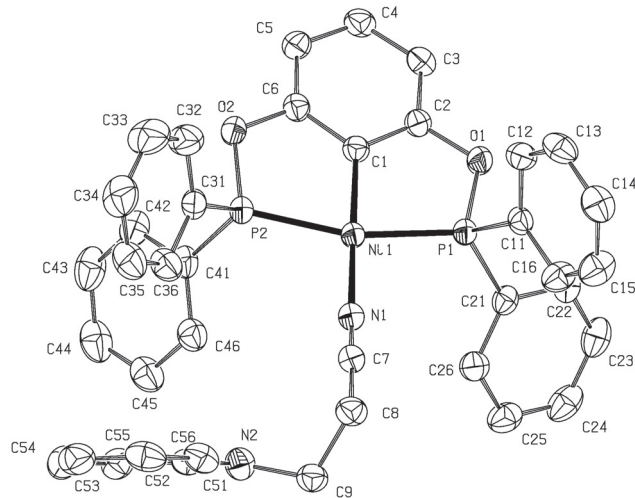


Figure 3.9. ORTEP diagram for complex **2e**. Thermal ellipsoids are set at the 50% probability level. The triflate anion, solvent (toluene) and the calculated hydrogen atoms are omitted for clarity. Selected distances (\AA) and angles ($^{\circ}$): Ni-C1= 1.883(2); Ni-P1= 2.1711(6); Ni-P2= 2.1734(6); Ni-N1= 1.874(2); N1-C7= ; C1-Ni-N1= 175.05(8); P1-Ni-P2= 163.15(2); C1-Ni-P1= 81.63(6); C1-Ni-P2= 81.55(6); P1-Ni-N1= 98.13(5); P2-Ni-N1= 98.72(5); C7-N1-Ni= 168.9(2).

We conclude from the above observations that aniline cannot displace coordinated acrylonitrile in **2b** to form an aniline adduct; instead, it adds to the olefinic moiety of coordinated acrylonitrile to generate the hydroamination product (Figure 3.10). On the other hand, a number of observations have indicated that NEt_3 does bind competitively to the Ni center. For instance, adding NEt_3 to the mixture of **1** and acrylonitrile (in the absence of aniline) led to emergence of a new ^{31}P NMR signal at ca. 136 ppm and a concomitant reduction in the intensity of the original signal; a complete conversion of **1** was observed with a 1:2 ratio of NEt_3 : acrylonitrile. That the new signal at 136 ppm is due to the NEt_3 adduct $[(\text{POCOP}^{\text{Ph}}\text{Ni}(\text{NEt}_3))\text{[OTf}]$ was confirmed by the

observation that the same species formed when 5-10 equiv of NEt_3 were added to a sample of **1** (in the absence of acrylonitrile and aniline, Figure 3.10).

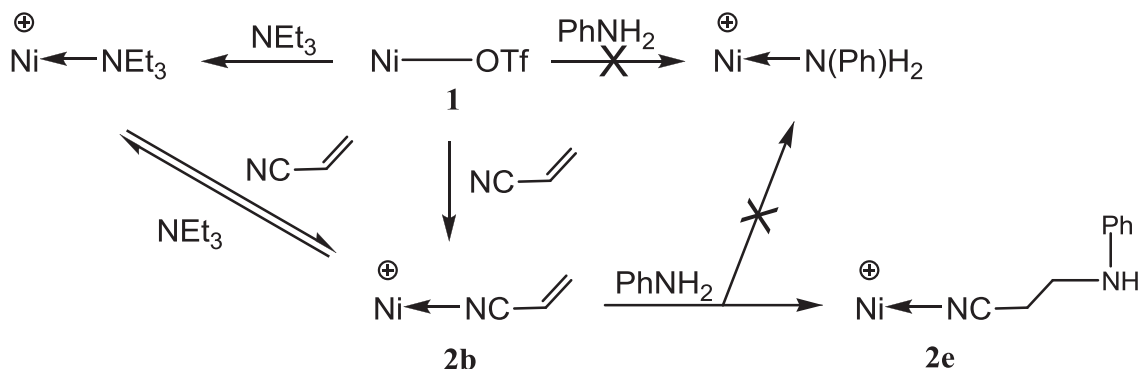


Figure 3.10. Reactivity of complexes **1** and **2b**

The proposed competitive binding of NEt_3 would be expected to have a detrimental effect on the hydroamination efficacy. Indeed, repeating a standard catalytic run in the presence of a large excess of NEt_3 revealed a significant inhibition of the catalysis: stirring a 1 : 200 : 200 : 400 mixture of **1** : acrylonitrile : aniline : NEt_3 for 3 h at 60 °C gave only traces of the anticipated hydroamination product. All of these observations are consistent with the hydroamination mechanism illustrated in Figure 3.11.

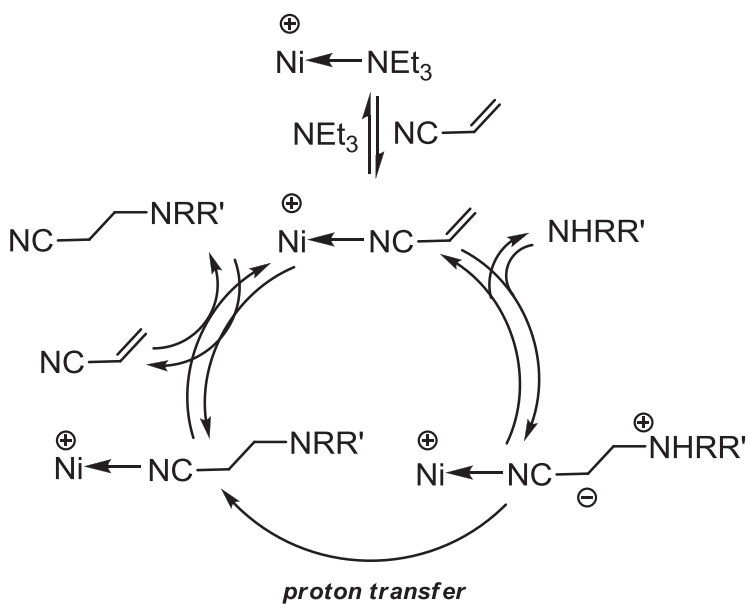


Figure 3.11. Proposed mechanism of hydroamination of acrylonitrile

The observation that NEt_3 binds to the $[(\text{POCOP}^{\text{Ph}})\text{Ni}]^+$ moiety but not to the analogous $[(\text{POCOP}^{i\text{-Pr}})\text{Ni}]^+$ moiety^{23m} underlines the significant influence of *P*-substituents on the substitutional lability of the acrylonitrile adducts $[(\text{POCOP}^{\text{R}})\text{Ni}(\text{NCCH}=\text{CH}_2)]^+$. This finding also provides partial explanation for the generally less beneficial influence of NEt_3 on the hydroamination reactions promoted by 1. Finally, the competitive binding of NEt_3 implies a similar reactivity for Et_2NH , and we found that addition of this amine to 1 gave rise to multiple new species (7 new ^{31}P NMR signals detected), presumably because of side reactions arising from the activation of the N-H bond. These observations can help justify the observation of lower hydroamination reactivity for the more nucleophilic Et_2NH vs. $\text{EtN}(\text{Ph})\text{H}$ (Table 3.4, Runs 4 and 11).

According to the mechanism proposed above (Figure 3.11), hydroamination should proceed equally well with acrylonitrile, crotonitrile, and methacrylonitrile as long

as these substrates are similarly activated toward amine nucleophiles by binding to the electrophilic Ni center. It was found, however, that even though all three substrates can generate the requisite cationic intermediates $[(\text{POCOP}^{\text{Ph}})\text{Ni}(\text{NCR})][\text{OTf}]$, hydroamination is much more sluggish for crotonitrile and methacrylonitrile. In the absence of solid state structures that could provide some indication of how effectively these substrates can bind to the Ni center, we have used IR spectroscopy to probe the question of whether or not the relative inertness of crotonitrile and methacrylonitrile might be due to a less effective binding of these substrates to Ni, which would in turn lead to insufficient activation of their double bonds. Given the sensitivity of the $\nu(\text{CN})$ value to the nature of electronic interaction in $\text{RCN} \rightarrow \text{M}$, we reasoned that IR data for $[(\text{POCOP}^{\text{Ph}})\text{Ni}(\text{NCR})][\text{OTf}]$ might serve as an indirect measure of the extent to which the conjugated double bond of the respective cyano olefin is activated towards nucleophilic attack upon coordination to the electrophilic metal center. As seen from the data tabulated in Table 3.6, the discrepancy in the values of $\Delta\nu(\text{CN})$ for acrylonitrile (25 cm^{-1}), crotonitrile (23 cm^{-1}), and methacrylonitrile (24 cm^{-1}) is not sufficient to explain the greater reactivity of acrylonitrile. Moreover, the similar $\Delta\nu(\text{CN})$ values indicate that the RCN adducts studied here bind equally effectively to Ni, and so the lower susceptibility of the conjugated double bond in crotonitrile and methacrylonitrile towards amine nucleophiles must be due to another phenomenon.

Table 3.6. Values of ν (CN) for various RCN and their Ni adducts

RCN	ν (CN) (cm^{-1})		$\Delta\nu$ (CN) (cm^{-1})
	Free RCN	$[(\text{POCOP}^{\text{Ph}})\text{Ni}(\text{NCR})][\text{OTf}]$	
Acetonitrile	2253	2297	44
Acrylonitrile	2229	2254	25
Crotonitrile	2222	2245	23
Methacrylonitrile	2228	2252	24

The IR data listed in Table 3.6 also reveal two other noteworthy points. First, the greater $\Delta\nu$ (CN) value for the acetonitrile adduct of POCOP^{Ph} (44 cm^{-1}) vs. $\text{POCOP}^{i\text{-Pr}}$ (39 cm^{-1})^{23g} supports our contention that the POCOP^{Ph} system is more electrophilic compared to its *i*-Pr analogue. Second, observation of comparable $\Delta\nu$ (CN) values for acetonitrile adducts of our d^8 Ni systems and that of the d^0 complex $[\text{Cp}_3\text{Zr}(\text{NCMe})_3][\text{BPh}_4]$ ²⁹ ($39\text{-}47$ vs. 42 cm^{-1}) implies that the Ni-N interaction in the complexes under study is dominated by N \rightarrow Ni σ -donation (no π -backbonding), which serves to reinforce the C≡N bond.

3.3.7. On the mechanism of alcoholysis reactions catalyzed by 1.

There are some indications that the alcoholysis reactions catalyzed by 1 do not follow the same Lewis-acid type mechanism as the hydroamination reactions discussed above. First, the alcoholysis of acrylonitrile promoted by 1 proceeds better with the less nucleophilic, more acidic alcohols. Moreover, a number of observations have indicated

that a charge-neutral Ni-OR species might be involved in the alcoholysis reactions.³⁰ For instance, while **1** does not appear to react with 3,4,5-trimethoxybenzyl alcohol (ca. 5 equiv), addition of base to this mixture resulted in a color change from yellow to orange and the $^{31}\text{P}\{\text{H}\}$ NMR spectrum showed the complete conversion of the triflate precursor to a new species displaying a singlet resonance at ca. 138 ppm. Similarly, addition of *m*-cresol and NEt₃ to a C₆D₆ solution of **1** gave an orange-red species displaying a ^{31}P signal slightly upfield of the corresponding signal for the NEt₃ adduct (135.7 vs. 136.2 ppm). We carried out two other experiments to confirm that this new species is not the NEt₃ adduct. First, we repeated the reaction of **1** with *m*-cresol in the presence of Na₂CO₃, KOH, and NPh₃ as base; observation of the same signal (135.7 ppm) confirmed that this new species is likely the aryloxide species (POCOP^{Ph})Ni{O(3-Me-C₆H₄)}, **5**. In addition, adding 1.2 equiv of NaO(3-Me-C₆H₄) to a toluene solution of **1** gave rise to a new peak at 134.7 ppm, which was not affected by addition of excess NEt₃. Addition of a few equivalents of *m*-cresol to this mixture resulted in a downfield shift of the initial signal to ca. 135.7 ppm, while addition of acrylonitrile gave the expected hydroamination product.

The above observations lead us to propose a charge-neutral Ni-OR species as the resting state in the catalytic cycle for the alcoholysis of acrylonitrile. As shown in Figure 3.12, we propose that this Ni-OR species promotes a heterolytic activation of the alcohol O-H bond, which makes possible the conjugate addition.³¹ Consistent with this scenario, the more reactive alcohols are those possessing a more acidic O-H moiety and giving Ni-OR moieties resistant to decomposition. What is still unclear is whether the simultaneous κ^N -binding of acrylonitrile to this Ni-OR (or a different Ni moiety) is required for the

alcoholysis reaction, as was proposed by Yi et al. for their Ru-catalyzed alcoholysis of acrylonitrile.^{17a}

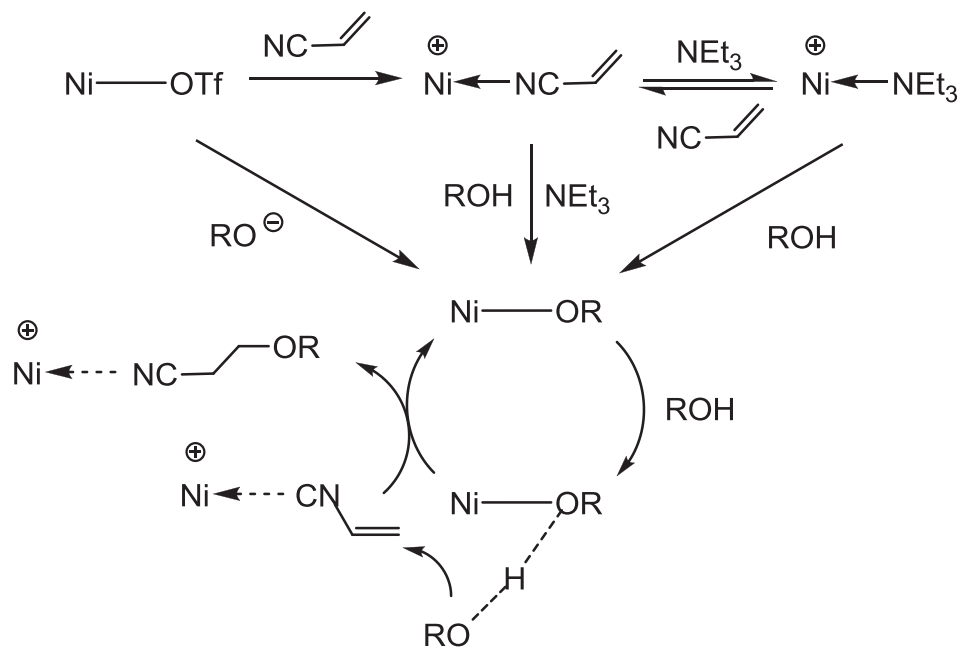


Figure 3.12. Mechanism of alcoholysis of acrylonitrile

3.4. Conclusion

The results presented in this report outline some of the differences between POCOP-type pincer complexes of nickel bearing PPh_2 and $\text{P}(i\text{-Pr})_2$ donor moieties. For instance, the small but significant difference between the $\nu(\text{CN})$ values in $[(\text{POCOP}^{\text{R}})\text{Ni}(\text{NCMe})]^+$ (2297 cm^{-1} for $\text{R} = \text{Ph}$ and 2292 cm^{-1} for $\text{R} = i\text{-Pr}$) indicates greater $\text{N} \rightarrow \text{Ni}$ σ -donation to the $[(\text{POCOP}^{\text{Ph}})\text{Ni}]^+$ fragment, implying that the cationic adducts bearing *P*-Ph substituents are more electrophilic. Contrary to our predictions, this enhanced electrophilicity of the POCOP^{Ph} system does not lead to a greater reactivity for the Ni-

catalyzed hydroamination of acrylonitrile. As discussed above, the complex ($\text{POCOP}^{i\text{-Pr}}$)- $\text{Ni}(\text{OTf})$ is a more competent pre-catalyst, both on its own and in combination with NEt_3 , than its POCOP^{Ph} analogue; on the other hand, the latter compound promotes hydroamination much more effectively when water is used as a proton-transfer agent instead of NEt_3 . Moreover, (POCOP^{Ph}) $\text{Ni}(\text{OTf})$ proved to be more reactive than its *i*-Pr counterpart for the alcoholysis of acrylonitrile.

The observed differences in the hydroamination reactivities of the two triflate derivatives are due, in part, to the different reactivities of these compounds with water and NEt_3 . For example, we noted that the competitive binding of NEt_3 (and likely other amines) to nickel is much more effective in the POCOP^{Ph} derivative; this binding can hinder catalytic reactions involving cationic intermediates. Interestingly, small amounts of water proved to be much more potent in promoting hydroamination reactions catalyzed by (POCOP^{Ph}) $\text{Ni}(\text{OTf})$ even though this derivative is much more prone to hydrolysis in comparison to its $\text{POCOP}^{i\text{-Pr}}$ analogue. Structural characterization of complex **4**, which was obtained from the hydrolytic/aerobic decomposition of **1**, has served to identify the hydrolytic protonation and oxidation steps involved in such decomposition processes.

The above conclusions, combined with our earlier observation that the compounds (POCOP^{Ph}) $\text{Ni}(\text{alkyl})$ are inherently less stable than their $\text{POCOP}^{i\text{-Pr}}$ analogues,^{23r} suggest that future catalytic studies involving the (POCOP^{Ph}) Ni system should be focused on the reactions they promote best, namely Michael type alcoholysis. We plan to expand the range of substrates that can be used in this reaction, and also to

study the synthesis and stabilities of Ni-OR derivatives with the objective of elucidating the precise role played by these compounds in the alcoholysis of acrylonitrile.

3.5. Experimental Section

3.5.1. General.

All manipulations were carried out using standard Schlenk and glove box techniques under a nitrogen atmosphere. When necessary, solvents were dried by passage through activated aluminum oxide columns (MBraun SPS) followed by freeze-thaw degassing to water contents of less than 10 ppm (determined using a Mettler Toledo C20 coulometric Karl Fischer titrator). C₆D₆ was dried over 4 Å molecular sieves and then freeze-thaw degassed. The preparation and characterization of **1** and its bromo precursor have been reported earlier.^{23r} The following were purchased from Aldrich and, unless otherwise noted, used without further purification: Ni (metal), chlorodiphenylphosphine, triethylamine, and all the amines, alcohols and olefins used in the catalytic studies. A Bruker AV 400 spectrometer was used for recording ¹H, ¹³C{¹H} (101 MHz), and ³¹P{¹H} (162 MHz) and Bruker AV 300 was used to record ¹⁹F NMR spectra. ¹H and ¹³C chemical shifts are reported in ppm downfield of TMS and referenced against the residual C₆D₆ signals (7.15 ppm for ¹H and 128.02 ppm for ¹³C); ³¹P chemical shifts are reported in ppm and referenced against the signal for 85% H₃PO₄ (external standard, 0 ppm). ¹⁹F chemical shifts are referenced to CFCl₃ (0 ppm), which results in a single resonance for C₆F₆ at -164.9 ppm. Coupling constants are reported in Hz. The correlation and

assignment of ^1H and ^{13}C NMR resonances were facilitated by spectral analysis and reference to literature values. GC/MS measurements were made on an Agilent 6890N spectrometer, UV-Vis spectra were measured on a Varian Cary 500i, and IR spectra were recorded on Bruker Alpha-P FTIR (4000-400 cm^{-1}).

3.5.2. Synthesis of $\{\kappa^P,\kappa^C,\kappa^P\text{-2,6-(Ph}_2\text{PO)}_2\text{C}_6\text{H}_3\}\text{Ni(NCCH}_3\text{)}\}[\text{OSO}_2\text{CF}_3]$ (2a).

Method A: To a solution of **1** (120 mg, 0.175 mmol) in 10 mL of toluene was added acetonitrile (9 μL , 0.175 mmol) and the mixture was stirred for 15 min. The product was obtained as orange crystals by slow diffusion of hexane into a saturated toluene solution (100 mg, 80%). **Method B:** To a mixture of $\{\kappa^P,\kappa^C,\kappa^P\text{-2,6-(Ph}_2\text{PO)}_2\text{C}_6\text{H}_3\}\text{NiBr}$ (140 mg, 0.23 mmol) and AgOTf (52 mg, 0.23 mmol) in 25 mL of dichloromethane was added acetonitrile (12 μL , 0.24 mmol). After 5h of stirring, the mixture was filtered by cannula and passed through a short column of silica gel. Evaporation to dryness gave 110 mg of a yellow powder (73% crude yield).

^1H NMR (400 MHz, C_6D_6) : δ 6.70 (d, $^3J_{\text{HH}} = 8$, 2H, ArH 3), 7.10 (t, $^3J_{\text{HH}} = 8$, 1H, ArH 4), 7.44 (m, 12H, *p*+*m*-H in PPh $_2$), 7.74 (m, 8H, *o*-H in PPh $_2$), 2.23 (s, 3H, NCCH $_3$), ^{13}C { ^1H } NMR (101 MHz, C_6D_6) : δ 132.08 (^vt , $J_{\text{cp}} = 11$, 4C, *i*-C in PPh $_2$), 130.18 (^vt , $J_{\text{cp}} = 8$, 8C, *o*-C in PPh $_2$), 132.04 (^vt , $J_{\text{cp}} = 6$, 8C, *m*-C in PPh $_2$), 133.39 (4C, *p*-C in PPh $_2$), 165.04 (^vt , $J_{\text{cp}} = 8$, 2C, ArC 2), 107.99 (^vt , $J_{\text{cp}} = 7$, 2C, ArC 3), 131.31 (1C, ArC 4), 129.51 (t, $J_{\text{cp}} = 8$, 1C, ArC 1), 30.40 (1C, CH $_3$), 143.44 (1C, NC-Me) ^{31}P { ^1H } NMR (160 MHz, C_6D_6) : δ 149.7 (s, 2P). ^{19}F NMR (179 MHz, C_6D_6) : δ -78.15 (s, 3F). IR (solid state, cm^{-1}): 1026 (SO $_3$), 1104 (CF $_3$), 1289 (SO $_3$), 1438 (C=C $^{\text{Ar}}$), 1583 (C=C $^{\text{Ar}}$) 2297 (N≡C). UV-Vis(CH $_2\text{Cl}_2$, 1.25×10^{-4}) [λ_{max} , nm (ϵ , mol $^{-1}$ cm 2)] : 386(1001),

324(3846). Elemental Anal. For $C_{33}H_{26}O_5P_2N_1S_1F_3Ni$ Calc.(found) % :C, 54.57 (54.44); H, 3.61 (3.59); S, 4.42 (4.36); N, 1.93 (1.96).

3.5.3. General procedure for preparation of $[\{\kappa^P,\kappa^C,\kappa^P\text{-}2,6\text{-}Ph_2PO\}_2C_6H_3\}Ni(NCR)][OSO_2CF_3]$ (2).

To a solution of **1** (125 mg, 0.18 mmol) in 25 mL of dichloromethane under nitrogen atmosphere, was added one equivalent of acrylonitrile, crotonitrile, or methacrylonitrile. An immediate color change from deep to pale yellow was noted in all cases. The solvent was evaporated slowly under a nitrogen current to give an oily yellow solid. (N.B. Placing the product under vacuum leads to partial decomposition of the product, presumably due to dissociation of RCN.) Only one of the four products could be isolated in analytically pure form, but comparison of the spectra for the remaining compounds (below) to those for the completely characterized acetonitrile analogue **2a** allowed us to confirm the identities of all RCN adducts **2** with confidence.

3.5.3.1. $[\{\kappa^P,\kappa^C,\kappa^P\text{-}2,6\text{-}(Ph_2PO)_2C_6H_3\}Ni(NCCH=CH_2)][OSO_2CF_3]$ (2b).

Crude yield: 90%. 1H NMR (400 MHz, C_6D_6) : δ 6.79 (d, $^3J_{HH} = 8$, 2H, ArH³), 6.95 (t, $^3J_{HH} = 6$, 1H, ArH⁴), 7.07 (m, 12H, *p*+*m*-H in PPh₂), 8.08 (m, 8H, *o*-H in PPh₂), 4.67 (dd, $^3J_{trans} = 12$, $J_{cis} = 8$, 1H, CH-CN-Ni), 4.90 (dd, $^2J=20$, $^3J_{cis}=8$, 1H, CH_{cis} H-CH₂ - CN-Ni), 5.30 (dd, $^3J_{trans} = 8$, $^2J=12$, 1H, CH_{trans} H -CH₂-CN-Ni) . $^{13}C\{^1H\}$ NMR (101 MHz, C_6D_6) : δ 135.7 (m, 4C, *i*-C in PPh₂), 131.3-132.2 (unresolved multiplet, 22C, *o*+*m*+*p*-C in PPh₂+ ArC⁴+ArC¹) (quaternary carbons are not observed), 106.9 (m, ArC³), 126.05 (1C, C=C-CN), 116.92 (1C, C=C-CN). $^1P\{^1H\}$ NMR (160 MHz, C_6D_6) : δ 150.53

(s,2P). ^{19}F NMR (179 MHz, C_6D_6) : δ -78.15 (s,3F). IR (solid state, cm^{-1}): 1028 (SO_3), 1105 (CF_3), 1260 (SO_3), 1439 ($\text{C}=\text{C}^{\text{Ar}}$), 1584 ($\text{C}=\text{C}^{\text{Ar}}$) $\nu=2254$ ($\text{N}\equiv\text{C}$). UV-Vis(CH_2Cl_2 , $1.25 \cdot 10^{-4}$) [λ_{max} , nm (ε , $\text{mol}^{-1} \text{cm}^2$)]: 390 (2266).

3.5.3.2. $[\{\kappa^P,\kappa^C,\kappa^P\text{-}2,6\text{-}(\text{Ph}_2\text{PO})_2\text{C}_6\text{H}_3\}\text{Ni}(\text{NCCH}=\text{CHMe})][\text{OSO}_2\text{CF}_3]$ (2c).

Crude yield: 87%. ^1H NMR (400 MHz, C_6D_6) : δ 6.69 (d, $^3J_{\text{HH}} = 8$, 2H, ArH^3), 6.96 (t, $^3J_{\text{HH}} = 8$, 1H, ArH^4), 7.03 (m, 12H, $p+m$ -H in PPh_2), 8.04 (m, 8H, o -H in PPh_2), 4.56 (m, 1H, $CH\text{-CN-Ni}$), 5.58 and 5.29 (m, 1H, $\text{CH}_3\text{-}CH_{cis}\text{-CH-CN-Ni}$) and (m, 1H, $\text{CH}_3\text{-}CH_{trans}\text{-CH-CN-Ni}$), 1.04 and 1.46 (d, $^4J_{\text{cis}}=2$, $^3J=7$, 3H, $\text{CH}_3\text{-CH}$) and (d, $^4J_{\text{trans}}=2$, $^3J_{\text{HH}} = 7$, 3H, $\text{CH}_3\text{-CH}$). ^{13}C { ^1H } NMR (101 MHz, C_6D_6) : δ 132.4 (m, 4C, i -C in PPh_2), 129.4-130.3 (unresolved multiplet, 22C, $o+m+p$ -C in $\text{PPh}_2 + \text{ArC}^4 + \text{ArC}^1$) (quaternary carbons are not observed), 105.06 (m, ArC^3), 47.23 (1C, CH_3), 119.27 (1C, $\text{C}=\text{C-CH}_3$), 116.02 (1C, $\text{C}=\text{C-CH}_3$). ^{31}P { ^1H } NMR (160 MHz, C_6D_6) : δ 150.80 (s,2P). ^{19}F NMR (179 MHz, C_6D_6) : δ -78.15 (s,3F). IR (solid state, cm^{-1}): 1030 (SO_3), 1106 (CF_3), 1262 (SO_3), 1439 ($\text{C}=\text{C}^{\text{Ar}}$), 1585 ($\text{C}=\text{C}^{\text{Ar}}$) 2283 ($\text{N}\equiv\text{C}$). UV-Vis(CH_2Cl_2 , $1.25 \cdot 10^{-4}$) [λ_{max} , nm (ε , $\text{mol}^{-1} \text{cm}^2$)]: 395 (963).

3.5.3.3. $[\{\kappa^P,\kappa^C,\kappa^P\text{-}2,6\text{-}(\text{Ph}_2\text{PO})_2\text{C}_6\text{H}_3\}\text{Ni}(\text{NCC(Me)}=\text{CH}_2)][\text{OSO}_2\text{CF}_3]$ (2d).

Crude yield: 74%. ^1H NMR (400 MHz, C_6D_6) : δ 6.79 (d, $^3J_{\text{HH}} = 8$, 2H, ArH^3), 6.95 (t, $^3J_{\text{HH}} = 6$, 1H, ArH^4), 7.15 (m, 12H, $p+m$ -H in PPh_2), 8.09 (m, 8H, o -H in PPh_2), 4.82 (m, 1H, $CH_{cis}\text{H-C-CN-Ni}$), 5.17 (m, 1H, $CH_{trans}\text{H-C-CN-Ni}$), 1.30 (t, $^4J_{\text{HH}} = 2$, 3H, CH_3). ^{13}C { ^1H } NMR (101 MHz, C_6D_6) : δ 132.68 (m, 4C, i -C in PPh_2), 129.43 (unresolved multiplet, 12C, $m+p$ -C in PPh_2), 168.04 (2C, ArC^2) , 132.34 (unresolved

multiplet, 10C, *o*-C in $\text{PPh}_2^+ \text{ArC}^4 + \text{ArC}^1$), (quaternary carbons are not observed), 107.65 (m, ArC^3), 30.40 (1C, CH_3), 124.09 (1C, $\text{C}=\text{C}-\text{CH}_3$), 123.06 (1C, $\text{C}=\text{C}-\text{CH}_3$). $^{31}\text{P}\{\text{H}\}$ NMR (160 MHz, C_6D_6) : δ 150.79 (s, 2P). ^{19}F NMR (179 MHz, C_6D_6) : δ -78.15 (s, 3F). IR (solid state, cm^{-1}): 1030 (SO_3), 1105 (CF_3), 1265 (SO_3), 1439 ($\text{C}=\text{C}^{\text{Ar}}$), 1584 ($\text{C}=\text{C}^{\text{Ar}}$), 2252 ($\text{N}\equiv\text{C}$). UV-Vis(CH_2Cl_2 , 1.25×10^{-4}) [λ_{max} , nm (ϵ , $\text{mol}^{-1} \text{cm}^2$)] : 390 (660).

3.5.3.4. $[\{\kappa^p, \kappa^c, \kappa^p\text{-}2,6\text{-}(\text{Ph}_2\text{PO})_2\text{C}_6\text{H}_3\}\text{Ni}(\text{NCCH}_2\text{CH}_2\text{N}(\text{Ph})\text{H})][\text{OSO}_2\text{CF}_3](2e)$.

To a solution of **1** (100 mg, 0.15 mmol) in 10 mL of toluene was added 3-(phenylamino)propionitrile (22 mg, 0.15 mmol), the mixture was stirred for 15 min and orange-yellow crystals were obtained obtained by slow diffusion of hexane (70% crude yield).

^1H NMR (400 MHz, C_6D_6) : δ 7.89 (qq, $J_{\text{HH/HP}} = 8$, 8H, *o*-H in PPh_2), 7.41-7.31 (t, $J_{\text{HH/HP}} = 8$, 12H, *p*+*m*-H in PPh_2), 7.23 (t, $^3J_{\text{HH}} = 8$, 2H, *m*-H in Ph), 7.15 (t, $^3J_{\text{HH}} = 8$, 1H, ArH^4), 6.75 (t, $^3J_{\text{HH}} = 8$, 1H, *p*-H in Ph), 6.66 (d, $^3J_{\text{HH}} = 8$, 2H, ArH^3), 6.42 (d, $^3J_{\text{HH}} = 8$, 2H, *o*-H in Ph), 2.75 (t, $^3J_{\text{HH}} = 8$, 2H, NH-CH_2), 2.63 (t, $^3J_{\text{HH}} = 8$, 2H, NC-CH_2), 5.00 (s, 1H, NH). $^{13}\text{C}\{\text{H}\}$ NMR (101 MHz, C_6D_6) : δ 168.37 (^vt , $J_{\text{cp}} = 13$, 2C, ArC^2), 133.19 (4C, *p*-C in PPh_2), 132.33 (^vt , $J_{\text{cp}} = 5$, 8C, *m*-C in PPh_2), 131.0 (^vt , $J_{\text{cp}} = 30.3$, 4C, *i*-C in PPh_2), 131.23 (1C, ArC^4), 130.06 (^vt , $^2J_{\text{cp}} = 7$, 8C, *o*-C in PPh_2), 129.53 (1C, ArC^1), 128.39 (2C, *m*-C in NH-Ph), 118.33 (1C, *p*-C in NH-Ph), 113.65 (2C, *o*-C in NH-Ph), 39.50 (1C, NC-CH_2), 107.50 (^vt , $J_{\text{cp}} = 6$, 2C, ArC^3), 147.68 (1C, NC-CH_2), 77.39 (1C, $\text{NCCH}_2\text{-CH}_2\text{-NH}$). $^{31}\text{P}\{\text{H}\}$ NMR (160 MHz C_6D_6) : δ 149.8 (s, 2P). ^{19}F NMR (179 MHz, C_6D_6) : δ -78.15 (s, 3F). IR (solid state, cm^{-1}): 1026 (SO_3), 1104 (CF_3), 1289 (SO_3), 1438 ($\text{C}=\text{C}^{\text{Ar}}$), 1583 ($\text{C}=\text{C}^{\text{Ar}}$) 2279 ($\text{N}\equiv\text{C}$).

3.5.4. Synthesis of $\{\kappa^P,\kappa^C,\kappa^P\text{-}2,6\text{-(Ph}_2\text{PO)}_2\text{C}_6\text{H}_3\}\text{Ni}\{\text{O(3-Me-C}_6\text{H}_4\}\text{ (5).}$

To a solution of **1** (100 mg, 0.15 mmol) in 25 mL of dichloromethane under nitrogen atmosphere was added *m*-cresol (31 μL , 0.30 mmol) and NEt₃ (21 μL , 0.15 mmol). An immediate color change was noted, from deep yellow to deep red. Evaporation of the solvent under vacuum gave a red, oily powder (65 mg, 70% crude yield). All attempts to isolate an analytically pure sample ended in the formation of a thick oil.

¹H NMR (400 MHz, *C*₆D₆) : δ 6.45 (d, ³J_{HH} = 7, 2H, ArH³), 6.97 (t, ³J_{HH} = 7, 1H, ArH⁴), 7.07 (m, 12H, *p*+*m*-H in PPh₂), 8.03 (m, 8H, *o*-H in PPh₂), 6.85 (m, 4H), 1.30 (s, 3H, CH₃). ¹³C {¹H} NMR (101 MHz, *C*₆D₆) : δ 133.20 (^vt, *J*_{cp} = 14, 4C, *i*-C in PPh₂), 128.91 (^vt, ²J_{cp} = 10, 8C, *o*-C in PPh₂), 132.04 (^vt, *J*_{cp} = 7, 12C, *m*+*p*-C in PPh₂), 166.57 (2C, ArC²), 107.14 (^vt, *J*_{cp} = 5, 2C, ArC³), 131.76 (1C, ArC⁴), 129.50 (t, *J*_{cp} = 4, 1C, ArC¹), 21.62 (1C, CH₃), 158.46 (1C, *i*-C in O-Ph), 116.33 (1C, *o*₁-CH in O-Ph), 139.64 (1C, *m*-C in O-Ph), 120.56 (1C, *p*-C in O-Ph), 130.68 (1C, *m*-CH in O-Ph), 113.62 (1C, *o*₂-C in O-Ph), ³¹P{¹H} NMR (160 MHz, *C*₆D₆) : δ 135.7 (s, 2P). UV-Vis(CH₂Cl₂, 1.26 10⁻⁵) [λ_{max} , nm (ϵ , mol⁻¹ cm²)] : 488(2380).

3.5.5. Typical procedure used for catalytic hydroamination of cyano olefins.

The reaction vessel (a screw-capped vial) was charged with the olefin (e.g., 0.106 g of acrylonitrile, 2.00 mmol), the amine (e.g., 0.186 g of aniline, 2 mmol), and dodecane as the internal standard (0.012g, 0.07 mmol). The precatalyst (**1** or **3**) was then added (1.00 mL of a 0.0199 M solution in toluene). The mixture was stirred at 50 °C for a predetermined length of time (normally 3 h) and then analyzed by GC/MS to identify the

products and determine the yield using a previously prepared calibration curve. The identities of the products that are known compounds were confirmed by comparison of their spectra to literature data;²³ⁱ characterization of the new products is given below:

3-(phenylamino) propionitrile. ^1H NMR (300 MHz, C_6D_6) : δ 2.60 (t, $^3J = 7$, 2H, CH_2CN), 3.41 (t, $^3J = 7$, 2H, CH_2-CH_2CN), 6.52 (d, $^3J = 11$, 2H, *o*-H in Ph), 6.90 (t, $^3J = 12$, 1H, *p*-H in Ph), 7.02 (t, $^3J = 12$, 2H, *m*-H in Ph), 8.01 (s, 1H, NH). ^{13}C { ^1H } NMR (101 MHz, C_6D_6) : δ 19.02 (1C, CH_2-CN), 46.7 (1C, $C-CH_2CN$), 113.5 (1C, *o*-C in Ph), 117.71 (1C, CN), 118.0 (s, 1C, *p*-C in Ph), 129.8 (1C, *m*-C in Ph). 147.9 (1C, *i*-C in Ph).

3.5.6. Typical procedure used for catalytic alcoholysis of acrylonitrile.

The reaction vessel was charged with acrylonitrile (e.g., 0.106 g, 2.00 mmol) and the alcohol (e.g., 0.401g, 4 mmol of 2,2,2-trifluoroethanol), and the catalyst **1** was then added (1.00 mL of a 0.0199 M solution in toluene). The mixture was stirred at 60 °C for a predetermined length of time (normally 3 h) and then analyzed by GC/MS to identify the products and determine the yield using GC/MS. All of the products are known compounds.²³ⁱ

3.5.7. Crystal Structure Determinations.

Single crystals of **4** were obtained by exposing a toluene solution of **1** to ambient air over 2 days, whereas crystals for **2a**, **2e** and **3** were grown under a nitrogen atmosphere by exposing concentrated toluene solutions of these complexes to vapors of hexane. The crystallographic data for these complexes were collected using : a Bruker smart diffractometer equiped with a APEX II CCD detector and a graphite Monochromator (**3** and **4**); a FR591 generator from Nonius equipped with a Helios

optics, a Kappa rotating anode and a CCD 6K detector (**2a**); a Bruker Microstar generator (micro source) equipped with a Helios optics, a Kappa Nonius goniometer and a Platinum135 (**2e**).

Cell refinement and data reduction were done using SAINT³². An empirical absorption correction, based on the multiple measurements of equivalent reflections, was applied using the program SADABS³³. The space group was confirmed by XPREP³⁴ routine in the program SHELXTL³⁵. The structures were solved by direct-methods and refined by full-matrix least squares and difference Fourier techniques with SHELX-97³⁶. Anisotropic displacement parameters were used for refining all non-hydrogen atoms except for the severely disordered carbon atoms of the hexane solvate present in the unit cell of **2e**. Hydrogen atoms were set in calculated positions and refined as riding atoms with a common thermal parameter.

3.6. Acknowledgements.

The authors gratefully acknowledge financial support received from Université de Montréal (fellowships to A.B.S.) and NSERC of Canada (Discovery and Research Tools & Instruments grants to D.Z.). Dr. D. M. Spasyuk is thanked for many helpful discussions.

3.8. References

¹ For one of the earliest reports on pincer complexes see: Moulton, C. J.; Shaw, B. L. *J. C. S., Dalton Trans.* **1976**, 1020.

² For reviews on catalytic applications of pincer complexes see: (a) Singleton J. T. *Tetrahedron*, **2003**, 59, 1837. (b) Selander, N.; Szabó, K. J. *Chem. Rev.* **2011**, 111, 2048.

For some primary reports on catalytic applications of pincer complexes see: (c) Ohff, M.; Ohff, A.; van der Boom, M. E.; Milstein, D. *J. Am. Chem. Soc.*, **1997**, 119, 11687. (d) Miyazaki, F.; Yamaguchi, K.; Shibasaki, M. *Tetrahedron Lett.* **1999**, 40, 7379. (e) Bedford, R. B.; Draper, S. M.; Scully, P. N.; Welch, S. L. *New J. Chem.* **2000** 24, 745. (f) Dijkstra, H. P.; Meijer, M. D.; Patel, J.; Kreiter, R.; van Klink, G. P. M.; Lutz, M.; Spek, A. L.; Canty, A. J.; van Koten, G. *Organometallics* **2001**, 20, 3159. (g) Sebelius, S.; Olsson, V. J.; Szabó, K. J. *J. Am. Chem. Soc.* **2005**, 127, 10478. (h) Goldman, A. S.; Roy, A. H.; Huang, Z.; Ahuja, R.; Schinski, W.; Brookhart, M. *Science* **2006**, 312, 257. (i) Naghipour, A.; Sabounchei, S. J.; Morales-Morales, D.; Canseco-González, D.; Jensen, C. M. *Polyhedron*, **2007**, 26, 1445. (j) Gunanathan, C.; Ben-David, Y.; Milstein, D. *Science* **2007**, 317, 790. (k) Bernskoetter, W. H.; Brookhart, M. *Organometallics* **2008**, 27, 2036. (l) Zweifel, T.; Naubron, J.-V.; Grützmacher, H. *Angew. Chem. Int. Ed.*, **2009**, 48, 559.

³ For a selection of primary reports on various aspects of pincer chemistry see: (a) van der Ploeg, A. F. M. J.; van Koten, G.; Brevard, C. *Inorg. Chem.* **1982**, 21, 2878. (b) Gozin, M.; Aizenberg, M.; Liou, S.-Y.; Weisman, A.; Ben-David, Y.; Milstein, D. *Nature* **1994**, 370, 42. (c) Gusev, D. G.; Fontaine, F.-G.; Lough A. J.; Zargarian, D. *Angew. Chemie Int. Ed. Eng.*, **2003**, 42, 216. (d) Ingleson, M. J.; Fullmer, B. C.; Buschhorn, D. T.; Fan,

H.; Pink, M.; Huffman, J. C.; Caulton, K. G. *Inorg. Chem.*, **2008**, *47*, 407. (e) Azerraf, C.; Gelman, D. *Organometallics* **2009**, *28*, 6578. (f) Schultz, K. M.; Goldberg, K. I.; Gusev, D. G.; Heinekey, D. M. *Organometallics* **2011**, *30*, 1429. (g) Hebden, T. J.; St. John, A. J.; Gusev, D. G.; Kaminsky, W.; Goldberg, K. I.; Heinekey, D. M. *Angew. Chem. Int. Ed.* **2011**, *50*, 1873.

⁴ For a few general reviews on pincer complexes see: (a) Slagt, M. Q.; van Zwieten, D. A. P.; Moerkerk, A. J. C. M.; Gebbink, R. J. M. K.; van Koten, G. *Coord. Chem. Rev.* **2004**, *248*, 2275; (b) Benito-Garagorri, D.; Kirchner, K. *Acc. Chem. Res.* **2008**, *4*, 201. (c) van der Boom, M. E.; Milstein, D. *Chem. Rev.* **2003**, *103*, 1759. (d) Liang, L.-C. *Coord. Chem. Rev.* **2006** *250*, 1152. (e) Nishiyama, H. *Chem. Soc. Rev.* **2007**, *36*, 1133. (f) Leis, W.; Mayer, H. A.; Kaska, W. C. *Coord. Chem. Rev.* **2008**, *252*, 1787. (g) Albrecht, M.; van Koten, G. *Angew. Chem., Int. Ed.* **2001**, *40*, 375. For some primary reports on applications of pincer complexes in the area of materials see: (h) Batema, G. D.; Lutz, M.; Spek, A. L.; van Walree, C. A.; Donegá, C. d. M.; Meijerink, A.; Havenith, R. W. A.; Pérez-Moreno, J.; Clays, K.; Büchel, M.; van Dijken, A.; Bryce, D. L.; van Klink, G. P. M.; van Koten, G. *Organometallics* **2008**, *27*, 1690. (i) Albrecht, M.; Lutz, M.; Spek, A. L.; van Koten, G. *Nature* **2000**, *406*, 970. (j) Rivera, E. J.; Figueroa, C.; Colón, J. L.; Grove, L.; Connick, W. B. *Inorg. Chem.* **2007**, *46*, 8569. (k) Tastan, S.; Krause, J. A.; Connick, W. B. *Inorg. Chim. Acta* **2006**, *359*, 1889. (l) Aleksanyan, D. V.; Kozlov, V. A.; Nelyubina, Y. V.; Lyssenko, K. A.; Puntus, L. N.; Gutsul, E. I.; Shepel, N. E.; Vasil'ev, A. A.; Petrovskii, P. V.; Odinets, I. L. *Dalton Trans.* **2011**, *40*, 1535.

⁵ (a) Seligson, A.; Trogler, W.C. *Organometallics* **1993**, *12*, 738. (b) Seligson, A. L.; Trogler, W. C. *Organometallics* **1993**, *12*, 744.

⁶ (a) Brunet, J. J.; Neibecke, D.; in *Catalytic Heterofunctionalization*, ed. A. Togni and H. Grützmacher, VCH, Weinheim **2001** pp. 91–141. (b) Müller, T.; Beller, M. *Chem. Rev.* **1998**, *98*, 675. (c) Beller, M.; Seayad, J.; Tillack, A.; Jiao, H. *Angew. Chem. Int. Ed. Engl.*, **2004**, *43*, 3368. (d) Nobis, M.; Drießen-Hölscher, B. *Angew. Chem. Int. Ed. Engl.*, **2001**, *40*, 3983.

⁷ Brunet, J. J.; Commenges, G.; Neibecker, D.; Philippot, K. J. *J. Organomet. Chem.* **1994**, *469*, 221.

⁸ (a) Ackermann, L.; Bergman, R. G.; *Org. Lett.* **2002**, *4*, 1475. (b) Ackermann, L.; Kaspar, L. T.; Gschrei, C. J. *Org. Lett.* **2004**, *6*, 2515. (c) Bexrud, J. A.; Beard, J. D.; Leitch, D. C.; Leitch, L. L. *Org. Lett.* **2005**, *7*, 1959; (d) Thomson, R. K.; Bexrud, J. A.; Schafer, L. L. *Organometallics* **2006**, *25*, 4069. (e) Wood, M. C.; Leitch, D. C.; Yeung, C. S.; Kozak, J. A.; Schafer, L. L. *Angew. Chem. Int. Ed. Engl.* **2007**, *46*, 354.

⁹ Beller, M.; Trauthwein, H.; Eichberger, M.; Breindl, C.; Müller, T. *Eur. J. Inorg. Chem.* **1999**, 1121.

¹⁰ (a) Casalnuovo, A. L.; Calabrese, J. C.; Milstein, D. *J. Am. Chem. Soc.* **1988**, *110*, 6738. (b) Dorta, R.; Egli, P.; Zürcher, F.; Togni, A. *J. Am. Chem. Soc.* **1997**, *119*, 10857.

¹¹ (a) Pawlas, J.; Nakao, Y.; Kawatsura, M.; Hartwig, J. F. *J. Am. Chem. Soc.* **2002**, *124*, 3669. (b) Fadini, L.; Togni, A. *Chem. Comm.* **2003**, 30. (c) Fadini, L.; Togni, A. *Tetrahedron: Asymmetry* **2008**, *19*, 2555.

¹² (a) Kawatsura, M.; Hartwig, J. F. *J. Am. Chem. Soc.* **2000**, *122*, 9546. (b) Löber, O.; Kawatsura, M.; Hartwig, J. F. *J. Am. Chem. Soc.* **2001**, *123*, 4366. (c) Nettekoven, U.; J. F. Hartwig, *J. Am. Chem. Soc.* **2002**, *124*, 1166. (d) Kawatsura, M.; Hartwig, J. F. *Organometallics* **2001**, *20*, 1960.

¹³ Karshtedt, D.; Bell, A. T.; Tilley, T. D. *J. Am. Chem. Soc.* **2005**, *127*, 12640.

¹⁴ (a) Munro-Leighton, C.; Blue, E. D.; Gunnoe, T. B.; *J. Am. Chem. Soc.*, **2006**, *128*, 1446. (b) Munro-Leighton, C.; Delp, S. A.; Blue, E. D.; Gunnoe, T. B. *Organometallics* **2007**, *26*, 1483. (c) Corberán, R.; Marrot, S.; Dellus, N.; Merceron-Saffon, N.; Kato, T.; Peris, E.; Baceiredo, A. *Organometallics* **2009**, *28*, 326. (d) van Lingen, H. L.; Zhuang, W.; Hansen, T.; Rutjes, F. P. J. T.; Jørgensen, K.A. *Org. Biomol. Chem.* **2003**, *1*, 1953.

¹⁵ Gallagher, T. J. *J. Chem. Soc., Chem. Commun.* **1984**, 1554.

¹⁶ (a) Yang, C.-G.; He, C. *J. Am. Chem. Soc.* **2005**, *127*, 6966. (b) Kamiya, I.; Tsunoyama, H.; Tsukuda, T.; Sakurai, H. *Chem. Lett.* **2007**, *36*, 646. (c) Zhang, X.; Corma, A. *Dalton Trans.* **2008**, 397. (d) Volz, F.; Krause, N. *Org. Biomol. Chem.* **2007**, *5*, 1519 (e) T. Hirai, A. Hamasaki, A. Nakamura, M. Tokunaga, *Org. Lett.* **2009**, *11*, 5510.

¹⁷ (a) Yi, C.S.; Yun, S.Y.; He, Z.; *Organometallics* **2003**, *22*, 3031. (b) K. Hori, H. Kitagawa, A. Miyoshi, T. Ohta, I. Furukawa, *Chem. Lett.* **1998**, 1083.

¹⁸ Kawamoto, T.; Hirabayashi, S.; Guo, X.-X.; Nishimura, T.; Hayashi, T. *Chem. Commun.* **2009**, 3528.

¹⁹ (a) Hosokawa, T.; Shinohara, T.; Ooka, Y.; Murahashi, S.-I. *Chem.Lett.* **1989**, 2001. (b) Miller, K. J.; Kitagawa, T. T.; Abu-Omar, M. M. *Organometallics* **2001**, *20*, 4403. (c) Matsukawa, Y.; Mizukado, J.; Quan, H.; Tamura, M.; Sekiya, A. *Angew. Chemie Int. Ed. Engl.* **2005**, *44*, 1128. (d) Gligorich, K. M.; Schultz, M. J.; Sigman, M. S. *J. Am. Chem. Soc.* **2006**, *128*, 2794. (e) Zhang, Y.; Sigman, M. S.; *Org. Lett.* **2006**, *8*, 5557. (f) Patil, N. T.; Lutete, L. M.; Wu, H.; Pahadi, N. K.; Gridnev, I. D.; Yamamoto, Y. *J. Org. Chem.* **2006**, *71*, 4270.

²⁰ Qian, H.; Han, X.; Widenhoefer, R. A. *J. Am. Chem. Soc.* **2004**, *126*, 9536.

²¹ (a) Noyce, D. S.; DeBruin, K. E *J. Am. Chem. Soc.* **1968**, *90*, 372. (b) Fedor, L. R.; De, N. C.; Gurwara, S. K. *J. Am. Chem. Soc.* **1973**, *95*, 2905. (c) Jensen, J. L.; Carré, D. J. *J. Org. Chem.* **1974**, *39*, 2103. (d) Bell, R. P.; Preston, J.; Whitney, R. B. *J. Chem. Soc.* **1962**, *1166*. (e) Lemechko, P.; Grau, F.; Antoniotti, S.; Dunach, E. *Tet. Lett.* **2007**, *48*, 5731.

²² (a) Stewart, I. C.; Bergman, R. G.; Toste, F. D. *J. Am. Chem. Soc.* **2004**, *125*, 8696; (b) Kisanga, P. B.; Ilankumaran, P.; Fetterly, B.M.; Verkade, J. G. *J. Org. Chem.* **2002**, *67*, 3555.

²³ (a) Groux, L. F.; Bélanger-Gariépy, F.; Zargarian, D. *Can. J. Chem.* **2005**, *83*, 634. (b) Castonguay, A.; Charbonneau, F.; Beauchamp, A. L.; D. Zargarian, *Acta Cryst.* **2005**, *E61*, m2240. (c) Castonguay, A.; Sui-Seng, C.; Zargarian, D.; Beauchamp, A. L. *Organometallics* **2006**, *25*, 602. (d) Sui-Seng, C.; Castonguay, Chen, A. Y.; Gareau, D.; Groux, L. F.; Zargarian, D. *Topics in Catalysis* **2006**, *37*, 81. (e) Castonguay, A.; Beauchamp, A. L.; D. Zargarian, *Acta Cryst.* **2007**, *E63*, m196. (f) Pandarus, V.; Zargarian, D. *Chem. Commun.* **2007**, 978. (g) Pandarus, V.; Zargarian, D. *Organometallics* **2007**, *26*, 4321. (h) Castonguay, A.; Beauchamp, A. L.; Zargarian, D. *Organometallics* **2008**, *27*, 5723. (i) Castonguay, A.; Spasyuk, D. M.; Madern, N.; Beauchamp, A. L.; Zargarian, D. *Organometallics* **2009**, *28*, 2134. (j) Castonguay, A.; Beauchamp, A. L.; Zargarian, D. *Inorg. Chem.* **2009**, *48*, 3177. (k) Spasyuk, D. M.; Zargarian, D.; van der Est, A. *Organometallics* **2009**, *28*, 6531. (l) Spasyuk, D. M.; Zargarian, D. *Inorg. Chem.* **2010**, *49*, 6203. (m) Lefèvre, X.; Durieux, G.; Lesturgez, S.; Zargarian, D. *J. Mol. Catal. A*. **2011**, *335*, 1. (n) Spasyuk, D. M.; Gorelsky, S. I.; van der

Est, A.; Zargarian, D. *Inorg. Chem.* **2011**, *50*, 2661. (o) Lefèvre, X.; Spasyuk, D. M.; Zargarian, D. *J. Organomet. Chem.* **2011**, *864*. (p) A. Salah, D. Zargarian, *Acta Cryst.* **2011**, *E67*, m940. (q) A. Salah, D. Zargarian, *Acta Cryst.* **2011**, *E67*, m437. (r) Salah, A. B.; Zargarian, D. *Dalton Trans.* **2011** DOI:10.1039/C1DT10381D.

²⁴ For reports by other groups on POCOP-type Ni complexes see : (a) Valente, G. B. ; Oscar, B. P.; Cesar, H- A.; Toscano, R. A.; Morales-Morales, D. *Tetrahedron lett.* **2006**, *47*, 5059. (b) Chakraborty, S.; Krause, J. A.; Guan, H. *Organometallics* **2009**, *28*, 582. (c) Zhang, J.; Medley, C.; Krause, J. A.; Guan, H. *Organometallics* **2010**, *29*, 6393. (d) Chakraborty, S.; Zhang, J.; Krause, J. A.; Guan, H. *J. Am. Chem. Soc.* **2010**, *132*, 8872. (e) Huang, F.; Zhang, C.; Jiang, J.; Wang, Z.-X., Guan, H. *Inorg. Chem.* **2011**, *50*, 3816.

²⁵ Note that [(POCOPⁱ-Pr)Ni(NCMe)][OTf] does not display a reversible redox process under similar conditions.

²⁶ The solid state structure of this aquo adduct has been reported previously (ref. 23o).

²⁷ It should be mentioned that Poli's group has reported the use of water in the Pt-catalyzed hydroamination of ethylene (Dub, A. P.; Rodriguez-Zubiri, M.; Baudequin, C.; R. Poli, *Green Chem.* **2010**, *12*, 1392.

²⁸ Tests have indicated that addition of small amounts of water (up to 50 equivalents) to mixtures of **1** or **3** and acrylonitrile in toluene does not lead to detectable levels of decomposition due to hydrolysis, whereas a much larger excess (75 equiv or more) can lead to decomposition of the triflate derivative **1**.

²⁹ Jordan, R. F.; Echols, S. F. *Inorg. Chem.* **1987**, *26*, 383.

³⁰ It should be added that we have proposed recently that addition of alcohols to acrylonitrile is also catalyzed very efficiently by a charge-neutral dimeric pincer complex of nickel. See ref. 231.

³¹ A recent report has shown that in-situ generated NHC carbenes can promote the conjugate addition of alcohols to α,β -unsaturated carbonyl compounds; the authors argue that the carbene acts like a Brønsted base to deprotonate the alcohol, thus activating it for the addition step: Phillips, E. M.; Riedrich, M.; Scheidt, K. A. *J. Am. Chem.* **2010**, *132*, 13179.

³² SAINT Release 6.06; Integration Software for Single Crystal Data. Bruker AXS Inc., Madison, Wisconsin, USA., **1999**.

³³ Sheldrick, G.M. SADABS, Bruker Area Detector Absorption Corrections. Bruker AXS Inc., Madison, Wisconsin, USA., **1999**.

³⁴ XPREP Release 5.10; X-ray data Preparation and Reciprocal space Exploration Program. Bruker AXS Inc., Madison, Wisconsin, USA., **1997**.

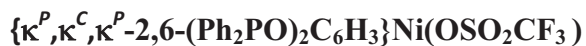
³⁵ SHELXTL Release 5.10; The Complete Software Package for Single Crystal Structure Determination. Bruker AXS Inc., Madison, Wisconsin, USA., **1997**.

³⁶ Sheldrick, G.M.. SHELXS97, Program for the Solution of Crystal Structures. Univ. of Gottingen, Germany. **1997**.

(b) Sheldrick, G.M. SHELXL97, Program for the Refinement of Crystal Structures. UniversityofGottingen,Germany,**1997**.

3.7. Supporting Information.

Tables of ^1H and ^{13}C NMR data for complexes **2** (**a-e**) and **5**, and UV-Vis spectra for complexes **2** (**a-d**) and **5** are provided as supporting information. This material is available free of charge via the Internet at <http://pubs.acs.org>. Complete details of the X-ray analyses for complexes **1**, **2a**, **2e**, **3** and **4** have been deposited at the Cambridge Crystallographic Data Centre (CCDC) and can be retrieved with the following reference numbers: 814532 (**1**), 830945 (**2a**), 830946 (**2e**), 830947 (**3**), 830948 (**4**). This data can be obtained free of charge via www.ccdc.cam.ac.uk/data_request/cif, or by emailing data_request@ccdc.cam.ac.uk, or by contacting The Cambridge Crystallographic Data Centre, 12, Union Road, Cambridge CB2 1EZ, UK; fax: +44 1223 336033.

Supporting Information**For****Hydroamination and Alcoholysis of Acrylonitrile Promoted by the Pincer Complex**

Abderrahmen B. Salah, Caroline Offenstien, and Davit Zargarian*

Département de chimie, Université de Montréal, Montréal (Québec), Canada H3C 3J7

List of items :

1. Table of ^1H NMR data for complexes **2a-e** and **5**
2. Table of ^{13}C NMR data for complexes **2a-e** and **5**
3. UV-Vis curves for complexes $(\text{POCOP}^{i\text{-Pr}})\text{Ni}-\text{NCCH}_3][\text{OSO}_2\text{CF}_3]$, **5** and complexes **2a-d**

Table 3.7. ^1H NMR data for complexes **2a-e** and **5**

	<i>o</i> -H (8H) (qq)*	<i>m</i> -H (qt)	<i>p</i> -H (t)	H3/H5 (d)	H4 (t)
2a	7.74 (m)		7.44 (m,12H)	6.70(8)	7.10(8)
2b	8.08 (m)		7.07 (m,12H)	6.79(8)	6.95(8)
2c	8.04 (m)		7.03 (m,12H)	6.69(8)	6.96(8)
2d	8.09(m)		7.15 (m, 12H)	6.79(8)	6.95(6)
2e	7.89()		7.36 (t, 12H)	6.66(8)	7.15(8)
5	8.03 (m)		7.07 (m,12H)	6.45(7)	6.97(7)

* qq= quasi quadriplet; qt= quasi triplet

Table 3.8. $^{13}\text{C}\{^1\text{H}\}$ NMR data for complexes **2a-e** and **5**

	<i>i</i> -C ^vt , 4C ($^v\text{J}_{\text{P-C}}$)	<i>o</i> -C ^vt , 8C ($^v\text{J}_{\text{P-C}}$)	C1* t, 1C ($^2\text{J}_{\text{C-P}}$)	C4 s, 1C	<i>m</i> -C ^vt , 8C ($^v\text{J}_{\text{P-C}}$)	<i>p</i> -C ^vt , 4C ($^v\text{J}_{\text{C-P}}$)	C2/C6 ^vt , 2C ($^v\text{J}_{\text{P-C}}$) *	C3/C5 ^vt , 2C ($^v\text{J}_{\text{P-C}}$)
2a	132.08(11)	130.18(8)	129.51(8)	131.31		133.39(6)	165.04(8)	107.99(7)
2b	135.7 (m)				131.3-132,2 unresolved multiplet		Non observed	106.92(2)
2c	132.4(m)				129.4-130.3 unresolved multiplet		Non observed	105.06(s)
2d	132.68 (m)		132.33 unresolved multiplet		129.43 unresolved multiplet		168.33(s)	107.65 (s)
2e	131.0(30)	130.06(7)	129.53	131.23	132.33(5)	133.19(s)	168.37 (13)	107.50(6)
5	133.20 (14)	128.91(10)	129.50 (4)	131.76		132.04 (7)	166.57(s)	107.14 (5)

* The signals of the quaternary carbons are very weak.

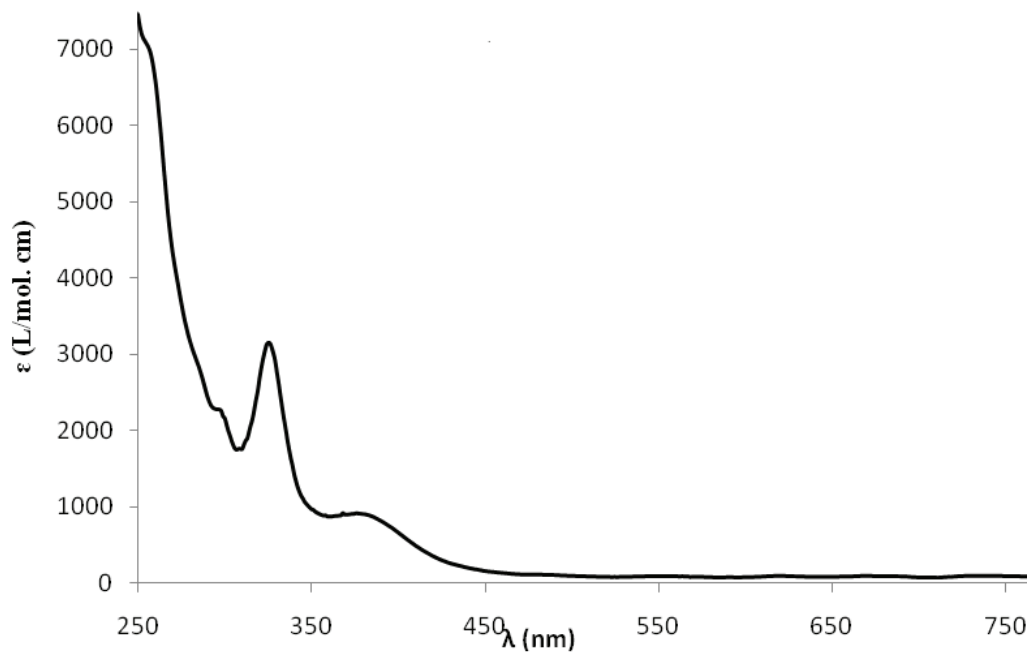


Figure 3.13. UV-Vis of $(\text{POCOP}^{\text{i-Pr}})\text{NiNCMe}$ in CH_2Cl_2 . Concentration = $1.25 \cdot 10^{-4}$ mol/L

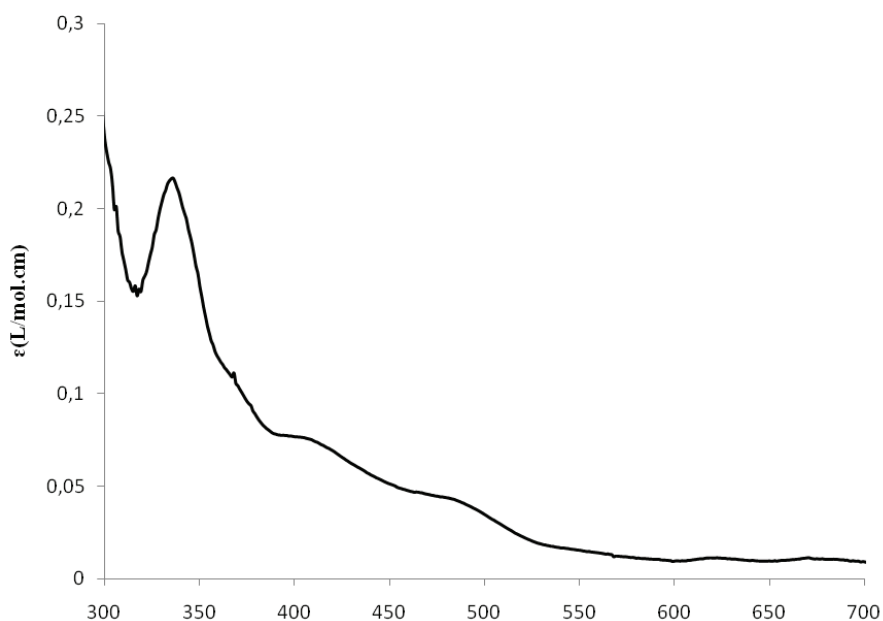


Figure 3.14. UV-Vis of complex 5 in CH_2Cl_2 (Concentration = $1.26 \cdot 10^{-5}$ mol/L)

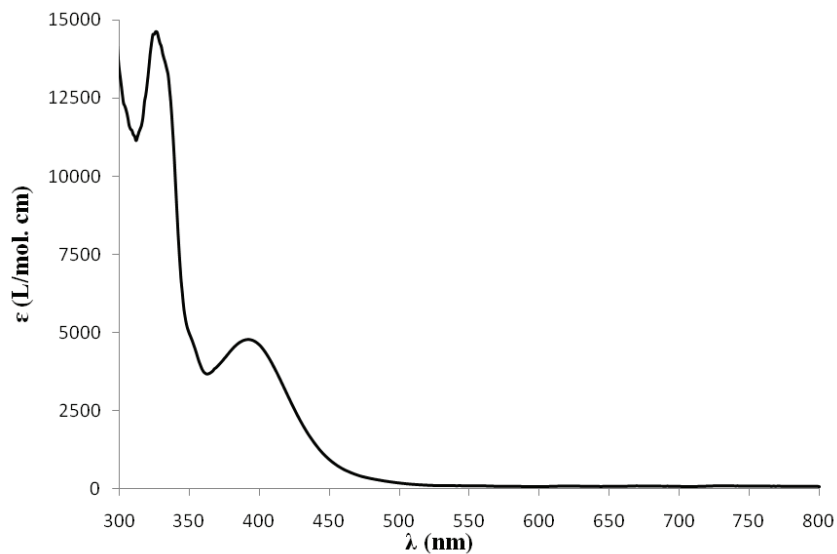


Figure 3.15. UV-Vis of complex **2a** in CH_2Cl_2 (Concentration = 1.25×10^{-4} mol/L)

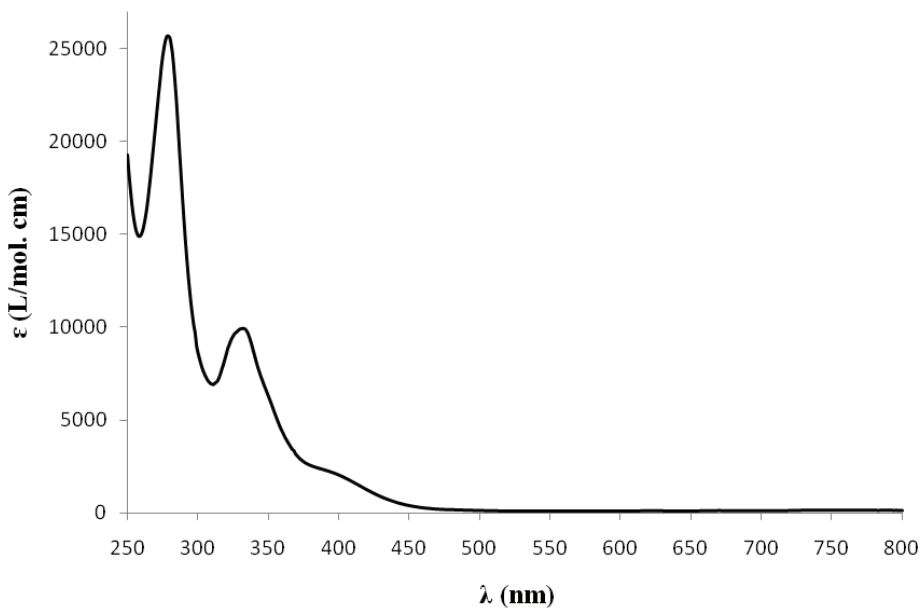


Figure 3.16. UV-Vis of complex **2b** in CH_2Cl_2 (Concentration = 1.25×10^{-4} mol/L)

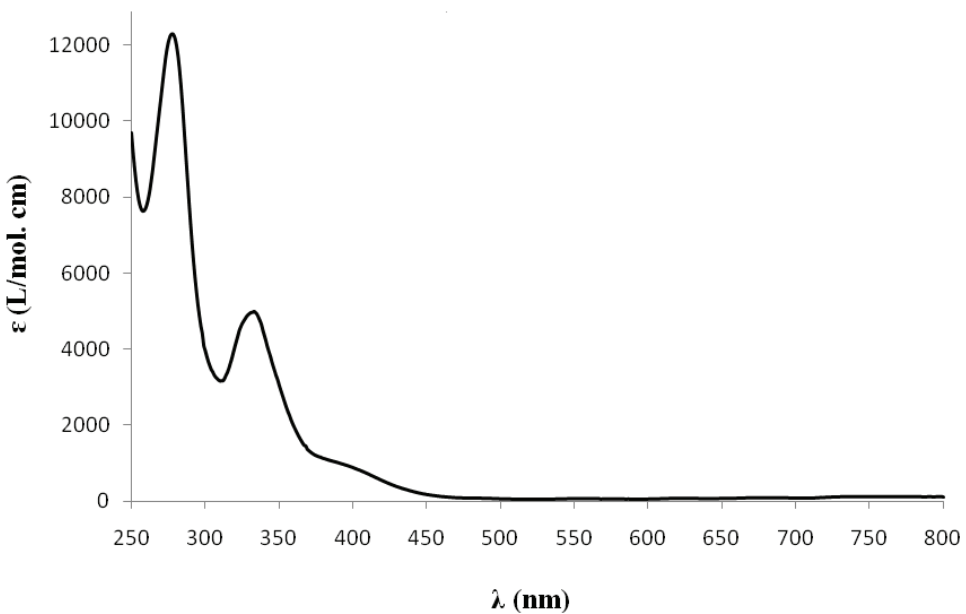


Figure 3.17. UV-Vis of complex **2c** in CH_2Cl_2 (Concentration = $1.25 \cdot 10^{-4}$ mol/L)

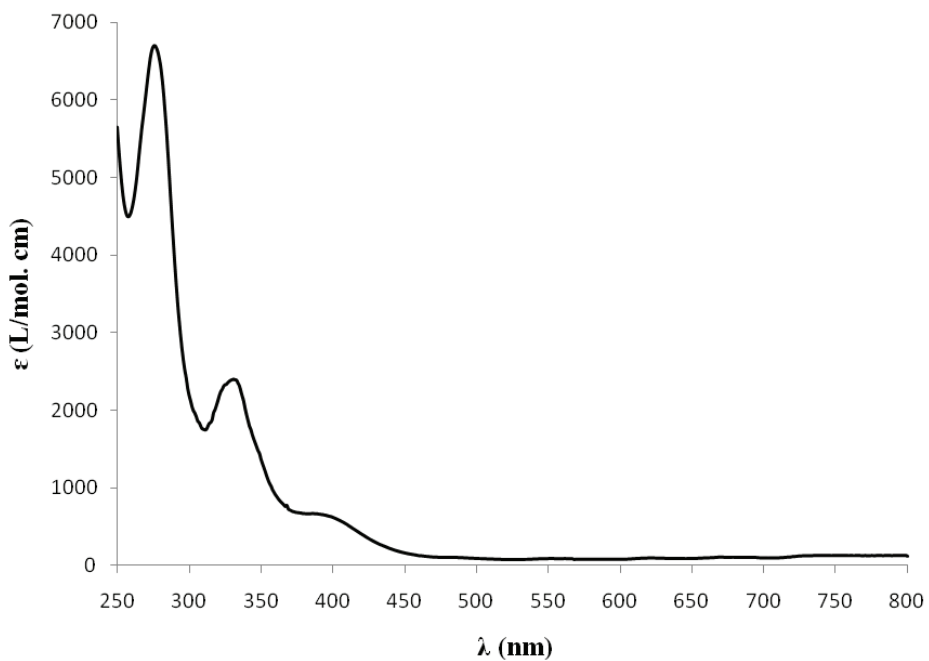


Figure 3.18. UV-Vis of complex **2d** in CH_2Cl_2 (Concentration = $1.25 \cdot 10^{-4}$ mol/L)

Chapitre 4: Conclusion générale

Dans ce mémoire, nous avons mis au point la synthèse d'une nouvelle série de composés pinceurs diphosphinito du nickel(II) comportant différentes phosphines. Ainsi, nous avons exploré l'effet du changement des substituants phosphines sur les propriétés spectroscopiques, électrochimiques et catalytiques de ces composés.

4.1 Synthèse des ligands et des complexes

La synthèse du ligand $\text{POC}_{\text{sp}^2}\text{OP}$ avec de bons rendements est déjà bien connue en littérature. Généralement, ces méthodes utilisent des solvants d'extraction à haut point d'ébullition comme le toluène, un excès de base telle que la 4-diméthylaminopyridine (DMAP), des températures élevées et/ou des durées importantes. Toutes ces conditions ont été révisées en changeant la base, la température, la durée mais également en utilisant l'hexane pour l'extraction du ligand (figure 4.1).

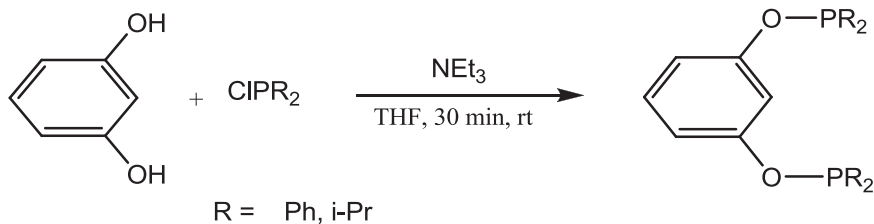


Figure 4.1. Synthèse des ligands

La cyclométallation des ligands a été effectuée en faisant réagir le précurseur $\text{NiBr}_2(\text{NCCH}_3)_x$ avec le ligand en présence d'un équivalent de base pour neutraliser l'acide libéré ce qui conduit à de meilleurs rendements.

Une série des dérivés du complexe $(\text{POCOP}^{\text{Ph}})\text{NiBr}$ a été synthétisée en vue de comprendre l'effet de substitution des phosphines sur les propriétés spectroscopiques et

électrochimiques des complexes pinceurs de type POCOP de Ni(II). L'utilisation des sels d'argent paraît être la solution la plus fiable pour obtenir de bons rendements. Certes, l'utilisation des sels de potassium mène aussi à des composés cibles, mais cette approche exige de l'énergie thermique et conduit à de faibles rendements. D'ailleurs, les sels de sodium sont inefficaces, ce qui indique que le lien Ni-Br est un lien très fort. Les tentatives de synthèse des dérivés alkyles à partir de la réaction du complexe (POCOP^{Ph})NiBr avec les réactifs Grignard (ou les organolithiens) ont été infructueuses, et ce, à différentes conditions. Ces résultats n'étaient pas surprenants sachant que différents groupes de recherche, partout dans le monde, ont tenté la préparation de ce type de composé en vain (figure 4.2). D'autre part, les dérivés alkyles du complexe (POCOP^{i-Pr})NiBr semblent être très faciles à obtenir et à isoler, ce qui montre l'important rôle que jouent les substituants des phosphines dans la formation et la stabilisation de ces composés.

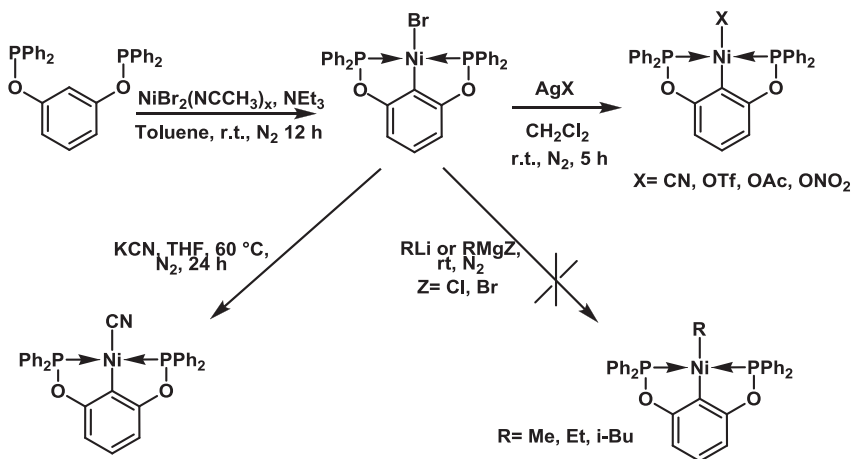


Figure 4.2. Synthèse des complexes

4.2 L'effet du changement des phosphines sur les propriétés catalytiques et spectroscopiques

Du point de vue spectroscopique, le changement des groupes i-Pr par des Ph sur les phosphores rend les complexes plus distordus (distorsion tétraédrique) et déplace le pic de MLCT vers la région des UV et, par la suite, augmente le potentiel d'oxydation du centre métallique.

Les études catalytiques d'hydroamination et d'hydroalkoxylation de l'acrylonitrile ont été faites avec les complexes $(POCOP^{\text{Ph}})_2\text{NiOTf}$ et $(POCOP^{\text{i-Pr}})_2\text{NiOTf}$ dans le but d'étudier l'effet des substituants des phosphines sur les propriétés catalytiques des complexes. Tout d'abord, nous avons optimisé les conditions expérimentales (3 h et 60°C) ainsi que le choix du solvant (toluène) avec la polarité adéquate dans le but d'obtenir de meilleurs rendements, tout en évitant la double hydroamination de l'acrylonitrile. En ce qui concerne la réaction d'hydroamination, les deux complexes $(POCOP^{\text{Ph}})_2\text{NiOTf}$ et $(POCOP^{\text{i-Pr}})_2\text{NiOTf}$ sans ajout d'additifs ont montré une activité catalytique comparable. Par contre, en présence d'une base (triéthylamine), le deuxième complexe semble être plus réactif que son homologue; en outre, l'inverse a été observé lorsque l'eau a été utilisée comme additif.

La réaction d'hydroalkoxylation a bien été étudiée avec le système $POCOP^{\text{Ph}}$. Comme pour la réaction d'hydroamination, il a été démontré que la présence du précatalyseur $(POCOP^{\text{Ph}})_2\text{NiOTf}$ est indispensable à la réaction. A l'exception du $\text{CF}_3\text{CH}_2\text{OH}$, la réaction d'hydroalkoxylation de l'acrylonitrile ne fonctionne pas avec les alcools aliphatiques car ils détruisent le catalyseur. De plus, le méthacrylonitrile et le crotonitrile sont inactifs pour cette réaction. Pour avoir une meilleure conversion, le ratio substrat : alcool devrait être au moins 1 : 2 et la présence d'une base (triéthylamine) est

essentielle; c'est le contraire pour la réaction d'hydroamination, où la présence de la base (triéthylamine) diminue les rendements dans le cas de POCOP^{Ph} .

Du point de vue mécanistique, la formation du produit d'hydroamination passe à travers une attaque nucléophile par l'amine sur le double lien du substrat qui est coordonné au nickel via son groupe nitrile; par la suite, il y aura un transfert du proton pour fournir le produit final. Lors de cette réaction, de nombreuses observations ont été notées dans le cas du complexe $(\text{POCOP}^{\text{Ph}})\text{NiOTf}$, telles que la coordination de la triéthylamine qui diminue le rendement (figure 4.3).

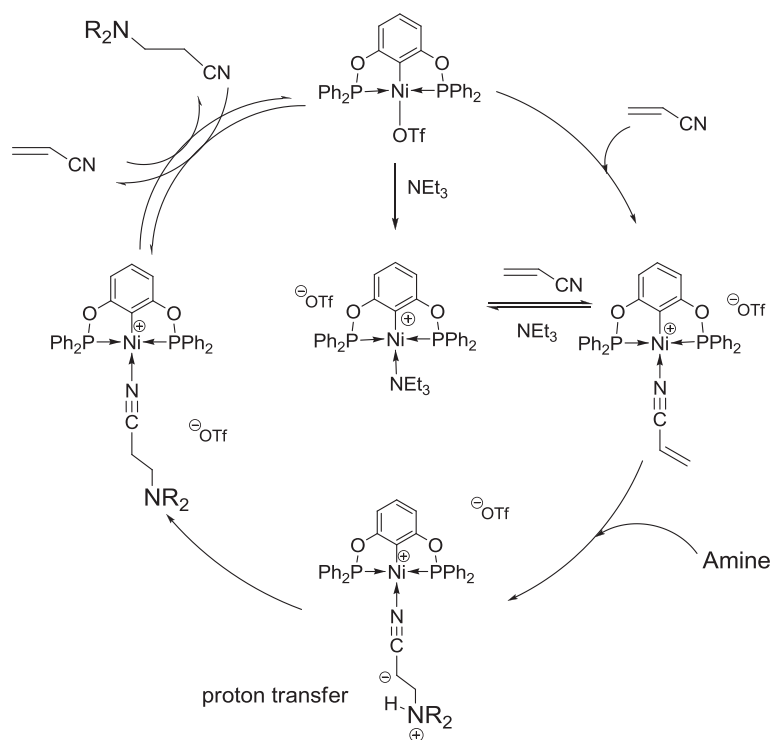


Figure 4.3. Mécanisme de l'hydroamination

Par ailleurs, le mécanisme de l'hydroalkoxylation est totalement différent par rapport à celui de l'hydroamination. Il a été démontré que l'espèce active est le dérivé $(\text{POCOP}^{\text{Ph}})\text{Ni-OAr}$ qui se forme suite à l'ajout du mélange de l'alcool et de la base sur le cation $[(\text{POCOP}^{\text{Ph}})\text{NiNCCHCH}_2]^+$. On présume que les interactions hydrogène jouent un

rôle clé dans le mécanisme en augmentant la nucléophilie de l'oxygène de l'alcool, ce qui rend l'attaque sur le double lien très facile (Figure 4.4).

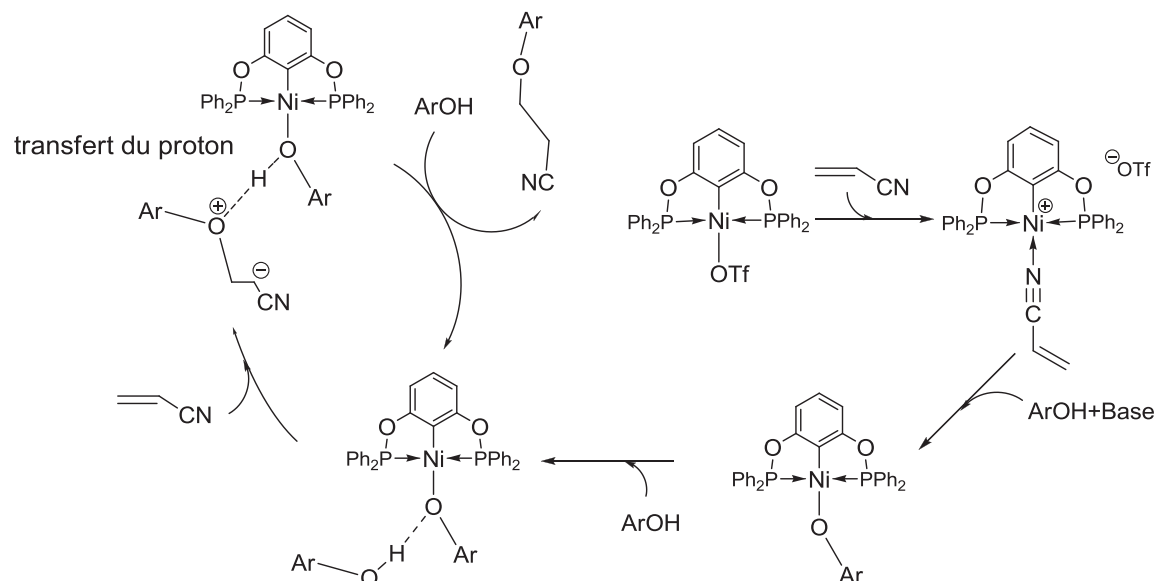


Figure 4.4. Mécanisme d'hydroalkoxylation

4.3 Limitation et perspectives

La plupart des objectifs visés pour ce mémoire ont été atteints à l'exception de l'isolation et de la caractérisation de certains dérivés ou intermédiaires dans les cycles catalytiques. De plus, le nombre limité des travaux académiques qui s'intéresse à l'étude de l'effet de changement des phosphines sur l'activité catalytiques et les propriétés spectroscopiques des complexes pinceurs du nickel rend ce travail très important. Ainsi, nous avons pu prouver que le fait de changer des phosphines plus donneuses par d'autres moins donneuses augmente le caractère électrophile du nickel. Cela facilite davantage les réactions de type d'addition de Michaelis-Menten sur les oléfines activées. Cependant, il a été remarqué expérimentalement que l'augmentation excessive du caractère électrophile du nickel peut parfois causer des problèmes, tels que la coordination des additifs

(triéthylamine). En outre, sur le plan stérique, il s'est avéré que la synthèse des dérivés alkyles nécessite des phosphines plus encombrantes pour protéger le lien Ni-R, ce qui constitue une faiblesse dans ce projet. Également, cette étude est limitée à certain type de phosphines, en raison de leur prix moins élevé par rapport à d'autres phosphines. Toutefois, on peut estimer la réactivité du reste des phosphines grâce à notre étude en tenant compte des effets stériques et électroniques des phosphines étudiées.

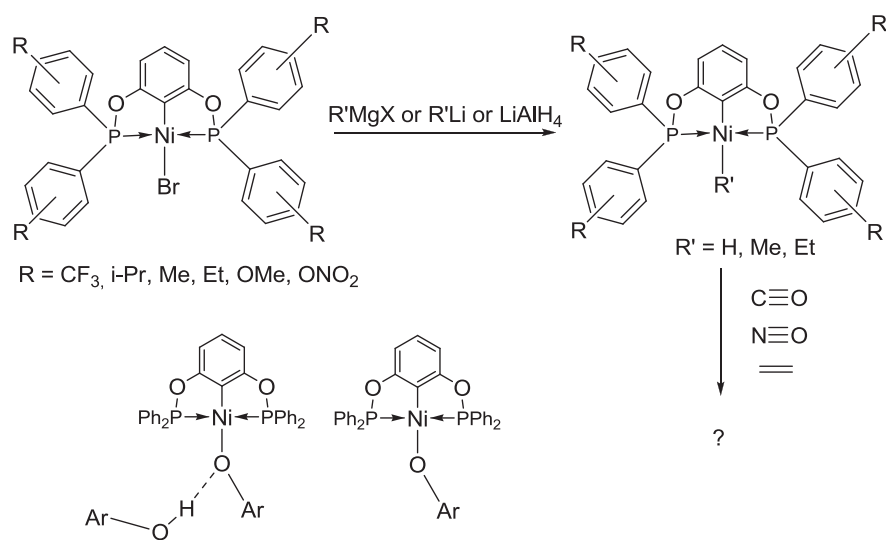


Figure 4.5. Nouveau complexes et intermédiaire réactionnels de type POCOP

Cette étude peut être améliorée par la fonctionnalisation des groupes phényles des phosphines. En effet, en ajoutant des groupes électro-donneurs ou électro-attracteurs, on peut conduire à de nouvelles réactivités catalytiques ou stœchiométriques intéressantes comme l'insertion des gaz toxiques, ou encore à l'isolation des composés très réactifs tel l'hydrure. Une idée intéressante pour l'hydroamination serait d'utiliser une base moins nucléophile ou plus encombrante que la triéthylamine afin empêcher la compétition entre la base et le substrat pour la coordination au centre métallique.

A propos de la réaction d'hydroalkoxylation, l'isolation de certains intermédiaires et leur caractérisation semble être indispensable pour la validation du mécanisme.

Finalement, pour résoudre le problème de réaction des alcools aliphatiques sur l'acrylonitrile, une idée à vérifier consiste simplement à faire réagir 1 équivalent d'un alcool aromatique avec le composé $(POCOP^{Ph})NiOTf$ en présence d'une base pour former le dérivé $(POCOP^{Ph})NiOAr$. Puis, ajouter un excès d'alcool aliphatique et selon le mécanisme précédent, il semble fort probable que la réaction d'addition du lien O-H sur l'acrylonitrile fonctionne sans destruction du catalyseur (figure 4.5).

ANNEXES

Des DVD comportant les rapports et les fichiers cif. des structures ont été soumis avec ce mémoire.